UNIVERSITY OF BELGRADE

FACULTY OF MEDICINE

Teodora M. Rodić

BONE QUALITY ANALYSIS OF JAW BONES IN TYPE 2 DIABETES AND ALCOHOLIC LIVER CIRRHOSIS: ANATOMICAL AND MICROSTRUCTURAL EVALUATION

Doctoral Dissertation

Belgrade, 2022

UNIVERSITY OF BELGRADE

FACULTY OF MEDICINE

Teodora M. Rodić

BONE QUALITY ANALYSIS OF JAW BONES IN TYPE 2 DIABETES AND ALCOHOLIC LIVER CIRRHOSIS: ANATOMICAL AND MICROSTRUCTURAL EVALUATION

Doctoral Dissertation

Belgrade, 2022

УНИВЕРЗИТЕТ У БЕОГРАДУ

МЕДИЦИНСКИ ФАКУЛТЕТ

Теодора М. Родић

АНАЛИЗА КВАЛИТЕТА ВИЛИЧНИХ КОСТИЈУ КОД ТИПА 2 ДИЈАБЕТЕСА И АЛКОХОЛНЕ ЦИРОЗЕ ЈЕТРЕ: АНАТОМСКА И МИКРОСТРУКТУРНА АНАЛИЗА

Докторска дисертација

Београд, 2022.

PhD advisor: Assist. Prof. Dr. Petar Milovanović, Faculty of Medicine, University of Belgrade

Members of the Committee:

1. Prof. Dr. Marija Đurić, Faculty of Medicine, University of Belgrade;

2. Prof. Dr. Jelena Sopta, , Faculty of Medicine, University of Belgrade;

3. Assist. Prof. Dr Miroslav Vasović, Faculty of Medical Sciences, University of Kragujevac.

Date of defense: _____

Acknowledgements

I am thankful to many people without whom my PhD thesis would not have come to life.

To my late grandmother Slobodanka Bojić and to my aunt Slađana Mijanović, for financing my bachelor and PhD studies and for always being genuinely interested to hear about my successes.

To my sister, Dragana Rodić, and my brother, Dragoljub Rodić, for making me see a bigger picture, for reminding me of my path when I got entangled, for rejoucing together with me on every milestone and for visiting me in Hamburg during memorable days.

To my parents, Miomir Rodić and Stojanka Rodić Vujinović, to whom I dedicate my PhD thesis. It is only with the love, support and understanding of my parents that I have finished my formal education and became the person that I am today. My PhD thesis is, among else, a symbol and a reward of everything my parents have done for me. Your daughter loves you.

Bone Quality Analysis of Jaw Bones in Type 2 Diabetes and Alcoholic Liver Cirrhosis: Anatomical and Microstructural Evaluation

Abstract:

Increasing prevalence of type 2 diabetes mellitus (T2DM) in general population due to the aging society, sedentary lifestyle, and obesity results in growing numbers of T2DM patients in dental practice. Recent studies have suggested increased bone fragility in patients with T2DM; however, the mechanisms of T2DM-associated bone changes in jaw bones are still poorly understood. Indeed, patients with T2DM often present with a need for dental implant placement in the edentulous alveolar bone. Furthermore, titanium fixation screws, which need to be placed in the mandibular angle in case of a fracture located in that region are sometimes required in T2DM patients. T2DM-related alterations in jaw bone quality, which may have direct effects on osseointegration and implant survival in this patient population, have not yet been investigated. The question remains as to whether alterations in jaw bone quality in T2DM contribute to implant failure.

Alcoholic liver cirrhosis (ALC) has a proven negative influence on bone quality at various skeletal sites, such as femur and spine. On the other hand, evidence about the influence of ALC on jaw bone quality is scarce. Dental patients with a history of alcohol abuse and possibly compromised liver function sometimes need surgical interventions on the jaw bone, in post-traumatic cases, tooth extractions etc. Information about the jaw bone quality in patients with ALC is needed to make an evidence-based decision about the possibilities for oral and maxillofacial surgery in these patients.

There is still poor understanding of bone quality in patients with T2DM and ALC; however, these patients, especially T2DM patients, are often met in the dental practice and decisions to treat or not to treat them are usually based on personal opinion of a physician. Therefore, there is a great need for evidence-based recommendations in clinical practice. In that context, we believe that understanding how T2DM and ALC affect bone quality on several hierarchical levels of observation could have significant clinical relevance in medicine and dentistry. Currently, patients treated with different antidiabetic medications are not distinguished clearly in clinical practice and the current clinical approach is not based on strong evidence. Therefore, the focus on the effects of T2DM treatment options (Insulin vs. OAD) on bone quality may also be of great practical value in oral and maxillofacial surgery. And it is important to clarify whether T2DM and ALC should be considered absolute or relative contraindications for oral interventions on bone, at least when it comes to the bone tissue status of these patients.

The aim of this thesis was to explore bone quality of T2DM and ALC patients compared with healthy control group on several hierarchical levels in the edentulous region of the lower first molar and the mandibular angle, so as to provide structural evidence to estimate possibilities of for common treatments in oral and maxillofacial surgery.

The following specific objectives were stated:

i.   to compare the jaw bone microstructural, compositional, and cellular properties between patients with T2DM and healthy controls;
ii. to investigate the influence of OAD vs. insulin in T2DM individuals in a site-specific manner, and to
iii. to compare the jaw bone microstructural, compositional, and cellular properties between individuals with ALC and healthy controls, in a site-specific manner.

Mandible bone samples were collected during autopsy at the Faculty of Medicine, University of Belgrade, from male individuals aged over 65 years. The specimens were divided into three groups: T2DM group (n=10), ALC group (n=6), and age- and sex-matched healthy controls (n=11). Bone microstructure of the angulus and the molar regions was assessed using micro-computed tomography (Skyscan 1172 micro-CT, Bruker, Kontich, Belgium) at a spatial resolution of 10 μm. A separate analysis was performed for the cortical and trabecular compartments, providing 3D quantitative parameters of bone microarchitecture. Morphological analysis of osteons and osteocyte lacunae analysis was performed in ImageJ software. Next, evaluation of bone matrix mineralization using quantitative backscattered electron microscopy (qBEI) was performed. The composition of bone mineral and collagen phases, which indicate mechanical properties of bone matrix, was evaluated by Raman spectroscopy. Cellular and tissue characteristics of bone specimens were assessed using histomorphometry. Tissue sections were stained with toluidine blue and Masson-Goldner. Osseous cell and tissue indices, which indicate bone cell properties and ratios between active and inactive bone surfaces, were determined using OsteoMeasure histomorphometry system (Osteo Metrics, Atlanta, GA, USA).

The parameters of jaw bone microstructure, composition, and bone cells were compared between individuals with T2DM and healthy controls in a site-specific manner. In the mandibular angle, T2DM showed lower porosity of the lingual cortex (p=0.004). In the trabecular bone of the mandibular angle higher trabecular thickness (p=0.008), fewer mineralized osteocyte lacunae (p=0.049), and smaller lacunae (p=0.03) were found in the T2DM group. More highly mineralized bone packets were found in the buccal cortex of the mandibular angle in insulin-treated compared to OAD-treated T2DM group (p=0.034). In the molar region, we found higher heterogeneity of trabecular calcium content in T2DM insulin than in the Control (p=0.015) and T2DM OAD (p=0.019) groups. The trabecular bone of the molar region showed a lower fractal dimension (p=0.028) and higher osteoclast number per bone perimeter in T2DM vs. the Control group (p=0.042). The lingual cortex of the molar region showed no difference in T2DM. The buccal cortex of the molar region had a lower mineralized osteocyte lacunar bone number (p=0.04) and a higher carbonate-to-phosphate ratio in T2DM (p=0.009). Inter-site comparisons (angulus vs. molar region) in the T2DM group and T2DM subgroups showed higher cortical porosity in the molar region compared with the angulus region in T2DM (p=0.007).

Similar to T2DM jaw bone quality study, there was substantial variability in bone quality between ALC and healthy controls. The trabecular bone of the molar region showed smaller lacunae in ALC than in the Control group (p=0.002). The lingual cortex of the molar region showed higher closed porosity in ALC compared with the Control group (p=0.003). The buccal cortex of the molar region had higher closed porosity (p=0.02) and a higher carbonate-to-phosphate ratio in ALC (p=0.008). The trabecular bone of the angulus region had lower calcium content (p=0.042), fewer highly mineralized bone packets (p=0.036), fewer octeoclasts (p=0.032), and a tendency towards lower osteoblast number in ALC compared with the Control group (p=0.056). The lingual cortex of the angulus region showed a tendency towards higher open porosity (p=0.098) and pore diameter in ALC (p=0.002). The buccal cortex of the angulus region showed higher closed porosity (p=0.007) in ALC compared with the Control group. Inter-site comparisons (angulus region vs. molar region) in the ALC group showed microstructural differences in trabecular geometry, such as higher degree of anisotropy in the angulus region (p=0.001) and higher fractal dimension in the molar region (p=0.033).

The results indicated that T2DM caused microarchitectural alterations of the jaw bone, manifested by simpler microarchitectural geometry of the trabecular molar region and higher trabecular thickness at the trabecular angulus. Both insulin and OAD therapy affected bone remodeling, with OADs causing more intense resorption in the trabecular molar region several years after tooth extraction, and Insulin therapy predominantly causing alterations in mineralization. OAD therapy caused a filling effect of cortical pores in the lingual cortex of the angulus region. Insulin therapy was associated with packets of highly mineralized bone and layers of bone tissue of different calcium content in both observed regions of the mandible. Bone tissue in cases receiving OAD therapy had altered carbonate content compared with the healthy bone. The lower number of mineralized lacunae in T2DM compared with controls might suggest even younger tissue age due to DM-related faster remodeling. Cortical thickness of the jaw remained unchanged in T2DM. Taken together, all alterations to bone quality must have developed under a combination of local and systemic factors specific for each bony site of the jaw. Further research is required to explain the mechanisms of such bone tissue alterations in patients with diabetes. Based on the current data, there is generally no contraindication for the implant placement in T2DM patients as far as bone microstructure and composition are concerned. Nevertheless, alterations to bone quality might affect implant's long-term stability, which requires further studies.

ALC caused microstructural alterations of the jaw bone, manifested by higher closed porosity in cortical bone and lower lacunar size in the trabecular bone of the molar region. Trabecular bone of the angulus region had lower calcium content and lower resorptive activity in the ALC individuals than in the corresponding regions of the healthy individuals. Bone chemical composition was altered in buccal cortex of the molar region, with higher carbonate content in ALC compared with healthy individuals. Such bone tissue characteristics must have developed under a combination of systemic and local factors specific for each bony site of the jaw. Our findings suggest that jaw bone quality is altered in ALC, in terms of microstructure, mineralization, tissue composition, and cellular activity. It is possible that jaw bone in ALC has altered mechanical characteristics, but this needs further research. Oral and maxillofacial surgeons should approach patients with ALC with caution during surgical procedures involving bone, due to alterations in jaw bone quality.

This results from this thesis showed that T2DM and ALC alter bone quality of the mandible, and that alterations caused by T2DM and ALC differentially affect various bony sites and compartments of the mandible. Moreover, differences in bone quality between the angulus region of the mandible and the edentulous alveolar bone in the region of first lower molar are of interest to oral and maxillofacial surgeons. This thesis indirectly provides more possibilities for dental implant insertion and the titanium screw placement in patients with T2DM. In ALC patients, surgeons should bear in mind altered jaw bone tissue characteristics when performing interventions involving bone tissue. Taken together, this thesis provides the structural basis for consideration during making a treatment plan in oral and maxillofacial surgery of these patients.

Key words: type 2 diabetes mellitus, alcoholic liver cirrhosis, jaw, bone, microstructure, mineralization, osteocytes

Scientific field: MEDICINE

Scientific subfield: Skeletal biology

UDK number:

Анализа квалитета виличних костију код типа 2 дијабетеса и алкохолне цирозе јетре: анатомска и микроструктурна анализа

Сажетак:

Повећана учесталост типа 2 дијабетес мелитуса (Т2ДМ) у општој популацији због старења друштва, неактивног стила живота и гојазности доводи до повећаног броја пацијената са Т2ДМ у стоматолошкој пракси. Недавна истраживања указују на повећану ломљивост костију пацијената са Т2ДМ. Упркос томе, још увек се врло мало зна о механизмима промена на костима које се јављају у Т2ДМ. Код пацијената са Т2ДМ често постоји потреба за уградњом зубних имплантата у безуби алвеоларни гребен. Осим тога, титанијумски шрафови за фиксацију, који се постављају у угао доње вилице у случају прелома локализованог у том региону, су некада потребни код пацијената са Т2ДМ. Промене у квалитету кости код Т2ДМ које могу имати директне ефекте на осеоинтеграцију и опстанак имплантата у овој популацији пацијената још увек нису истражени. Остаје питање да ли постоје промене у квалитету кости вилица у Т2ДМ које могу допринети губитку имплантата.

Алкохолна цироза јетре (АЦЈ) има доказано негативан утицај на квалитет костију на различитим местима скелета, попут бутне кости и кичме. Међутим, докази о утицају АЦЈ на квалитет кости вилице су оскудни. Стоматолошким пацијентима који конзумирају алкохол и потенцијално имају оштећену функцију јетре понекад су потребне хируршке интервенције на костима вилица (нпр. у посттрауматским случајевима, вађење зуба итд.). У том смислу су неопходни подаци о квалитету кости вилице код пацијената са АЦЈ, пре свега да би се донела одлука заснована на доказима о могућностима оралне и максилофацијалне хирургије код ових пацијената.

Још увек се мало зна о квалитету кости код особа са Т2ДМ и АЦЈ. Ипак, ови пацијенти, нарочито они са Т2ДМ, често се срећу у стоматолошкој пракси, где се одлуке о томе да ли да се они хируршки збрину или не често заснивају на субјективној процени лекара. Због тога у клиничкој пракси постоји потреба за препорукама заснованим на доказима. У том смислу, разумевање како Т2ДМ и АЦЈ утичу на квалитет кости на неколико хијерархијских нивоа посматрања би могло имати велики клинички значај у медицини и стоматологији. Данас се не прави јасна разлика између пацијената третираних различитим антидијабетицима, и савремени клинички приступ није базиран на чврстим доказима. Због тога би истраживање ефеката различитих терапијских опција код Т2ДМ (инсулин и орални антидијбетици (ОАД)) на квалитет кости такође могло бити од великог практичног значаја у оралној и максилофацијалној хирургији. Важно је и разјаснити да ли би Т2ДМ и АЛЦ требало посматрати као апсолутну или као релативну контраиндикација за оралнохируршке интервенције на кости, бар када је у питању коштани статус ових пацијената. Штавише, микроархитектурне и микроструктурне карактеристике виличних костију особа са Т2ДМ које узимају инсулин или ОАД су такође од клиничког значаја.

Општи циљ ове тезе је био да се на неколико хијерархијских нивоа посматрања истражи квалитет кости у безубој регији доњег првог молара и угла доње вилице код особа са Т2ДМ и АЦЈ у поређењу са здравом контролном групом, како би се поставила основа за унапређење процеса клиничког одлучивања у оралној хирургији, имплантологији и максилофацијалној хирургији код ових пацијената.

Специфични циљеви ове тезе су били:

(и) да се упореде микроструктура, састав и ћелијска својства кости доње вилице између особа са Т2ДМ-ом и здравих особа контролне групе;

(ии) да се испита да ли се коштане карактеристике пацијената са Т2ДМ разликују у зависности од начина лечења (орални антидијабетици (ОАД) или инсулин) и да ли зависе од посматраног региона доње вилице; и

(иии) да се упореде микроструктура, састав и ћелијска својства кости доње вилице између појединаца са АЦЈ-е и здравих особа контролне групе, као и да се испита да ли се коштане карактеристике разликују зависно од посматраног региона доње вилице.

У овој тези, узорци кости доње вилице сакупљени су од мушкараца старијих од 65 година током обдукција на Медицинском факултету Универзитета у Београду. Узорци су подељени у три групе: Т2ДМ група (n=10), АЦЈ група (n=6) и здрава контролна група одговарајућег узраста и пола (n=10).

Микроструктура кости региона ангулуса и безубог алвеоларног гребена доњег првог молара процењена је помоћу микрокомпјутеризоване томографије (Skyscan 1172 micro-CT, Bruker, Kontich, Белгија) при резолуцији од 10 µm. Одвојено су анализирани кортикални и трабекуларни одељак кости, чиме су утврђени 3Д квантитативни параметри микроархитектуре кости. Морфологија остеона (број остеона и дебљина њиховог зида) су анализирани у софтверу за обраду слика (ImageJ, Fiji). Процена коштане минерализације је извршена квантитативним имицингом повратним распршењем електрона (qBEI). Састав минералне и органске фазе кости, који указује на механичка својства коштаног матрикса, одређен је Раман спектроскопијом (inVia, WiRE 5.1., Renishaw). Карактеристике ћелија и узорака коштаног ткива су испитане применом хистоморфометрије. Исечци ткива су обојени толуидин плавим и Масон-Голднер трихромним бојењем. Индекси коштаних ћелија и ткива, који указују на својства коштаних ћелија и односе између активних и неактивних површина костију, утврђени су коришћењем система за хистоморфометрију OsteoMeasure (Osteo Metrics, Atlanta, GA, USA).

Упоредили смо параметре коштане микроструктуре, хемијског састава и ћелија између особа са Т2ДМ и здравих контрола нижу порозност лингвалног кортекса (p=0,004). У трабекуларној кости ангулуса доње вилице, већа дебљина трабекула (p=0,008), мањи број минерализованих остеоцитних лакуна (p=0,049) и мање лакуне (p=0,03) су нађени у Т2ДМ групи. Више пакета хиперминерализоване кости је нађено у букалном кортексу ангулуса доње вилице (p=0,034) у подгрупи Т2ДМ леченој инсулином у поређењу са подгрупом Т2ДМ леченој ОАД-има. У региону молара, нашли смо већу хетерогеност садржаја калцијума у трабекуларној кости особа лечених инсулином у поређењу са контролом (p=0,015) и подгрупом леченом ОАД-има (p=0,019). Такође, трабекуларна кост у региону молара је показала нижу фракталну димензију (p=0,028) и већи број остеокласта у Т2ДМ у поређењу са контролном групом (p=0,042). Лингвални кортекс у региону молара није показао промене у Т2ДМ у поређењу са контролом. Букални кортекс у региону молара је имао нижи број минерализованих лакуна остеоцита (p=0,04) и виши однос карбоната према фосфатима у Т2ДМ групи у поређењу са контролном групом (p=0,009). Унутаргрупна поређења између различитих региона (регион ангулуса у поређењу са регионом молара) у групи и подгрупама Т2ДМ су показала већу кортикалну порозност у региону молара у односу на регион ангулуса у Т2ДМ групи (p=0,007).

Слично као у делу студије о квалитету виличне кости у Т2ДМ, уочили смо значајну варијабилност у квалитету виличне кости између АЦЈ и здравих контрола. Трабекуларна кост региона молара је показала мање лакуне у АЦЈ у поређењу са контролном групом (p=0,002). Лингвални кортекс региона молара је показао мању затворену порозност у АЦЈ у поређењу са контролном групом (p=0,003). Букални кортекс региона молара је имао већу кортикалну порозност (p=0,02) и нижи однос карбоната према фосфатима у АЦЈ групи (p=0,008). Трабекуларна кост региона ангулуса је имала нижи садржај калцијума (p=0,042), мањи број пакета хиперминерализоване кости (p=0,036), мањи број остеокласта (p=0,032) и тенденцију ка нижем броју остеобласта (p=0.056) у АЦЈ групи у поређењу са контролном групом. Лингвални кортекс у региону ангулуса је показао тенденцију према већој отвореној порозности (p=0,098) и дијаметру пора у АЦЈ (p=0,002). Букални кортекс региона ангулуса је показао већу затворену порозност (p=0,007) у АЦЈ групи у поређењу са контролном групом. Унутаргрупна поређења између различитих региона (регион ангулуса у поређењу са регионом молара) у АЦЈ групи су показала микроструктурне разлике у трабекуларној геометрији, као што су виши степен анизотропије у региону ангулуса (p=0,001) и виша фрактална димензија у региону молара (p=0,033).

Добијени резултати сугеришу да Т2ДМ изазива микроструктурне промене виличне кости, што се испољава једноставнијом микроструктурном геометријом трабекуларне кости региона молара и већом дебљином трабекула у региону ангулуса. И инсулином и ОАД утичу на ремоделовање трабекуларне кости. ОАД су изазвали повећану ресорпцију у региону молара неколико година након вађења зуба, док је терапија инсулином доминантно изазвала поремећаје у минерализацији. ОАД терапија је изазвала ефекат попуњавања пора у лингвалном кортексу региона ангулуса. Терапија инсулином је изазвала стварање пакета хиперминерализоване кости и слојеве коштаног ткива различитог садржаја кацијума у свим посматраним регионима доње вилице. Коштано ткиво пацијената лечених ОАД-има је имало поремећен садржај карбоната у односу на кост здравих особа. Смањен број минерализованих лакуна у Т2ДМ у поређењу са здравим особама сугерише још млађу коштану старост због бржег ремоделовања изазваног Т2ДМ-ом. Дебљина виличног кортекса остаје непромењена у Т2ДМ.

Ове промене у квалитету кости су се морале развити под утицајем локалних и системских фактора специфичних за сваки регион виличне кости. Даља истраживања су потребна да би се објаснио механизам наведених промена квалитета кости код особа са Т2ДМ. На основу садашњих информација, генерално нема контраиндикација за уградњу зубних имплантата код особа са Т2ДМ, бар када су у питању микроструктура и састав кости. Ипак, промене у саставу кости би могле утицати на дугорочну стабилност имплантата, што захтева додатна истраживања.

Показали смо да АЦЈ изазива промену микроструктуре виличне кости, што се огледа у већој затвореној порозности у кортикалној кости, као и у мањој величини лакуна у трабелукарној кости у региону молара. Трабекуларна кост региона ангулуса има мањи садржај калцијума и мању ресорптивну активност код особа са АЦЈ него код здравих особа. Хемијска структура кости је промењена у букалном кортексу региона молара, са већим садржајем карбоната у АЦЈ у поређењу са здравим особама. Овакве карактеристике коштаног ткива су се морале развити под утицајем системских и локалних фактора за сваки коштани регион вилице. Наши резултаи указују на то да је квалитет виличне кости промењен у АЦЈ у смислу микроструктуре, минерализације, састава коштаног ткива и ћелијске активности. Могуће је да коштано ткиво у АЦЈ има

промењене механичке карактеристике, али ова претпоставка захтева додатна истраживања. Орални и максилофацијални хирурзи би требало да пацијентима са АЦЈ приступе са опрезом током хируршких процедура које укључују коштано ткиво, због промењеног квалитета кости у односу на здраве особе.

Резултати овог истраживања су показали да Т2ДМ и АЦЈ мењају квалитет кости доње вилице, као и да промене изазване Т2ДМ-ом и АЦЈ-ом различито утичу на поједине коштане регионе и одељке доње вилице. Осим тога, регионалне специфичности у квалитету кости региона ангулуса и безубог региона доњег првог молара су од значаја за оралне и максилофацијалне хирурге. Ова теза индиректно пружа више могућности за уградњу зубних имплантата и постављање титанијумских шрафова код пацијената са Т2ДМ. Код пацијената са АЦЈ, хирурзи би требало да имају на уму промењене карактеристике коштаног ткива када изводе интервенције које укључују кост. Резултати ове докторске тезе чине структурну основу за разматрање током израде плана терапије у ораланој и максилофацијалној хирургији пацијената са Т2ДМ и АЦЈ.

Кључне речи: тип 2 дијабетес мелитус, алкохолна цироза јетре, вилица, кост, микроструктура, минерализација, остеони

Научна област: МЕДИЦИНА

**Ужа научна област**: Биологија скелета

УДК број:

Contents

1. Introduction

1.1 Bone hierarchical organization

Bone is a complex nanocomposite material that can be observed on several hierarchical levels. At microscale bone is composed of osteons, osteonal lamellae and trabecular packets. At nanoscale bone is composed of bone cells and bone matrix **(Figure 1)**. Osteons, cylindrical formations of bone tissue, are a basic unit of cortical bone structure. Osteons consist of several lamellae with collagen fibers oriented in opposite directions in every next lamella. One lamella consists of many collagen fibers oriented in a uniform direction. One collagen fiber consists of many collagen fibrils. Bone cells, osteocytes, are immersed in bone matrix. Bone matrix is made of organic component, mostly type I collagen, and inorganic component, mostly hydroxyapatite.
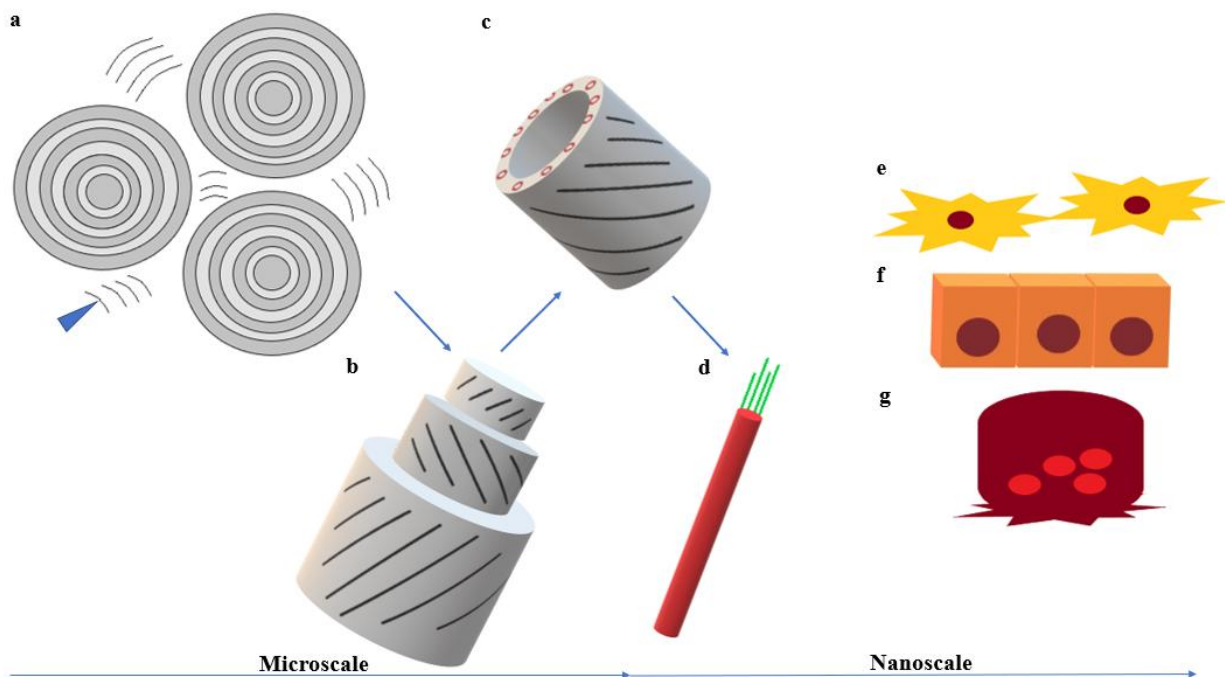
Figure 1: Hierarchical organization of bone structure. **a)** Three cross-sectioned osteons with interstitial lamellae between them (blue arrowhead). **b)** Osteon consists of several lamellae with collagen fibers oriented in opposite directions. **c)** One lamella consists of many collagen fibers oriented in a uniform direction. Red circles represent endings of collagen fibers. **d)** One collagen fiber (red tube) consists of many collagen fibrils (green lines). **a-c)** Microscale bone composition. **e-g)** Bone cells. **d-g)** Bone collagen and bone cells belong to nanoscale bone composition. **e)** Osteocytes, mutually connected via their processes inside bone canaliculi, form a network that orchestrates bone remodeling. **f)** Osteoblasts are bone-forming cells found on bone surfaces. **g)** Osteoclasts are multinucleated cells that resorb bone tissue.

1.2 Bone quality

Bone tissue is often observed as a material, since it also has mechanical function. Bone strength is the ability of bone tissue to resist force: it is determined by bone mineral density (BMD) and bone quality **(Figure 2)**. BMD is measured by dual X-ray absorptiometry (DXA). BMD is a main clinical indicator for the assessment of the quantity of mineralized

substance per bone surface or volume. Bone quality is a complex term that encompasses bone microarchitecture, bone tissue material properties and microdamage. [Saito 2014]. Bone microarchitecture refers to microstructural organization of bone tissue which is described by bone porosity, tissue volume, trabecular connectivity etc. Bone microdamage in form of microcracks is usually seen in aged bone tissue. Altered bone tissue material properties can lead to increased bone fragility [Palermo 2017].
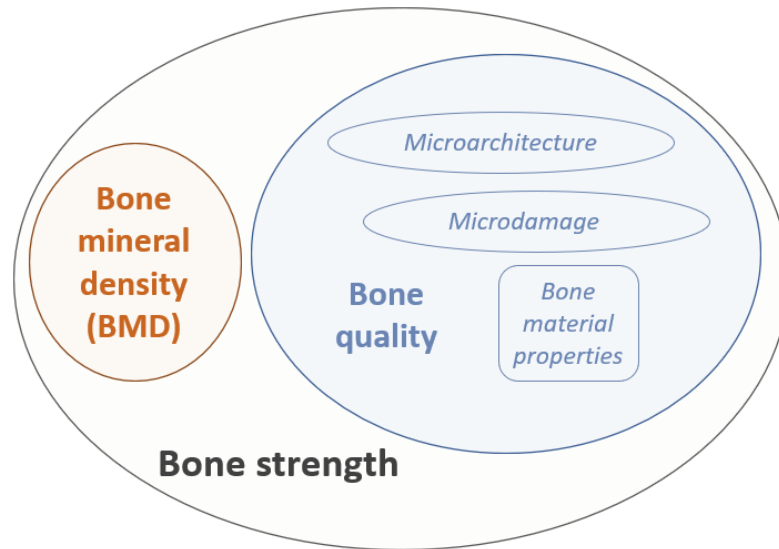
Figure 2: Bone strength is determined by bone mineral density (BMD) and bone quality. Bone quality is a complex term that encompasses: bone microarchitecture, bone tissue material properties and microdamage. Altered bone strength can lead to increased bone fragility.

1.3 Type 2 diabetes mellitus and bone quality

Diabetes mellitus (DM) is a metabolic disease characterized by absence of insulin production or resistance to insulin. DM affected 463 million adults worldwide (9% of the global population) in 2019. Around 90% of patients with DM have type 2 DM (T2DM) [WHO, Lancet 2016].

Pathophysiological mechanisms underlying bone fragility in diabetes mellitus are complex, and can include:
- ❖ Advanced glycation endproducts (AGEs) formation,
- ❖ Microvascular complications,
- ❖ Mineralization alteration,
- ❖ Microarchitectural alterations,
- ❖ Changes to bone marrow adiposity,
- ❖ Osteocytes' apoptosis,
- ❖ Lower bone formation,
- ❖ Higher bone resorption [Napoli 2017, Palermo 2017] **(Figure 3).**
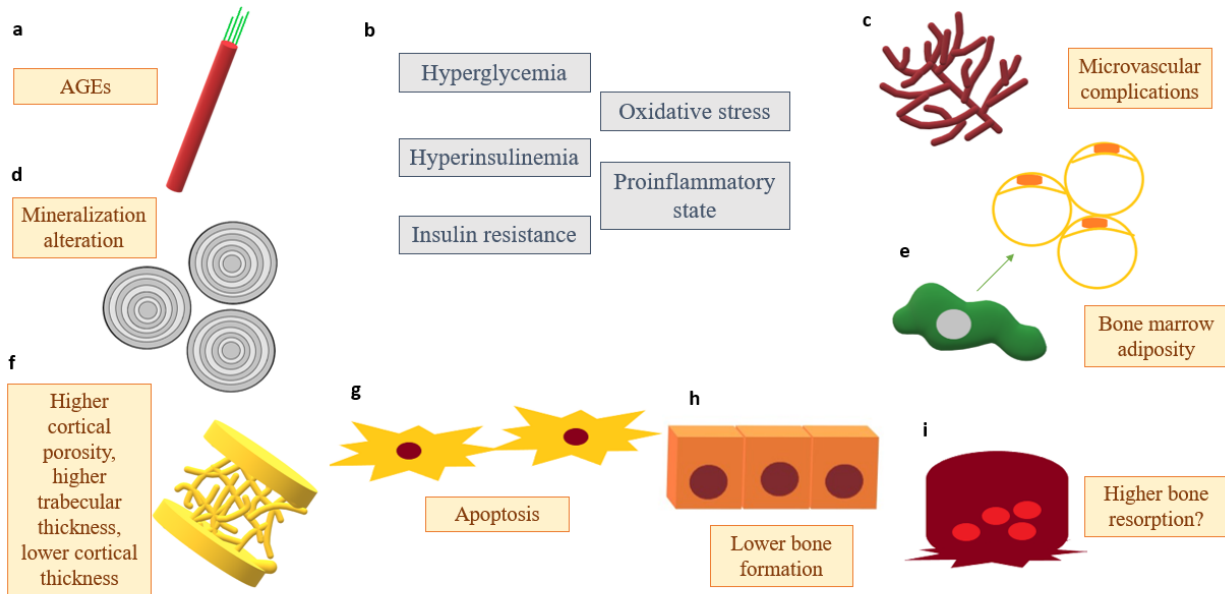
Figure 3: Pathophysiological mechanisms of bone quality alterations in T2DM. **a)** Non-enzymatic crosslinks or advanced glycation endproducts (AGEs) are formed inside collagen fibrils. Green lines inside red tube represent collagen fibrils inside one collagen fiber. **b)** General features of T2DM that cause bone quality alterations include: hyperglycemia, hyperinsulinemia, insulin resistance of cells, oxidative stress and generalized proinflammatory state. **c)** Microvascular complications, such as occlusion and deterioration of small blood vessels, occur in latter stages of T2DM. **d)** Mineralization in T2DM might be altered. **e)** Bone marrow stem cell (green cell) differentiates towards adipocytes (yellow cells) in T2DM, causing bone marrow adiposity. **f)** T2DM causes bone microarchitectural alterations, such as: higher cortical porosity, higher trabecular thickness and lower cortical thickness. **g)** Hyperglycemia has direct toxic effect on osteocytes, as it causes their apoptosis. **h)** Osteoblasts produce less new bone tissue in T2DM, i.e. bone formation is lower in T2DM. **i)** Osteoclastic bone resorption is either higher or unchanged in T2DM.

been proven to have superior mechanical features compared with bone matrix with dominant non-enzymatic collagen crosslinks (AGEs). In other words, the more AGEs bone matrix has, the more inferior bone quality is. [Woelfel 2020, Karim 2018 Bone]

Microvascular complications are another mechanism of bone quality alterations in T2DM. Small blood vessels in various organs such as kidneys, retina and heart, deteriorate in T2DM, causing low perfusion of these organs. Cirovic et al. (2022) found lower bone volume ratio (BV/TV) in femoral neck region of T2DM persons with microvascular complications compared to T2DM persons without microvascular complications, by using micro-computerized tomography (micro-CT).

Next, studies that used densitometry analysis (DXA) revealed normal or increased BMD in T2DM subjects compared to controls [Fan 2016]. Since fractures may occur in diabetic population regardless of BMD values, BMD cannot be observed as a sole indicator of bone mechanical competence in T2DM [Napoli 2016].

Importantly, most papers have reported microstructural alterations of several skeletal regions in T2DM, although some inconsistencies may be recognized. For example, Shanbhogue et al. (2016) performed high-resolution peripheral quantitative computed tomography (HR-pQCT) in T2DM and healthy patients and found lower cortical thickness and higher cortical porosity in distal radius of T2DM patients compared to healthy controls.

Burghardt et al. (2010) reported higher trabecular thickness and higher cortical porosity in T2DM patients' tibia compared to controls by using HR-pQCT. Next, Wölfel et al. (2020) found high cortical porosity in mid-diaphyseal region of individuals with T2DM by using micro-computed tomography (micro-CT). In contrast, Osima et al. (2017) reported lower cortical porosity of proximal femoral shaft in T2DM women compared to controls by using computerized tomography (CT). Finally, Karim et al. (2018) found that microarchitecture did not differ between T2DM and control group in trabecular cores from medial femoral neck. Variable results may be explained by the differences in skeletal site investigated, gender, presence of microvascular complications and other factors.

Furthermore, bone marrow adiposity has been proven to alter bone quality in T2DM patients [Andrade 2021]. Adipocytes and osteoblasts both originate from bone marrow stem cells. In diabetic conditions bone marrow stem cells differentiate towards adipocytes rather than towards osteoblasts, increasing bone marrow adiposity and reducing bone formation.

Next, osteocytes' apoptosis may be an issue in T2DM. Lacunae of apoptotic osteocytes may mineralize, which can be seen in aged bone tissue [Milovanovic 2015], usually in elderly persons. T2DM is also associated with negative effects on the mechanosensing properties of osteocytes [Picke 2019].

Pathophysiological mechanism that acts on osteoblasts and osteoclasts in T2DM includes oxidative stress and hyperglycemia. Oxidative stress found in T2DM promotes a generalized state of inflammation which causes inefficient bone tissue repair. Moreover, hyperglycemia has direct toxic effect on bone cells, osteoblasts and osteocytes. In hyperglycemic conditions osteoblasts produce less new bone tissue which might have qualitative irregularities in mineral or organic substance.

Regarding bone remodeling during DM, there is osteoblast insufficiency and enhanced bone resorption [Pietschmann 2010]. There is also evidence of low bone formation, although evidence of increased bone resorption in T2DM is not consistent [Picke 2019] [Palermo 2017, Murray 2019]. Gennari 2012 and Pacicca 2019 found elevated circulating sclerostin levels in persons with T2DM and in aged persons. Sclerostin is an inhibitor of bone formation and is produced by osteocytes. In vitro and animal studies report an unaltered rate of bone resorption [Cunha 2014, El Maghraoui 2015], whereas some studies have suggested increased osteoclastic activity in DM under certain conditions, such as in periodontal disease [Wu 2015, Pacios 2013] and osteoporosis [Yamagishi 2012]. DM affects periodontal bone tissue adjacent to teeth by increasing osteoclast number and activity and by increasing the osteoclast number and activity and by inducing osteoblasts apoptosis [Wu 2015]. Other studies have even reported inhibited osteoclast function and differentiation in a diabetic environment [Kasahara 2010, Wittrant 2008, He 2015].

Due to the conflicting evidence and generally negligent effect that has been observed in osteoclasts, it seems likely that the impaired bone remodeling in T2DM is primarily due to inhibited osteoblastic and progenitor cell activity rather than due to an alteration in bone resorption. However, further research is needed to clarify the effect of diabetes mellitus on osteoclastic function and differentiation. Bone cells' activity in an edentulous alveolar ridge after a tooth socket has been remodeled is still unknown.

1.4 Jaw bone quality in T2DM

Alveolar region has tremendous clinical significance as it hosts dental roots and is the region bearing dental implants. Since first molars are the center of occlusion and bear the strongest forces during mastication [Ferrato 2017], prosthetic replacement of these teeth is important in patients who lose them [Ferrato 2017]. Therapeutic options can include prosthetic restorations on dental implants, also in T2DM patients [Naujokat 2016].

Mandibular angle is important in maxillofacial surgery since titanium fixation screws need to be inserted there in case of a fracture of that jaw region (**Figure 4**).
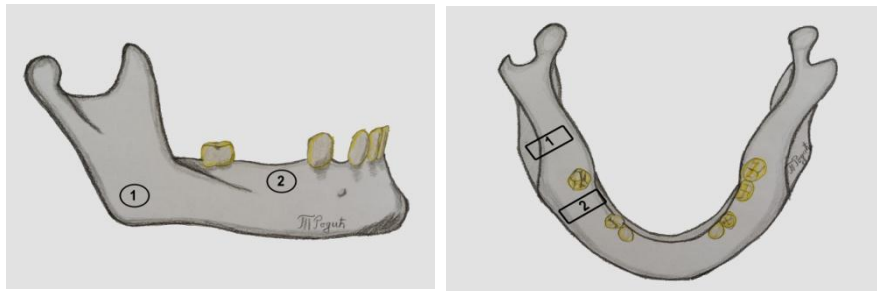
Figure 4: Circle marked with 1 represents location of titanium fixation screws which need to be inserted into the mandibular angle in case of a fracture of that jaw region. Circle marked with 2 represents alveolar bone in the region of 1ˢᵗ molar; alveolar bone hosts dental roots and is the region bearing dental implants after a tooth is lost. (Original drawings)

There is scarce evidence about the effects of T2DM on the human jaw bone. A clinical study on T2DM patients with dental implants (mean age 52 years, male and female) showed that plaque index, bleeding on probing, probing depth, marginal bone loss (using digital periapical radiographs), and advanced glycation end-products (AGEs) levels in peri-implant sulcular fluid were significantly higher in the diabetic and pre-diabetic group compared to controls [Alrabiah 2018]. Other clinical studies have offered data about the periodontal status of T2DM patients [Javid 2019, Mauri-Obradors 2018], and radiomorphometric indices measured on panoramic X-rays [Kurşun-Çakmak 2018]. A significant inverse correlation between HbA1c values and cortical and trabecular bone density in the posterior region of the mandible has been reported using cone-beam computed tomography (CBCT) and bone mineral density (BMD) measurements on alveolar bone in patients with T2DM and controls (mean age 51 years, male and female) [Nemtoi 2013]. However, no clinical research has evaluated bone quality of alveolar bone in T2DM patients on microstructural, compositional and cellular level.

Animal studies on T2DM bone tissue characteristics of alveolar bone have focused mostly on streptozotocin-induced diabetes models. Bulut et al. (2014) and Akyol et al. (2010) found that jaw bone defects in streptozotocin-induced diabetic rat model exhibited poorer healing than the non-diabetic group, as well as reduction in cellular proliferation and hampered conversion of connective tissue to bone. In a different study analyzing streptozotocin-induced diabetes in pigs, it was shown that jaws in diabetic pigs had thicker trabeculae and wider mineralization zones than jaws in control animals [von Wilmowsky 2016]. However, since streptozotocin is a substance that acts toxically on the pancreatic β-cells, streptozotocin diabetic animal models may not be an optimal model for T2DM, where insulin is still produced but resistance to its effects leads to increased blood glucose levels.

1.5 Effect of T2DM medications on jaw bone quality

The risk of hip fracture is higher in patients with T2DM. The risk is increased further in those treated with insulin, as well as in those with poor glycemic control [Palermo 2017, Napoli 2017].

Patients with T2DM who take oral antidiabetic medications (OAD) should not be observed together with T2DM patients treated with insulin. Indeed, it was noted by some authors that "there's an unfortunate tendency to lump all diabetics into one category, which

should not be the case" [Goss 2013]. Insulin has a proven anabolic effect on bone tissue, whereas OAD have various effects [Guja 2019, Thrailkill 2005]. So far, there is no evidence of the jaw bone microstructure of T2DM patients treated with OAD vs. insulin. Yet, these groups of patients are treated differently in oral surgical practice, in a manner adopted and based on the clinicians' experience. For example, a survey on the antibiotic-prescribing habits of dentists has shown that 27% of practitioners categorize poorly controlled T2DM on insulin as a high-risk condition for which they prescribe antibiotics prior to an invasive procedure, which is currently not recommended by existing guidelines [Tomczyk 2018, Power 2019].

1.6 Type 2 diabetes mellitus patients in oral surgical practice

Increasing prevalence of T2DM in the general population due to the aging society, sedentary lifestyle, and obesity results in growing numbers of T2DM patients in the dental practice. Patients with T2DM often present with a need for dental implant placement in the edentulous alveolar bone [Naujokat 2016]. Furthermore, titanium fixation screws, which need to be placed in the mandibular angle in case of a fracture located in that region are sometimes required in T2DM patients [Ward 2015, Chrcanovic 2014, Chrcanovic 2012, Rao 2007]. T2DM is considered a relative contraindication for implant placement [Kudiyirickal 2015, Singh 2020], and it is left to the surgeon to decide whether a patient with T2DM could receive an implant [Chrcanovic 2014]. This is usually decided based on the oral hygiene status and the glycemic control [Naujokat 2016, Castellanos-Cosano 2019, Marchand 2012]. Nevertheless, data from literature show that up to 14% of T2DM patients experience dental implant failure, manifested by peri-implantitis and implant loosening [Aguilar-Salvatierra 2016, Escow 2017, Oates 2014, Alsaadi 2008, Peled 2003, Parihar 2020].

Peri-implantitis is a progressive and irreversible disease of implant-surrounding hard and soft tissues and is accompanied with bone resorption, decreased osseointegration, increased pocket formation and purulence [Smeets 2014] **(Figure 5)**. T2DM-related alterations in jaw bone quality, which may have direct effects on osseointegration and implant survival in this patient population [Oates 2013], have not yet been investigated. Consequently, the question remains as to whether alterations in jaw bone quality in T2DM contribute to implant failure.
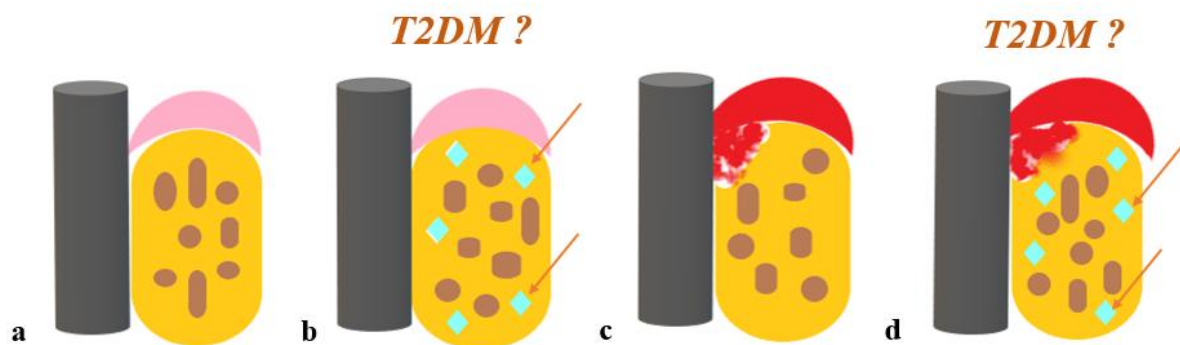
Figure 5: Possibilities for dental implant placement and peri-implantitis in healthy and diabetic patients. Grey cylinder represents dental implant. Yellow field with brown dots represents bone. Pink or red field is gingiva. **a)** Dental implant surrounded by bone and gingiva in healthy patients. **b)** Dental implant in T2DM patients might be placed in bone tissue with altered characteristics. Possible bone quality alterations are represented as light blue rhomboid shapes pointed to by arrows. **c)** Peri-implantitis in healthy patients. Bone resorption around implant is represented as damage of the yellow field. Pocket formation and inflamed gingiva are represented as red shapes. **d)** Peri-implantitis in T2DM patients. Possible jaw bone quality alterations in T2DM (blue rhomboid shapes) might favor peri-implantitis (yellow field damage and red shapes).

1.7 Alcoholic liver cirrhosis (ALC)

Liver cirrhosis is defined as diffuse histological development of regenerative nodules surrounded by fibrous bands in response to chronic liver injury, which leads to portal hypertension and end-stage liver disease [Schuppan 2008]. Liver cirrhosis may lead to severe complications, such as variceal bleeding, ascites, and hepatic encephalopathy [Schuppan 2008]. When liver cirrhosis occurs, the sinusoidal space between hepatocytes ensuring blood supply to the parenchyma decreases, sinusoidal endothelial cell fenestrations collapse, and numerous new vessels formed around the cirrhotic nodules bypass the obstructed normal route [Magdaleno 2017]. This vascular proliferation contributes to the remodeling of the liver architecture, collateral flow and portal hypertension [Magdaleno 2017].

Excess alcohol consumption is the most frequent cause of liver cirrhosis in Europe. In the United States, the prevalence of cirrhosis is 0.27%, corresponding to 633,323 adults in 2015 [Magdaleno 2017]. Thus, ALC is an important public health concern and a significant cause of morbidity and mortality worldwide. In most cases, in addition to alcohol consumption, lifestyle, gender, ethnic and socioeconomic factors may contribute or synergize in the progression of the disease.

1.8 ALC and bone quality

Factors that cause development of alcoholic bone disease in ALC include ethanol (with its direct toxic effect on bone cells), circulating proinflammatory cytokines, chronic pancreatitis, increased risk of trauma, malnutrition, vitamin D deficiency, calcium deficiency, leptin overproduction, hypogonadism, iron overload, neuropathy and myopathy (**Figure 6**). Proinflammatory cytokines, such as tumor necrosis factor α (TNFα) and interleukins 1 and 6 (IL-1, IL-6), are produced by Kupfer cells in the liver and are secreted into blood. These cytokines activate osteoclasts both directly and indirectly. IL-6 indirectly activates osteoclasts by stimulating osteoblast production of receptor activator of nuclear factor kB ligand (RANKL) [Handzlik-Orlik 2016]. Ethanol has direct toxic effects on bone cells by favoring osteocyte apoptosis, enhancing the activity of osteoclasts, and inhibiting the activity of osteoblasts through proinflammatory cytokines and RANKL. Disturbed metabolism of calcium and vitamin D results from impaired 25-hydroxilation of vitamin D precursor in the liver, intestinal malabsorption, malnutrition and decreased skin synthesis in patients with jaundice [Handzlik-Orlik 2016]. Leptin overproduction by adipocytes stimulates the synthesis of proinflammatory cytokines, TNFα and IL-1. Iron is deposited in the liver in ALC, which increases reactive oxygen species production [Madaleno 2017]. ALC is associated with several endocrinological disorders including hypogonadism, hyperparathyroidism and hypercortisolism, which disrupt mineralization, osteoblast proliferation and collagen synthesis [Lopez-Larramona 2013]. Muscle atrophy and neuropathy, which contribute to low BMD in ALC, are associated with vitamin D deficiency and low testosterone levels. Myopathy and neuropathy lead to increased risk of trauma in patients with ALC [Gonzalez-Reimers 2015]. Chronic pancreatitis is another feature of ALC that causes altered vitamin D and calcium absorption and malnutrition [Kizigul 2016].
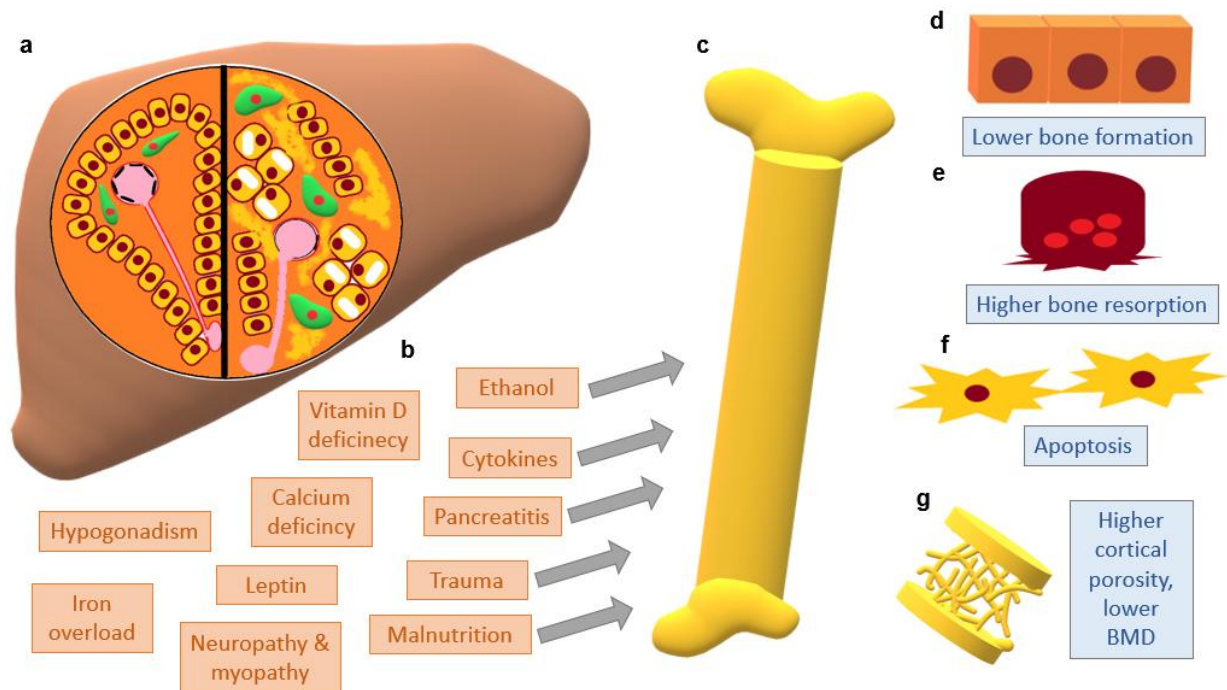
Figure 6: Pathogenesis of alcoholic bone disease in alcoholic liver cirrhosis (ALC). **a)** Schematic representation of histology of healthy liver vs. cirrhotic liver. Healthy liver tissue (left half of the circle) consists of lines of hepatocytes (yellow cells), blood vessels (pink tube) with endothelial fenestrations (thin black separated lines), and inactive myofibroblasts (thin green cells). Cirrhotic liver tissue (right half of the circle) features regenerative nodules of ballooned hepatocytes with lipid vesicles (large yellow cells with white circles), blood vessels (pink tube) without endothelial fenestrations (continuous black line), and active myofibroblasts (large green cells) that produce excessive amounts of extracellular matrix (irregular yellow fields between the cells). **b)** Factors that cause development of alcoholic bone disease in ALC include ethanol with its direct toxic effect on bone cells, circulating inflammatory cytokines, chronic pancreatitis, increased risk of trauma, malnutrition, vitamin D deficiency, calcium deficiency, leptin overproduction, hypogonadism, iron overload, neuropathy, and myopathy. **c)** Schematic representation of femoral bone. **d)-g)** Cellular and microstructural alterations in alcoholic bone disease in ALC proven in contemporary literature. **d)** Osteoblasts in ALC show lower bone formation compared to patients with healthy liver. **e)** Osteoclasts in ALC show higher bone resorption. **f)** Osteocytes in ALC might succumb to apoptosis. **g)** Bone quality and microstructure in ALC feature higher cortical porosity and lower areal BMD.

1.9 ALC effect on jaw bone quality

Notably, the evidence about the influence of ALC on jaw bone quality is scarce. The only available data encompass studies about alveolar bone status based either on panoramic X-ray images or on clinical parameters of periodontal health, such as number of present teeth, bleeding on probation, periodontal pocket depth [Rigawa 2013, Grønkjær 2016, Oetinger-Barack 2002]. For example, Rigawa et al. found an increased Russel's periodontal index, an index that estimates the degree of periodontal disease by measuring both bone loss around the teeth and gingival loss in patients with ALC [Rigawa 2013]. Grønkjær et al. found periapical radiolucencies in 46% of patients with ALC [Grønkjær 2016] and found greater vertical alveolar bone loss in patients with ALC compared to the controls.

No research so far has evaluated the alveolar bone microstructure and quality directly on bone samples originating from humans with ALC.

1.10 ALC patients in oral surgical practice

Dental patients with a history of alcohol abuse and possibly compromised liver function sometimes need surgical interventions on the jaw bone, such as in post-traumatic cases and tooth extractions [Silva-Santos 2012, Guggenheimer 2007]. Information about the jaw bone quality in patients with ALC is needed in order to make an evidence-based decision about the possibilities for oral and maxillofacial surgery in these patients. Since the first molar is the tooth that is the most often extracted [Chrcanovic 2012], the microstructure of this bony region is of interest also for ALC patients. Another important region for maxillofacial surgery is the angulus region of the mandible, since the fixation screws are placed there in case of a mandibular fracture [Sella-Tunis 2018].

Generally, it is already known that ALC leads to changes in bone structures of various skeletal regions. So far, it has not been investigated in what way and whether it affects the jaw bone. Since ALC patients often require oral surgery, it is necessary to examine bone quality in clinically important jaw bone sites. Information about the jaw bone quality in patients with ALC is needed to make an evidence-based decision about the possibilities for oral and maxillofacial surgery in these patients.

2. Research Aim and Objectives

General aim of this thesis was to explore bone quality of T2DM and ALC patients compared with healthy control group on several hierarchical levels in the edentulous region of the lower first molar and the mandibular angle region, in order to reveal information relevant for common treatments in oral and maxillofacial surgery.
Specific objectives were as follows:
1. to compare the jaw bone microstructural, compositional, and cellular properties between patients with T2DM and healthy controls,
2. to investigate the influence of OAD vs. insulin in a site-specific manner, and to
3. to compare the jaw bone microstructural, compositional, and cellular properties between individuals with ALC and healthy controls, in a site-specific manner.

3. Material and methods

3.1 Study design and sample characterization

Mandible bone cores were collected during autopsy at the Institute of Forensic Medicine, Faculty of Medicine, University of Belgrade, from male individuals aged over 65 years. The T2DM group (n=10, age: 70.6±4.5 years) was distinguished from healthy controls (n=11, age: 71.5±3.8 years) based on medical records. In the T2DM group, we differentiated between individuals with T2DM who had been treated with oral antidiabetic medications (OAD subgroup, n=5, age: 70.2±5.5 years) and those on insulin therapy (Insulin subgroup, n=5, age: 71±4.1 years). The cirrhosis group consisted of six individuals (n=6, age: 70.83±2.48 years). All individuals had their 1st lower molar extracted 3–6 years prior to post-mortem bone core collection. The inclusion criterion was the lack of the 1st lower molar, whereas the exclusion criteria encompassed malignant diseases, kidney disease, immunocompromised status, and hematological disorders. All individuals who participated in this study originated from similar socioeconomic backgrounds. They had access to medical resources, adequate nutrition, and little or no physical activity. The research protocol was approved by the Ethics Committee of the Faculty of Medicine, University of Belgrade.

The samples were collected using a dental hand piece instrument with a trephine burr attached to a micromotor. Bicortical bone cores were collected from two mandibular regions (**Figure 7**): the edentulous region of the first molar (Molar region) and the mandibular angle region (Angulus region). The mesiodistal diameter of all samples was 8 mm. The sample length (distance from buccal to lingual cortex, or the buccolingual dimension) showed variability between individuals and mandible regions, which is a feature already known in anthropological literature [Sella-Tunis, 2018]. The samples were immersed in 10% formalin solution until further use. The sample edges that were in direct contact with trephine burr were excluded from the region of interest for all bone quality assessment methods.
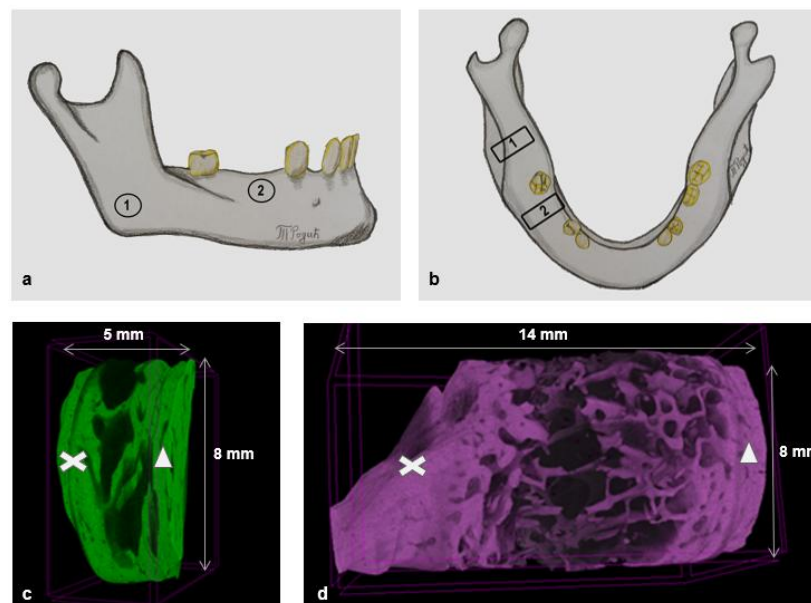
Figure 7: Bone core sites of bicortical human mandible samples and 3D sample reconstructions based on micro-CT scans (CT Vox software). (**a** and **b**) Drawings of mandible from different perspectives. Bone core site 1 is the mandibular angle (Angulus region), and bone core site 2 is the edentulous region of the 1st lower molar (Molar region). (**c**) Angulus sample. (**d**) Molar sample. (**c** and **d**) Triangle marks the lingual cortex and "x" marks the buccal cortex. The sample length slightly differed between the individuals due to normal variations in mandibular morphology.

3.2 Assessment of bone microarchitecture

Bone microstructure of the angulus and molar samples was assessed using a micro-computed tomography (micro-CT) system operated at a spatial resolution of 10 μm (Skyscan 1272, Bruker, Kontich, Belgium). The samples were kept hydrated with formalin in parafilm, mounted on a holder and scanned in native condition. Scans were acquired at 80 kV and 124 mA with an Al–Cu filter, an exposure time of 1220 ms and rotation step of 0.4°. Cortical and trabecular bone regions of interest were marked manually in the software. 3D bone morphology of the T2DM and the Control group bone cores was quantified based on 3D evaluation using CTAn software (Bruker, Kontich, Belgium). During the 3D analysis of jaw bone cores, a separate analysis was performed for the trabecular bone, buccal cortex, and lingual cortex of each jaw bone core.

For *cortical bone,* the following parameters were determined: bone volume per tissue volume, which represents volume of bone tissue within the sample volume (BV/TV, %); open porosity, which represents volume of pores that communicate with sample surface (Po(op), %); closed porosity, which represents volume of pores that do not communicate with sample surface (Po(cl), %); total porosity, which represents volume of pores that communicate with sample surface plus pores with no communication with the surface (Po(tot), %); and pore diameter (Po.Dm, mm). *Trabecular bone* microstructure was evaluated through the following parameters: bone volume per tissue volume (BV/TV, %); structure model index (SMI), which represents shape of trabeculae (the higher the number, the longer and thinner the trabeculae); degree of anisotropy (DA), which represents trabecular orientation in space (the higher the number, the more uniform trabecular orientation); fractal dimension (FD), which represents a measure of repetitiveness of geometry on several levels; trabecular thickness (Tb.Th, mm); trabecular number (Tb.N, mm); trabecular pattern factor (Tb.Pf, 1/mm), which represents trabecular connectivity; trabecular separation (Tb.Sp, mm); and connectivity density (Conn.Dn, $1/mm^3$), which represents the number of connections between trabeculae per volume (**Table 1**).

Table 1: Parameters of cortical and trabecular bone microstructure evaluated by micro-computed tomography (micro-CT)

Parameter	Unit	Definition	Bony site
BV/TV	%	Bone volume per tissue volume	Buccal cortex, Lingual cortex, Trabecular bone
Po.op	%	Open porosity	Buccal cortex, Lingual cortex
Po.cl	%	Closed porosity	Buccal cortex, Lingual cortex
Po.tot	%	Total porosity	Buccal cortex, Lingual cortex
Po.Dm	mm	Pore diameter	Buccal cortex, Lingual cortex
SMI	-	Structure model index	Trabecular bone
DA	-	Degree of anisotropy	Trabecular bone
FD	-	Fractal dimension, a measure of repetitiveness of geometry on several levels	Trabecular bone
Tb.Th	mm	Trabecular thickness	Trabecular bone
Tb.N	1/mm	Trabecular number	Trabecular bone

Tb.Pf	1/mm	Trabecular pattern factor	Trabecular bone
Tb.Sp	mm	Trabecular separation	Trabecular bone
Conn.Dn	1/mm^3	Connectivity density	Trabecular bone

3.3 Evaluation of bone matrix mineralization

After fixation in formalin, the samples underwent stepwise dehydration in increasing concentrations of ethanol, immediately before they were embedded in polymethyl methacrylate (PMMA). Sample blocks were cut perpendicular to the osteonal direction, and polished coplanar for bone mineralization analysis via quantitative backscattered electron imaging (qBEI).

Quantitative backscattered electron imaging (qBEI) is a type of scanning electron microscopy where a high-power electron beam is emitted, reflected and scattered backwards of a polished sample surface. Atoms with higher mass (high atomic number) scatter more electrons compared to atoms with lower mass (low atomic number). Stronger electron scatter (high mass atoms) produces darker image, and less intense electron scatter produces lighter image. qBEI produces images with areas that have various shades of grey. This contrast enables qBEI to be used for detection of different chemical content on the sample surface. [Jokanovic 2014. Instrumentalne metode. Chapter 14 Electron microscopy, p 696].

Prior to the qBEI imaging, the samples were carbon-coated. The specimens were examined using scanning electron microscope (LEO435 VP; LEO Electron Microscopy Ltd., Cambridge, UK) operated at 20 kV and 680 pA using a constant working distance of 20 mm (BSE Detector, Type 202; K.E. Developments Ltd., Cambridge, UK). Bone mineral density distribution was determined based on grey value images following previously described protocols [Milovanovic 2015, Roschger 2008]. Calibration of the system was performed using a carbon aluminum standard, allowing the quantification of bone mineral as calcium weight percentage. All parameters were obtained by using a custom routine in Matlab software. Determined parameters were as follows: mean calcium content (CaMean, wt%), peak calcium content (CaPeak, wt%), heterogeneity of bone mineral distribution (CaWidth (or StDev), wt%), amount of highly mineralized bone area (CaHigh, %B.Ar), and the amount of poorly mineralized bone area (CaLow, %B.Ar) (**Figure 8**, **Table 2**).
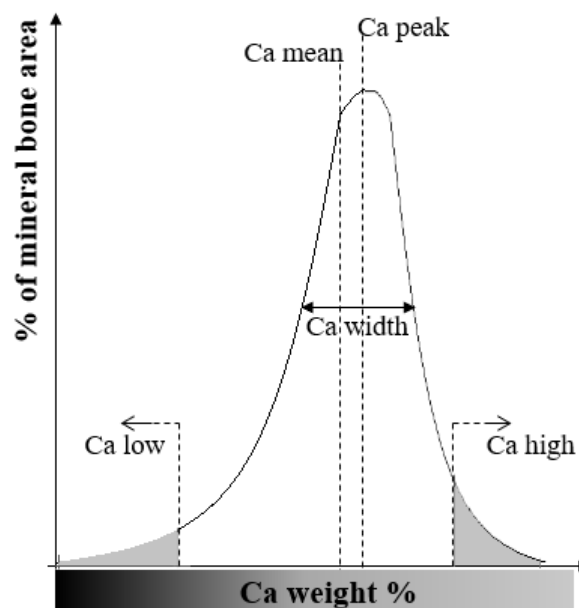
Figure 8: Quantification of bone matrix mineralization as calcium weight percentage

Table 2: Parameters of bone matrix mineralization evaluated by quantitative backscattered electron imaging (qBEI)

Parameter	Unit	Definition	Bony site
CaMean	wt%	Mean calcium content	Buccal cortex, Lingual cortex, Trabecular bone
CaPeak	wt%	Peak calcium content	Buccal cortex, Lingual cortex, Trabecular bone
CaWidth (or StDev)	wt%	Heterogeneity of bone mineral distribution	Buccal cortex, Lingual cortex, Trabecular bone
CaHigh	%B.Ar	Area of highly mineralized bone below the 5th percentile value of that group	Buccal cortex, Lingual cortex, Trabecular bone
CaLow	%B.Ar	Area of poorly mineralized bone above the 95th percentile value of that group	Buccal cortex, Lingual cortex, Trabecular bone

3.4 Morphological analysis of osteons

Osteonal morphology was analyzed in an open-source image processing software (ImageJ, Fiji) [Schneider 2012]. This analysis was performed on the qBEI images of the jaw bone cores. Osteons found in buccal and lingual cortical bone of the angulus and molar samples of all groups were analyzed. Only fully visible osteons were evaluated. Osteonal number per bone area (On.N/B.Ar, $1/mm^2$) and osteonal wall thickness (On.W.Th, μm) were accessed [Bernhardt 2013].

3.5 Osteocyte lacunar analysis

Osteocyte lacunae were analyzed in the ImageJ software and in a custom Matlab software, using the qBEI images. Parameters accessed for the *cortical* bone were as follows: mean osteonal osteocyte lacunar number (Mean On.Ot.Ln.N), mean osteonal mineralized lacunar number (Mean On.Mn.Lc.N), total osteonal mineralized lacunar number per osteonal bone area (Total Mn.On.Lc.N/On.B.Ar, $1/mm^2$), total mineralized lacunar number per bone area (Total Mn.Lc.N/B.Ar, $1/mm^2$), mean lacunar area (Mean Lc.Ar, $μm^2$), and lacunar number per bone area (Lc.N/B.Ar, $1/mm^2$). Parameters estimated for the *trabecular* bone were as follows: Lc.N/B.Ar, Mean Lc.Ar, and Total Mn.Lc.N/B.Ar (**Table 3**) [Schneider 2012, Dempster 2013, Bernhardt 2013, Milovanovic 2018, Rolvien 2018]. Mean Lc.Ar and Lc.N/B.Ar were accessed using the Matlab software, whereas other parameters were analyzed in the ImageJ software.

Table 3: Parameters of morphological analysis of osteons and osteocyte lacunae analysis evaluated by an image processing software (ImageJ, Fiji) and a custom Matlab software on the qBEI images of the jaw bone cores

Parameter	Unit	Definition	Bony site
T.Mn.Lc.N/B.Ar	$1/mm^2$	total mineralized lacunar number per bone area	Trabecular bone
Lc.N/B.Ar	$1/mm^2$	lacunar number per bone area	Buccal cortex, Lingual cortex, Trabecular bone
Mean lacunar size	μm^2	mean lacunar size	Buccal cortex, Lingual cortex, Trabecular bone
On.N/B.Ar	$1/mm^2$	osteon number per bone area	Buccal cortex, Lingual cortex
On.W.Th	μm	osteonal wall diameter	Buccal cortex, Lingual cortex
Mean On.Ot.Ln.N	#	mean osteonal osteocyte lacunar number	Buccal cortex, Lingual cortex
Mean On.Mn.Lc.N	#	mean osteonal mineralized lacunar number	Buccal cortex, Lingual cortex
Total Mn.On.Lc.N/On.B.Ar	$1/mm^2$	total mineralized osteonal lacunar number per osteonal bone area	Buccal cortex, Lingual cortex
T.Mn.Lc.N/B.Ar	$1/mm^2$	total mineralized lacunar number per bone area	Buccal cortex, Lingual cortex

3.6 Assessment of matrix composition

The composition of the mineral and collagen phases was evaluated by Raman spectroscopy using a laser wavelength of 785 nm and a spectral range from 350 cm^{-1} to 1750 cm^{-1} (inVia, Renishaw). On the buccal cortex, maps of 50 μm x 50 μm were acquired (10 μm step size, 20 s exposure time, 5 acquisitions per step, 36 points total). On trabecular bone, maps of 40 μm x 18 μm were acquired (8 μm step size, 20 s exposure time, 5 acquisitions per point, 18 points total) [Pascart 2017]. Post-processing and spectral analysis included polynomial baseline correction of background fluorescence, subtraction of PMMA signal reference spectrum acquired near the embedded bone specimens, and smoothing of the absorbance signal (WiRE 5.1, Renishaw) [Fiedler 2018].

As displayed in Figure 2, the phosphate peak (v_2PO_4) was located between 410 and 473 cm^{-1}, the proline peak between 838 and 862 cm^{-1} (pro), the phosphate peak (v_1PO_4) between 926 and 983 cm^{-1}, the carbonate peak (v_1CO_3) between 1020 and 1087 cm^{-1}, the amide III peak between 1225 and 1285 cm^{-1}, the CH$_2$ peak between 1432 and 1475 cm^{-1}, and the amide I peak between 1620 and 1700 cm^{-1} (**Figure 9, Table 4**). Bone tissue parameters were determined as ratios by dividing respective peak areas, including carbonate-to-phosphate ratio (carbonate/v_1PO_4), crystallinity (1/FWHM(v_1PO_4)), and mineral-to-matrix

ratios (v_1PO_4/amide I, v_1PO_4/CH_2, v_1PO_4/pro, v_1PO_4/amide III, and v_2PO_4/amide III) (**Table 5**) [Paschalis 2015, Paschalis 2017, Creecy 2016, Creecy 2018, Hammond 2014, Mandair 2015].
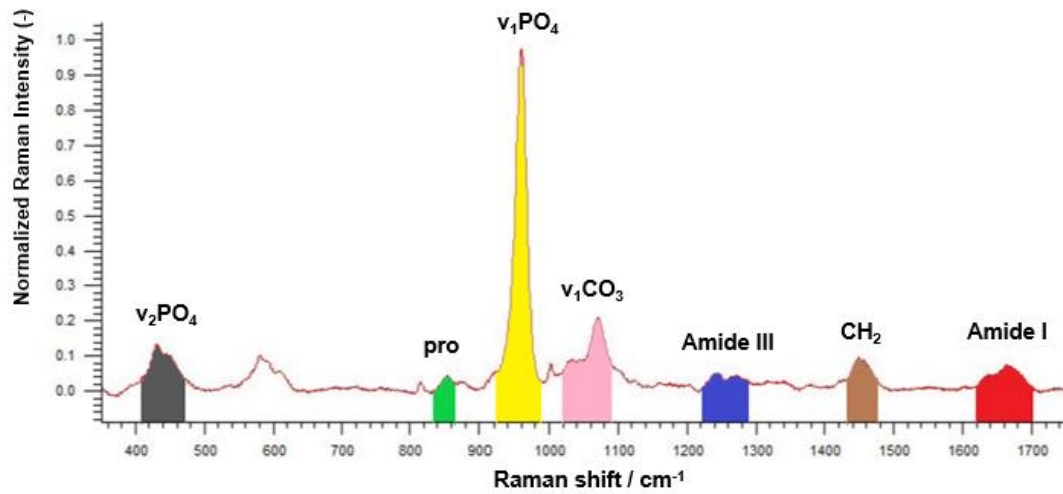
Figure 9: Acquired Raman spectra and evaluated peaks with their intervals

Table 4: Peaks of Raman spectra used for the assessment of mineral and matrix composition of bone cores were obtained by Raman spectroscopy (inVia, Renishaw)

Peak	Position	Definition	Bony site
v_2PO_4	410–473 cm^{-1}	Phosphate II peak	Trabecular bone
Pro	838–862 cm^{-}	Proline peak	Buccal cortex, Trabecular bone
v_1PO_4	926–983 cm^{-1}	Phosphate I peak	Buccal cortex, Trabecular bone
v_1CO_3	1020–1087 cm^{-1}	Carbonate peak	Buccal cortex, Trabecular bone
Amide III	1225–1285 cm^{-1}	Amide III peak	Buccal cortex, Trabecular bone
CH_2	1432–1475 cm^{-1}	CH_2 peak	Buccal cortex, Trabecular bone
Amide I	1620–1700 cm^{-1}	Amide I peak	Buccal cortex, Trabecular bone

Table 5: Ratios of mineral and matrix composition determined by Raman spectroscopy by dividing the respective peak areas

Parameter	Definition	Interpretation	Bony site
v_1CO_3/v_1PO_4	Area under the carbonate peak over the area under the phosphate I peak.	Carbonate-to-phosphate ratio	Buccal cortex, Trabecular bone
$1/FWHM(v_1PO_4)$	Reciprocal value of the full width at half-maximum of the phosphate I peak.	Crystallinity	Buccal cortex, Trabecular bone
$v_1PO_4/amide\ I$	Area under the phosphate I peak over the area under the amide I peak.	Mineral-to-matrix ratio	Buccal cortex, Trabecular bone
v_1PO_4/CH_2	Area under the phosphate I peak over the area under the CH_2 peak.	Mineral-to-matrix ratio	Buccal cortex, Trabecular bone
v_1PO_4/Pro	Area under the phosphate I peak over the area under the proline peak.	Mineral-to-matrix ratio	Buccal cortex, Trabecular bone
$v_1PO_4/amide\ III$	Area under the phosphate I peak over the area under the amide III peak.	Mineral-to-matrix ratio	Buccal cortex, Trabecular bone
$v_2PO_4/amide\ III$	Area under the phosphate II peak over the area under the amide IIII peak.	Mineral-to-matrix ratio	Trabecular bone

3.7 Histomorphometry

Cellular and tissue characteristics of bone specimens were assessed using histomorphometry. The samples embedded in PMMA were cut into 4-µm-thick sections perpendicular to the osteonal direction using a microtome and subsequently stained with toluidine blue and Masson-Goldner. Osseous cell and tissue indices were determined using the OsteoMeasure histomorphometry system (Osteo Metrics, Atlanta, GA, USA) with a 20x objective.

Cortical thickness of the buccal cortex and the lingual cortex (Ct.Th, µm) was determined. Also, the following parameters of cellular histomorphometry were determined for the trabecular bone: number of osteoblasts per bone perimeter (N.Ob/B.Pm, 1/mm), osteoid without osteoblasts area (OwoAr, mm^2), osteoid surface per bone surface (OS/BS), osteoid volume per bone volume (OV/BV), osteoid thickness (O.Th, µm), number of osteoclasts per bone perimeter (N.Oc/B.Pm, 1/mm), osteoclast surface per bone surface (Oc.S/BS, $1/mm^2$), eroded surface per bone surface (ES/BS), eroded surface without osteoclasts perimeter (ErSwo.Pm, mm), number of osteocytes per bone area (N.Ot/B.Ar, $1/mm^2$), number of empty osteocyte lacunae per bone area (N.eOt/B.Ar, $1/mm^2$), and number of newly embedded osteoblasts per bone area (N.Oot/B.Ar, $1/mm^2$) [Dempster 2013]. All evaluated structural and cellular parameters are shown in **Table 6**.

16

Table 6: Structural and cellular parameters of bone specimens assessed using the Osteo Measure histomorphometry system (Osteo Metrics, Atlanta, GA, USA)

Parameter	Unit	Definition	Bony site
N.Ob/B.Pm	1/mm	Number of osteoblasts per bone perimeter	Trabecular bone
N.Ot/B.Ar	$1/mm^2$	Number of osteocyte lacunae per bone area	Trabecular bone
OS/BS	-	Osteoid surface per bone surface	Trabecular bone
ES/BS	-	Eroded surface per bone surface	Trabecular bone
Oc.S/BS	-	Osteoclast surface per bone surface	Trabecular bone
O.Th	μm	Osteoid thickness	Trabecular bone
N.Oc/B.Pm	1/mm	Number of osteoclasts per bone perimeter	Trabecular bone
OwoB.Ar	mm^2	Osteoid without osteoblasts bone area	Trabecular bone
ErSwo.Pm	μm	Eroded surface without osteoclasts perimeter	Trabecular bone
N.eOt/B.Ar	$1/mm^2$	Number of empty osteocyte lacunae per bone area	Trabecular bone
N.Oot/B.Ar	$1/mm^2$	Number of newly embedded osteoblasts per bone area	Trabecular bone
Ct.Th	μm	Cortical thickness of the buccal cortex	Buccal cortex Lingual cortex

3.8 Statistical analysis

Statistical analysis was performed using SPSS (Version 17, Armonk, NY, USA). Normal distribution was tested using the Shapiro–Wilk test. Group comparisons were executed using either an independent-samples *t* test test for normally distributed data or non-parametric Mann–Whitney *U* test for not normally distributed data. The T2DM subgroups were compared to one another and to the control group either using one-way ANOVA with post-hoc tests under Bonferroni correction for the p value, or the Kruskal–Wallis with post-hoc Mann–Whitney test with Bonferroni correction, depending on the data distribution. Intergroup comparisons (T2DM: Angulus vs. Molar; ALC: Angulus vs. Molar) were performed using either paired samples ANOVA or Friedman's test, depending on the data distribution. *T* tests were performed two-tailed. An α level of or below 0.05 was regarded as statistically significant for all tests.

4. Results

4.1 T2DM Jaw Bone Quality. Intergroup comparisons: T2DM compared with the Control group

4.1.1 Lower cortical porosity and thicker trabeculae in T2DM angulus determined by micro-CT

Micro-CT 3D reconstructions of the mandible bone samples revealed differences between the groups regarding their microscopic morphology. Differences in macroscopic morphology were also seen among all of the angulus samples, but these were attributed to the normal variations in mandibular morphology [39]. Tables 1 and 2 show the values of microstructural parameters measured in the cortical and trabecular bone of the molar and angulus regions of the both T2DM groups and the control group. Significant differences in trabecular and cortical bone were found (**Tables 7 and 8**).

Lingual cortex of the angulus region showed higher BV/TV by 2% in the T2DM group (p=0.006) and by 2% in the T2DM OAD subgroup (p=0.005) compared with the Control group. Furthermore, open and total porosity and pore diameter were significantly lower in the same cortical region in the T2DM group compared with the Control group (open porosity by 56% (p=0.004); total porosity by 52% (p=0.006); pore diameter by 39% (p=0.029)) (**Figure 10**). Similarly, open and total porosity in the same cortical region were significantly lower in the T2DM OAD subgroup compared with the Control group (open porosity p=0.004; total porosity p=0.005). Higher values of BV/TV in the lingual cortex of the angulus compared with the control group were evident for the entire T2DM group and for the OAD subgroup, but not for the Insulin subgroup (p>0.05). Bone microstructure of both cortices in the molar region was similar between the T2DM groups and Control group (**Table 7**).

Regarding trabecular bone, Tb.Th was significantly higher in the T2DM group at the angulus region (by 28%, p=0.008) (**Figure 11**) compared with the Control group. Trabecular bone at the molar region showed lower FD in the combined T2DM group compared with the Control group (p=0.028), whereas the OAD and the Insulin subgroups separately presented no significant difference in FD compared with the Control group (p>0.05) (**Figure 12, Table 8**).
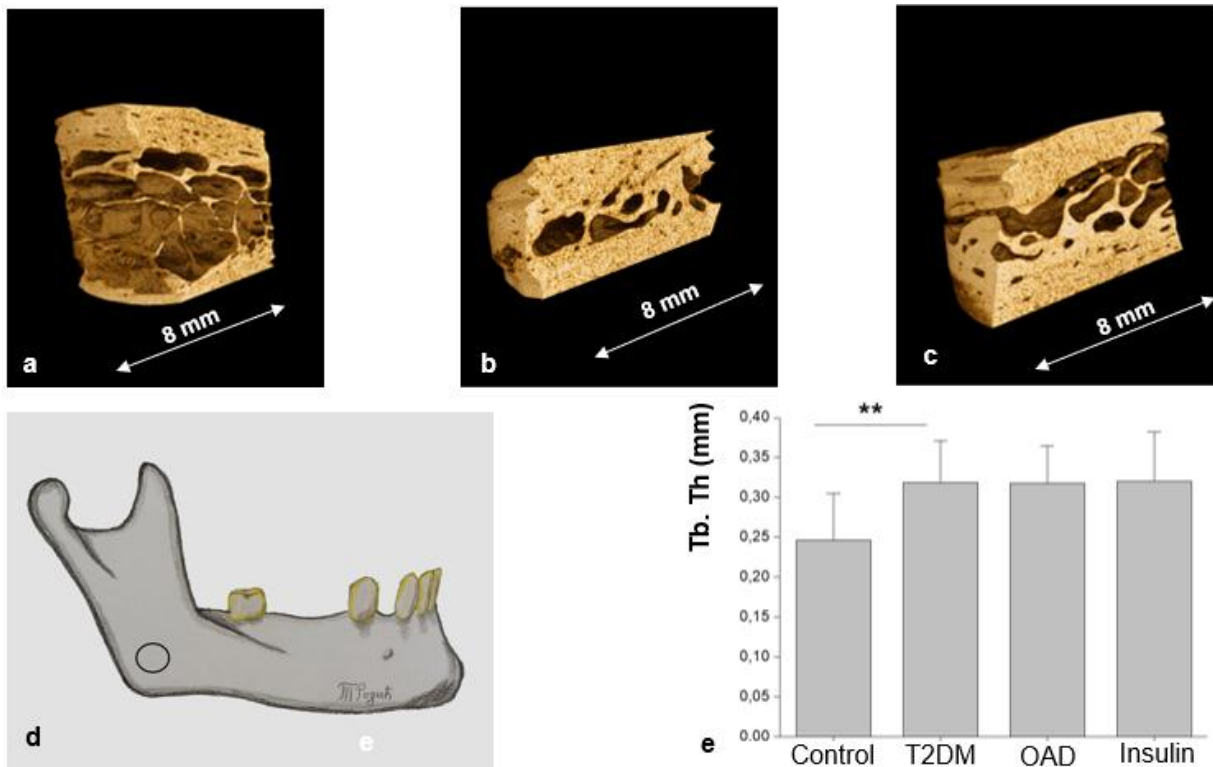
Figure 10: Trabecular thickness in the mandibular angulus (**a**) Control group with thin trabeculae. (**b**) T2DM OAD group with thicker trabeculae than the Control. (**c**) T2DM Insulin group with thicker trabeculae than the Control. (**a, b, c**) Representative reconstructions were cut virtually to enable better visualization of the trabeculae (CT Vox software). Differences in macroscopic morphology were attributed to the normal variations in mandibular morphology. (**d**) Drawing of a human mandible. Circle marks the bone core site at the mandibular angle. (**e**) Bar graph represents numerical values of trabecular thickness (Tb.Th) (Origin Pro software). Statistical significance was evident only between T2DM and Control groups ($p<0.01$(**)). T2DM OAD and T2DM Insulin subgroups separately did not reach significance compared with the Control group under strict Bonferroni correction of the p value.
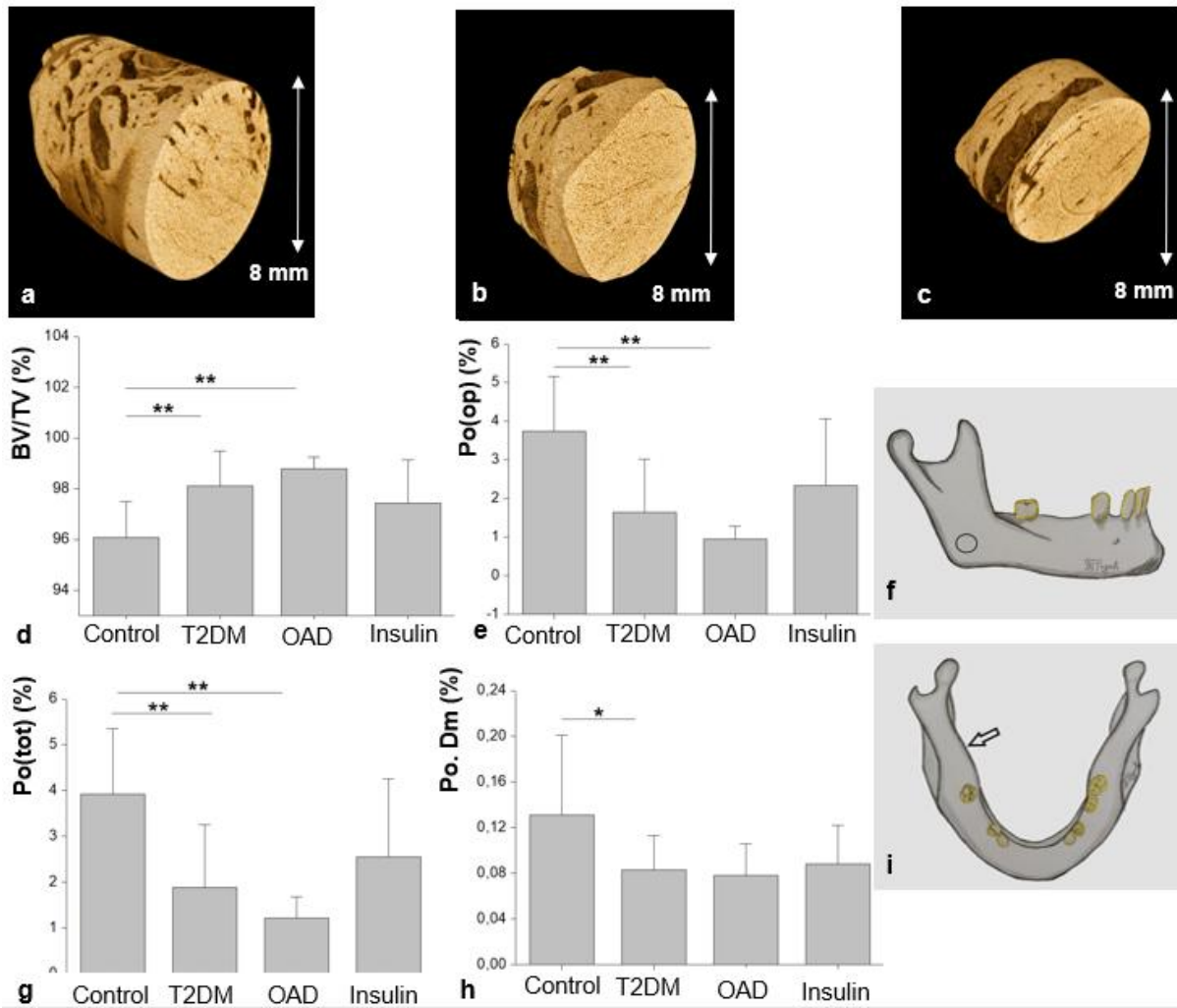
Figure 11: Porosity in the lingual cortex of the mandibular angulus (**a**) Control group. Pores are visible inside the cortex. (**b**) The T2DM OAD subgroup showed lower cortical porosity than the Control group. (**c**) The T2DM Insulin subgroup showed lower cortical porosity than the Control group. (**a-c**) Samples reconstructions were virtually cut parallel to the cortical surface to enable better visualization of cortical pores (CT Vox software). Differences in macroscopic morphology and size were attributed to the normal variations in mandibular morphology. (**d, e, g, h**) Bar graphs represent numerical values of several microarchitectural parameters (Origin Pro software). $p < 0.01$(**), $p < 0.05$(*). (**d**) Bone volume per tissue volume (BV/TV). (**e**) Open porosity (Po(op)). (**g**) Total porosity (Po(tot)). (**h**) Pore diameter (Po.Dm). (**f**) Drawing of a human mandible. Circle marks the bone core site at the mandibular angle. (**i**) Drawing of a human mandible. Arrow points to lingual cortex at the mandibular angle.
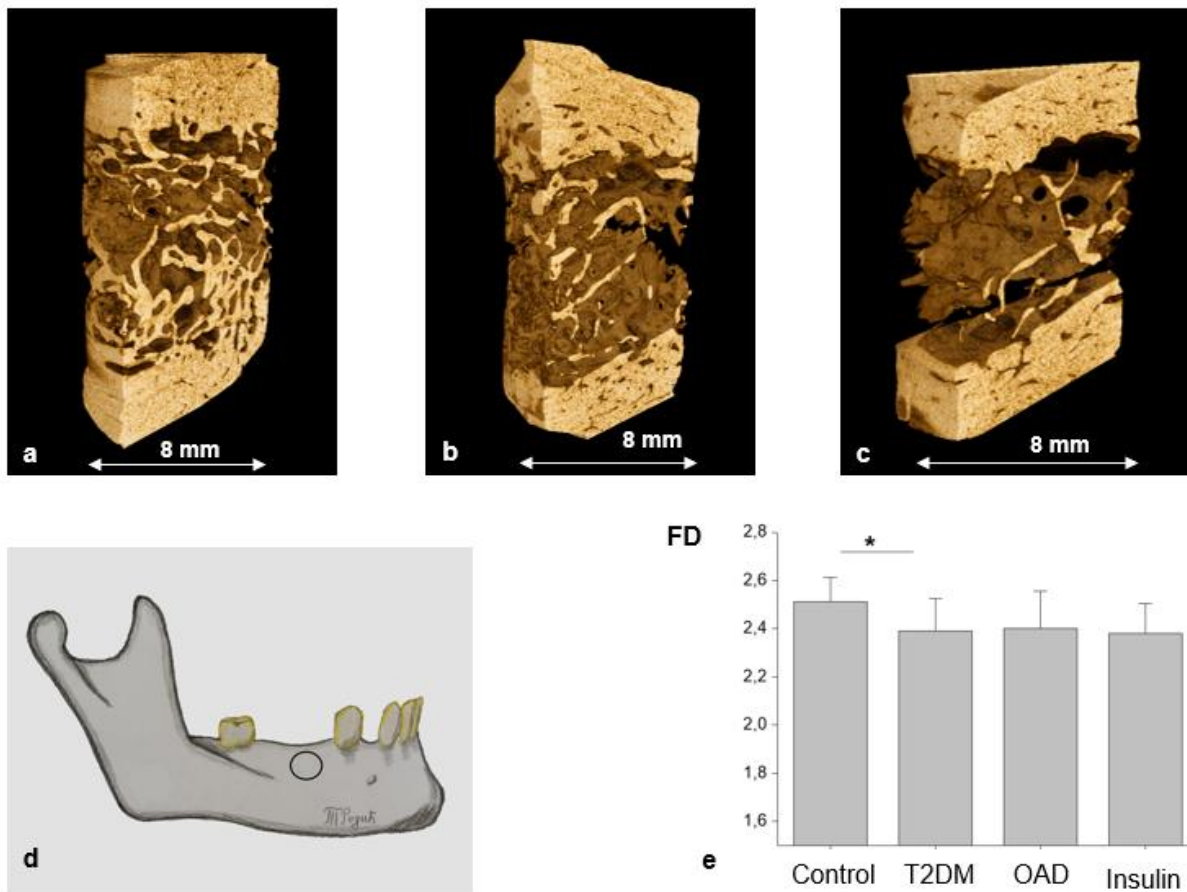
Figure 12: Geometry of trabecular bone in the molar region (**a, b, c**) Samples' reconstructions were virtually cut to enable better visualization of trabecular bone (CT Vox software). (**a**) The Control group sample shows complex trabecular bone pattern. (**b**) The T2DM OAD subgroup has simpler trabecular bone geometry compared with the Control group. (**c**) The T2DM Insulin subgroup has simpler trabecular bone geometry compared with the Control group. (**d**) Drawing of a human mandible. Circle marks the bone core site at the edentulous region of a lower first molar. (**e**) Bar graph represents numerical values of fractal dimension (FD) (Origin Pro software). Statistical significance was evident only between T2DM and Control groups ($p < 0.05$(*)). T2DM OAD and T2DM Insulin subgroups showed no significant differences compared with the Control under strict Bonferroni correction of the p value.

Table 7: Comparison of the 3D microstructural parameters in the cortical bone between the Control group and the T2DM groups.

	BV/TV [%]	Po.op [%]	Po.tot [%]	Po.Dm [mm]
Molar buccal cortex				
Control	94.07±2.81	5.71±5.58	5.92±5.49	0.11±0.07
T2DM	93.09±5.71 (N.S.)	6.72±5.75 (N.S.)	6.91±5.71 (N.S.)	0.13±0.05 (N.S.)
T2DM OAD	94.75±1.41 (N.S.)	5.05±1.42 (N.S.)	5.25±1.41 (N.S.)	0.12±0.03 (N.S.)
T2DM Insulin	91.42±8.03 (N.S.)	8.39±8.09 (N.S.)	8.57±8.02 (N.S.)	0.13±0.06 (N.S.)
Molar lingual cortex				
Control	96.07±1.42	4.45±1.85	4.7±1.85	0.1±0.03
T2DM	94.43±2.22 (N.S.)	5.27±2.21 (N.S.)	5.56±2.22 (N.S.)	0.11±0.04 (N.S.)
T2DM OAD	94.54±2.28 (N.S.)	5.2±2.31 (N.S.)	5.45±2.28 (N.S.)	0.11±0.04 (N.S.)
T2DM Insulin	94.32±2.42 (N.S.)	5.34±2.38 (N.S.)	5.66±2.42 (N.S.)	0.11±0.04 (N.S.)
Angulus buccal cortex				
Control	96.08±2.81	3.69±2.83	3.92±2.8	0.1±0.04
T2DM	90.25 ±20.6 (N.S.)	9.5±20.65 (N.S.)	9.74±20.6 (N.S.)	0.22±0.39 (N.S.)
T2DM OAD	84.34±29.45 (N.S.)	15.42±29.5 (N.S.)	15.65±29.42 (N.S.)	0.33±0.56 (N.S.)
T2DM Insulin	96.16±1.13 (N.S.)	3.59±1.17 (N.S.)	3.83±1.13 (N.S.)	0.11±0.03 (N.S.)
Angulus lingual cortex				
Control	96.07±1.42	3.74±1.42	3.92±1.42	0.13±0.07
T2DM	98.11±1.37 (**p=0.006**)	1.64±1.38 (**p=0.004**)	1.89±1.37 (**p=0.006**)	0.08±0.03 (**p=0.029**)
T2DM OAD	98.78±0.45 (**p=0.005**)	0.95±0.32 (**p=0.004**)	1.21±0.46 (**p=0.005**)	0.08±0.03 (N.S.)
T2DM Insulin	97.44±1.67 (N.S.)	2.33±1.72 (N.S.)	2.33±1.7 (N.S.)	0.09±0.03 (N.S.)

N.S.: not significant compared to the control group or between the T2DM groups;

p value: significant when <0.05; BV/TV: Bone volume per tissue volume; Po.op: Open porosity; Po.tot: Total porosity; Po.Dm: Pore diameter

Table 8: Comparison of the 3D microstructural parameters in the trabecular bone between the Control group and the T2DM groups.

	BV/TV [%]	SMI	DA	FD	Tb.Th [mm]	Tb.N [mm]	Tb.Pf [1/mm]	Tb.Sp [mm]	Conn.Dn [1/mm^3]
Molar trabecular									
Control	30.44±10.24	-0.06±1.24	1.8±0.66	2.51±0.1	0.24±0.06	1.18±0.3	-1.54±4.28	0.75±0.3	12.85±6.02
T2DM	27.44±13.98 (N.S.)	0.18±2.05 (N.S.)	1.59±0.26 (N.S.)	2.39±0.13 (**p=0.028**)	0.24±0.04 (N.S.)	0.99±0.48 (N.S.)	-0.11±4.86 (N.S.)	0.76±0.18 (N.S.)	9.27±4.88 (N.S.)
T2DM OAD	34.62±16.37 (N.S.)	-0.86±2.47 (N.S.)	1.61±0.24 (N.S.)	2.4±0.15 (N.S.)	0.27±0.03 (N.S.)	1.24±0.41 (N.S.)	-3.12±4.8 (N.S.)	0.75±0.26 (N.S.)	8.1±6.88 (N.S.)
T2DM Insulin	20.26±6.56 (N.S.)	1.23±0.77 (N.S.)	1.57±0.31 (N.S.)	2.38±0.12(N.S.)	0.22±0.03 (N.S.)	0.74±0.44 (N.S.)	2.94±2.59 (N.S.)	0.78±0.06 (N.S.)	10.45±1.69 (N.S.)
Angulus trabecular									
Control	32.21±18.51	-0.51±2.27	3.29±0.84	2.31±0.42	0.25±0.06	1.25±0.52	-1.73±4.25	0.76±0.27	2.29±13.27
T2DM	37.66±15.84 (N.S.)	0.57±2.33 (N.S.)	3.2±1.07 (N.S.)	2.32±0.12 (N.S.)	0.32±0.05 (**p=0.008**)	1.15±0.4 (N.S.)	0.73±5.74 (N.S.)	0.7±0.24 (N.S.)	14.72±13.56 (N.S.)
T2DM OAD	43.28±15.37 (N.S.)	0.53±2.6 (N.S.)	3.2±0.85 (N.S.)	2.36±0.14 (N.S.)	0.32±0.05 (N.S.)	1.33±0.38 (N.S.)	0.54±6.04 (N.S.)	0.63±0.3 (N.S.)	20.59±17.65 (N.S.)
T2DM Insulin	32.04±15.78 (N.S.)	0.61±2.34 (N.S.)	3.2±1.33 (N.S.)	2.29±0.11(N.S.)	0.32±0.06 (N.S.)	0.97±0.36 (N.S.)	0.92±6.13 (N.S.)	0.76±0.16 (N.S.)	8.86±4.05 (N.S.)

N.S.: not significant compared to the control group or between the T2DM groups
p value: significant when <0.05;

BV/TV: Bone volume per tissue volume; SMI: Structure model index; DA: Degree of anisotropy; FD: Fractal dimension; Tb.Th: Trabecular thickness; Tb.N: Trabecular number; Tb.Pf: Trabecular pattern factor; Tb.Sp: Trabecular separation; Conn.Dn: Connectivity density;

4.1.2 qBEI-determined irregularities in mineralization despite unchanged osteonal characteristics in T2DM

The results of qBEI assessment presented a higher number of highly mineralized bone packets in some jaw bone regions as well as higher heterogeneity of calcium values in other jaw bone regions (**Table 9**).

Ca High values were significantly higher in the buccal cortex of the angulus region in the T2DM Insulin subgroup compared with the T2DM OAD subgroup (by 76%, p=0.022), but were not significantly higher compared with the Control group (p>0.05) (Fig. 6). Next, trabecular bone of the molar region showed higher heterogeneity of calcium values in the T2DM Insulin subgroup compared with the T2DM OAD subgroup (by 25%, p=0.019) and the Control group (by 17%, p=0.015) (**Figure 13**, **Table 9**).

Osteonal analysis revealed no significant differences in osteonal number and wall thickness between the observed groups or subgroups (**Table 10**).

4.1.3 Fewer mineralized lacunae in the trabecular angulus region in T2DM

Osteocyte analysis revealed a 21% lower mean osteocyte lacunar size in the trabecular bone of the molar region in the T2DM group compared with the equivalent region of the Control group (p=0.03). There were fewer mineralized osteocyte lacunae per bone area in the trabecular bone of the angulus region in the T2DM group, in the OAD, and in the Insulin subgroups, as compared with the Control group (p=0.049, p=0.014, p=0.043, respectively) (**Figure 14**, **Table 11**).

Moreover, T2DM cortical bone showed some differences compared with the Control group. Specifically, total number of mineralized lacunae per bone area (Total Mn.Lc.N/B.Ar) was lower by 80% in the buccal cortex of the molar region (p=0.04) in the T2DM group compared with the Control group. Tables 4 and 5 show the values of osteocyte lacunar parameters for all of the observed groups and subgroups in the different regions.
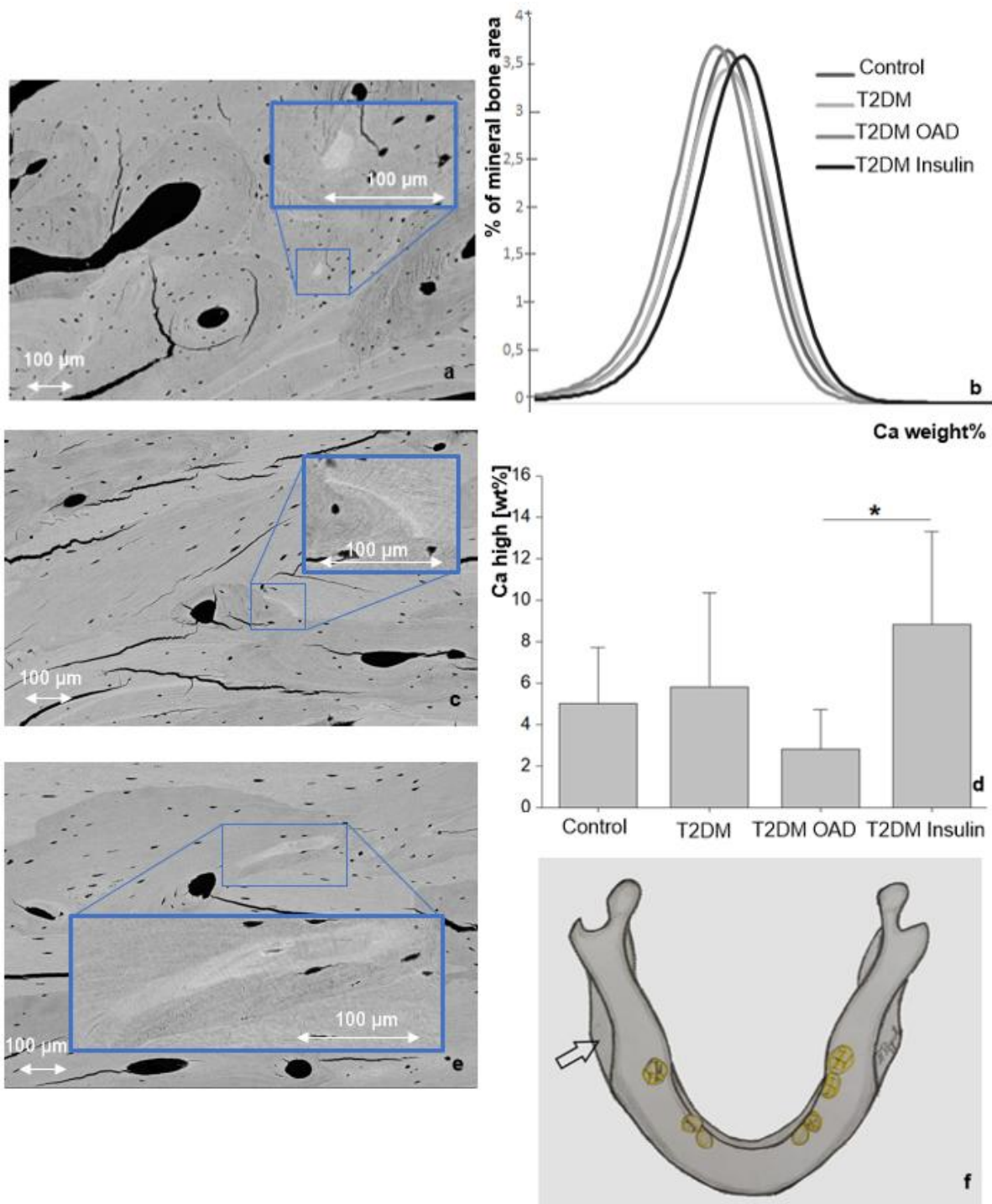
Figure 13: Packets of hypermineralized bone in buccal cortex of the angulus
(**a, c, e**) Quantitative backscattered electron microscopy images of buccal cortex in the angulus region. Areas of interest are shown in insets with higher magnification. (**a**) Packets of hypermineralized bone in the Control group. (**c**) The T2DM OAD subgroup showed less packets of hypermineralized bone compared with the Control group. (**e**) The T2DM Insulin subgroup showed more packets of hypermineralized bone compared with the Control group. (**b**) Distribution of calcium values in all of the groups. The T2DM Insulin curve is shifted towards higher calcium values compared with the curves of the other groups. The T2DM Insulin curve has the tallest tail, which represents high calcium values. The T2DM OAD curve is shifted towards lower calcium values compared with the curves of the other groups. (**d**) Bar graph represents numerical values of packets of hypermineralized bone (CaHigh parameter) in all groups (Origin Pro software). Statistical significance was evident between T2DM Insulin group and control, and between T2DM Insulin and T2DM OAD ($p<0.05$(*)). (**f**) Drawing of a human mandible. Arrow marks buccal cortex of the angulus region.
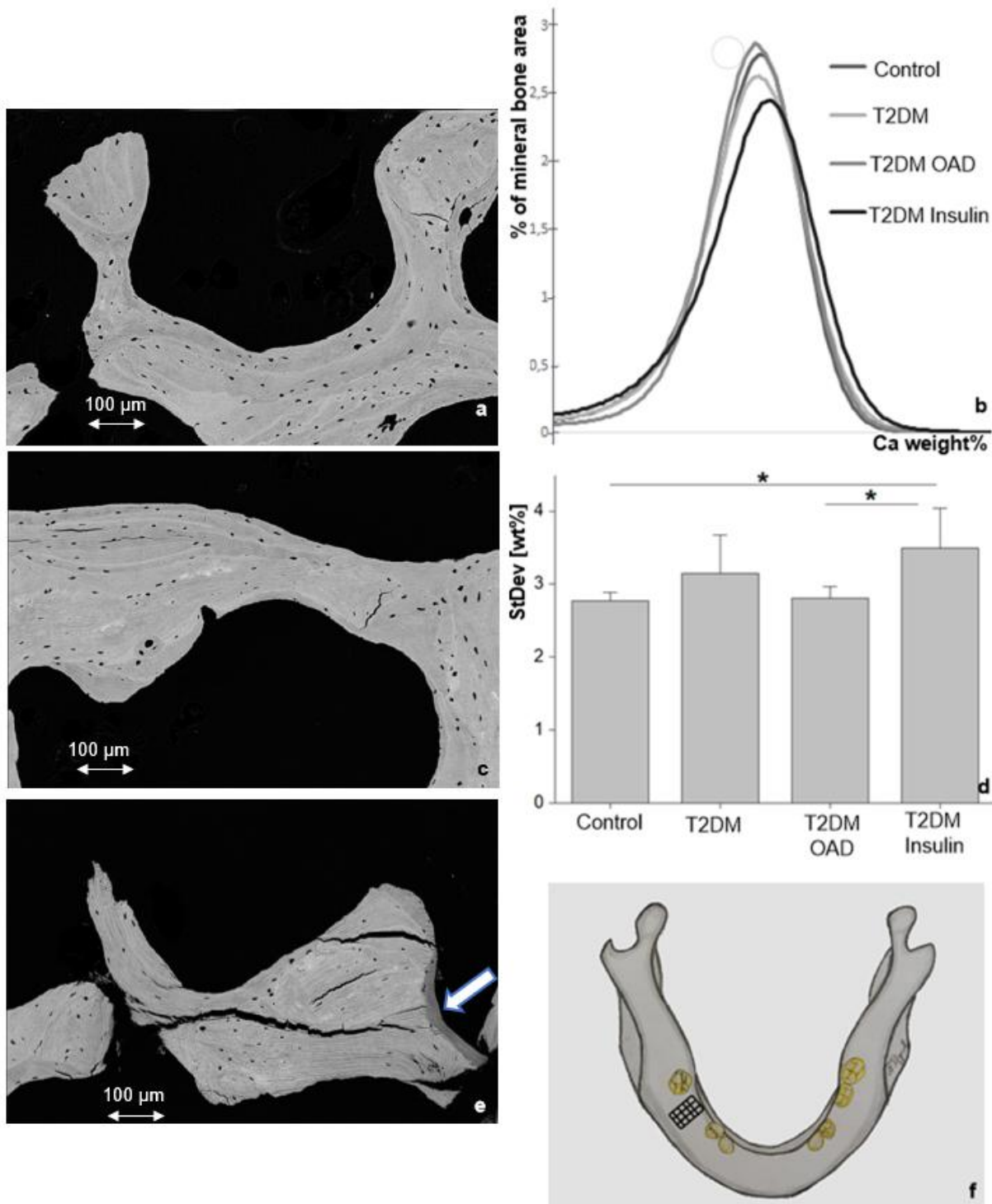
Figure 14: Higher mineralization heterogeneity of the trabecular bone in the molar region of T2DM Insulin group compared with the Control group

(**a, c, e**) Quantitative backscattered electron microscopy images of trabecular bone. (**a**) The Control group has low variability of calcium content in bone matrix, as reflected in similar shades of grey appearing on the image. (**c**) The T2DM OAD subgroup has low variability of calcium content in bone matrix, as reflected in similar shades of grey appearing on the image. (**e**) The T2DM Insulin subgroup has higher variability of calcium content in bone matrix compared with the other groups. Area of low calcium content (arrow) is darker than those with high calcium content. (**b**) Distribution of calcium values in all of the groups. The T2DM Insulin curve is wider than the curves of the other groups. (**d**) Bar graph represents numerical values of calcium content variability (StDev parameter) in all of the groups (Origin Pro software). Statistical significance was evident between the T2DM Insulin and the Control groups, and between the T2DM Insulin and T2DM OAD subgroups ($p<0.05$(*)). (**f**) Drawing of a human mandible. Grid marks trabecular bone of the edentulous region of lower first molar.
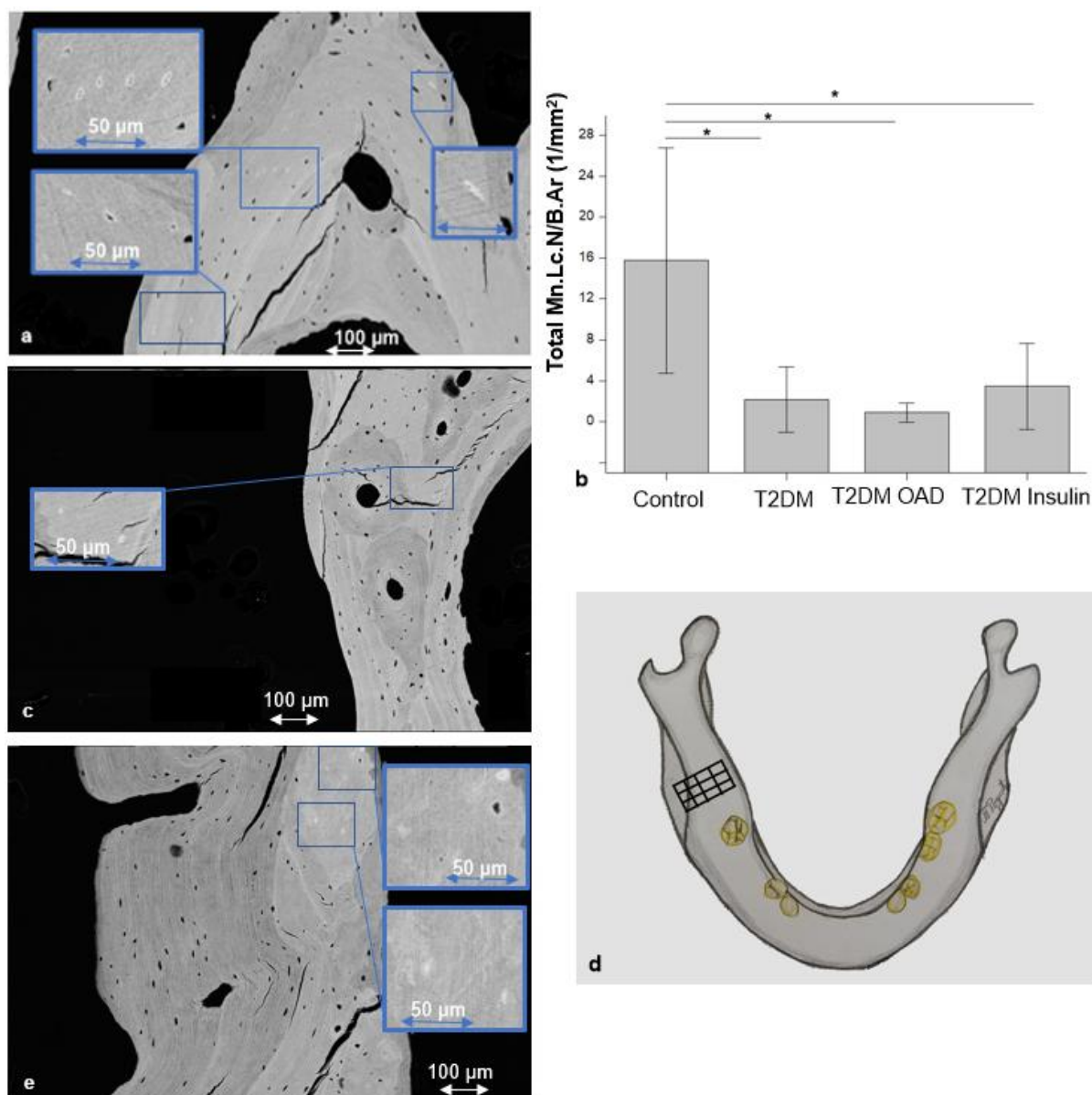
Figure 15: Mineralized osteocyte lacunae in trabecular bone of the angulus region
(**a, c, e**) Quantitative backscattered electron microscopy images of trabecular bone. Areas of interest are shown in figure insets with larger magnification. (**a**) The Control group has numerous partially and completely mineralized osteocyte lacunae, as seen in figure insets in larger magnification. (**c**) The T2DM OAD subgroup has fewer mineralized osteocyte lacunae compared with the Control group. (**e**) The T2DM Insulin subgroup has fewer mineralized osteocyte lacunae compared with the Control group. (**b**) Bar graph represents numerical values of mineralized osteocyte lacunae per bone area (Total Mn.Ot.Lc.N/B.Ar) (Origin Pro software). Statistical significance was evident between all T2DM groups and Control group ($p < 0.05$(*)). (**d**) Drawing of a human mandible. Grid marks the trabecular bone of the angulus region.

Table 9: Values of the qBEI parameters in the Control and the T2DM groups.

	CaMean [wt %]	CaPeak [wt %]	StDev [wt%]	CaLow [wt %]	CaHigh [wt %]
Molar buccal cortex					
Control	26.55±0.62	27.2±0.63	2.49±0.26	5.92±2.33	6.28±3.88
T2DM	26.07±0.92 (N.S.)	26.68±0.8 (N.S.)	2.64±0.3 (N.S.)	9.21±7 (N.S.)	5.08±3.89 (N.S.)
T2DM OAD	25.84±1.24 (N.S.)	26.44±0.93 (N.S.)	2.6±0.38 (N.S.)	10.87±10.04 (N.S.)	7.65±4.28 (N.S.)
T2DM Insulin	26.29±0.5 (N.S.)	26.91±0.67 (N.S.)	2.68±0.23 (N.S.)	7.55±1.64 (N.S.)	6.73±4.88 (N.S.)
Molar lingual cortex					
Control	25.92±0.39	26.59±0.24	2.78±0.35	5.34±2.42	4.96±1.54
T2DM	26.29±0.66 (N.S.)	26.84±0.64 (N.S.)	2.67±0.24 (N.S.)	4.03±1.44 (N.S.)	7.85±4.18 (N.S.)
T2DM OAD	26.49±0.6 (N.S.)	27.04±0.59 (N.S.)	2.51+0.13 (N.S.)	3.1±10.76 (N.S.)	3.43±1.86 (N.S.)
T2DM Insulin	26.09±0.72 (N.S.)	26.64±0.68 (N.S.)	2.83±0.23 (N.S.)	4.97±1.39 (N.S.)	7.5±4.58 (N.S.)
Angulus buccal cortex					
Control	26.59±0.5	27.17±0.35	2.58±0.6	4.82±3.35	5.01±2.7
T2DM	26.73±0.81 (N.S.)	27.17±0.72 (N.S.)	2.39±0.22 (N.S.)	4±2.83 (N.S.)	5.83±4.54 (N.S.)
T2DM OAD	26.24±0.69 (N.S.)	26.72±0.58 (N.S.)	2.36±0.29 (N.S.)	5.03±3.79 (N.S.)	2.81±1.93 (N.S.)
T2DM Insulin	27.23±0.62 (N.S.)	27.61±0.58 (N.S.)	2.41±0.14 (N.S.)	2.97±1.01 (N.S.)	8.85±4.46 (Insulin vs. OAD: **p=0.035**)
Angulus lingual cortex					
Control	26.37±0.49	26.94±0.46	2.35±0.14	5.04±2.09	5.63±3.28
T2DM	26.52±0.56 (N.S.)	27.03±0.43 (N.S.)	2.51±0.36 (N.S.)	5.18±2.87 (N.S.)	7.55±3.75 (N.S.)
T2DM OAD	26.24±0.58 (N.S.)	26.8±0.43 (N.S.)	2.54±0.43 (N.S.)	6.2±3.42 (N.S.)	5.51±3.26 (N.S.)
T2DM Insulin	26.8±0.41 (N.S.)	27.26±0.31 (N.S.)	2.48±0.32 (N.S.)	4.17±2.06 (N.S.)	9.56±3.29 (N.S.)
Molar trabecular					
Control	25.58±0.75	26.48±0.48	2.98±0.53	7.02±4.71	5.31±3.02
T2DM	25.56±0.93 (N.S.)	26.38±0.7 (N.S.)	3.15±0.52 (N.S.)	8.27±5.54 (N.S.)	7.69±3.91 (N.S.)
T2DM OAD	25.62±0.92 (N.S.)	26.2±0.83 (N.S.)	2.8±0.16 (N.S.)	5.85±3.45 (N.S.)	5.75±3.43 (N.S.)
T2DM Insulin	25.5±1.04 (N.S.)	26.56±0.56 (N.S.)	3.5±0.54 (Insulin vs. OAD: **p=0.019**) (Insulin vs. Control **p=0.015**)	10.69±6.51 (N.S.)	9.63±3.63 (N.S.)
Angulus trabecular					
Control	26.76±0.9	27.26±0.98	2.52±0.18	5.82±4.36	5.88±3.45
T2DM	26.11±1.29 (N.S.)	26.92±1.22 (N.S.)	3.05±0.6 (N.S.)	12.69±9.53 (N.S.)	6.04±3.51 (N.S.)
T2DM OAD	25.57±1.23 (N.S.)	26.44±1.24 (N.S.)	3.05±0.32 (N.S.)	15.82±9.95 (N.S.)	3.7±3.31 (N.S.)
T2DM Insulin	26.64±1.22 (N.S.)	27.39±1.11 (N.S.)	3.05±0.84 (N.S.)	9.56±9.0 (N.S.)	8.38±1.73 (N.S.)

N.S.: not significant compared to the Control group or between the T2DM groups; P value: significant when <0.05; CaMean: Mean calcium content; CaPeak; Peak calcium content; CaWidth: Heterogeneity of bone mineral distribution: CaHigh: Area of highly mineralized bone below the 5th percentile value of that group; CaLow: Area of poorly mineralized bone above the 95th percentile value of that group;

Table 10: Values of the osteonal morphology parameters of the trabecular bone in the molar region in the Control group and T2DM groups.

Molar trabecular	Lc.N/B.Ar (1/mm^2)	Mean Lc. size (µm^2)	Total Mn.Lc.N/B.Ar (1/mm^2)
Control	452.21± 61.54	17.19± 2.15	3.93 ± 5.47
T2DM	725.04± 377.81 (N.S.)	14.68± 3.21 (N.S.)	2.08 ± 4.68 (N.S.)
T2DM OAD	654.55 ± 237.73 (N.S.)	15.81 ± 3.29 (N.S.)	4.11 ± 6.25 (N.S.)
T2DM Insulin	795.53 ± 502.23 (N.S.)	13.56 ± 3.03 (N.S.)	0.05 ± 0.02 (N.S.)
Angulus trabecular			
Control	362.04± 117.91	16.97± 3.33	15.8 ± 11
T2DM	583.55± 248.46 (N.S.)	13.46± 2.23 (**p=0.03**)	2.16 ± 3.17 (**p=0.049**)
T2DM OAD	687.09 ± 317.41 (N.S.)	12.5 ± 1.67 (N.S.)	0.88 ± 0.92 (**p=0.014**)
T2DM Insulin	480 ± 106.53 (N.S.)	14.42 ± 2.47 (N.S.)	3.44 ± 4.2 (**p=0.043**)

N.S.: not significant compared to the Control group or between the T2DM groups; p value: significant when <0.05; T.Mn.Lc.N/B.Ar: total mineralized lacunar number per bone area; Lc.N/B.Ar: lacunar number per bone area; Mean Lc. size: mean lacunar size

Table 11: Values of the osteonal morphology and osteocyte lacunar parameters of the cortical bone in the Control and T2DM groups.

	On.N/B.Ar (1/mm^2)	On.W.Th (µm)	Mean On.Ot.Ln.N	Lc.N/B.Ar (1/mm^2)	Mean Lc. size (µm^2)	Mean On.Mn.Lc.N	Total Mn.On.Lc.N/ On.B.Ar (1/mm^2)	Total Mn.Lc.N/B.Ar (1/mm^2)
Molar buccal cortex								
Control	3.85 ± 2.48	14.59 ± 32.46	11±5	533.13 ± 66.76	15.31± 1.58	0.09 ± 0.12	1.72 ± 3.01	5.79 ± 5.69
T2DM	1.47 ± 2.04 (N.S.)	46.1 ± 36.19 (N.S.)	12.7±4.7 (N.S.)	557.5 ± 145.69 (N.S.)	15.75± 2.49 (N.S.)	0.11 ± 0.13 (N.S.)	8.32 ± 1.58 (N.S.)	1.12 ± 2.35 (**p=0.04**)
T2DM OAD	2.21 ± 2.31 (N.S.)	36.88 ± 37.1 (N.S.)	13.59 ± 4.21 (N.S.)	616.64 ± 161.66 (N.S.)	15.29 ± 2.9 (N.S.)	0.05 ± 0.04 (N.S.)	7.96 ± 1.37 (N.S.)	0.71 ± 0.71 (N.S.)
T2DM Insulin	0.73 ± 1.63(N.S.)	55.31 ± 36.86 (N.S.)	11.82 ± 5.47 (N.S.)	498.36 ± 113.49 (N.S.)	16.22 ± 2.23 (N.S.)	0.17 ± 0.16 (N.S.)	8.68 ± 1.93 (N.S.)	1.53 ± 3.4 (N.S.)
Molar lingual cortex								
Control	1.31 ±1.79	41.18 ± 39.18	15±6	627.12 ± 164.68	15.04± 3.15	0.11±0.08	5.96 ± 1.32	1.51 ± 2.13
T2DM	1.33 ±2.26 (N.S.)	54.02 ± 37.75 (N.S.)	13±3 (N.S.)	581.81 ± 121.79 (N.S.)	14.79 ± 1.99 (N.S.)	0.15±0.12 (N.S.)	0.51 ± 0.12 (N.S.)	0.64 ± 0.15 (N.S.)
T2DM OAD	2.65 ± 2.66 (N.S.)	40.04 ± 36.2 (N.S.)	14.07 ± 4.41 (N.S.)	508.61 ± 93.18 (N.S.)	16.09 ± 1.82 (N.S.)	0.11 ± 0.09 (N.S.)	1.07 ± 1.74 (N.S.)	1.24 ± 2.14 (N.S.)
T2DM Insulin	0.01 ± 0.01 (N.S.)	68.01 ± 37.51 (N.S.)	11.39 ± 1.09 (N.S.)	655 ± 106.28 (N.S.)	13.49 ± 1.16 (N.S.)	0.19 ± 0.14 (N.S.)	0.14 ± 0.15 (N.S.)	0.04 ± 0.05 (N.S.)
Angulus buccal cortex								
Control	1.78 ± 1.44	16.06 ± 35.76	9.28±3.01	662.93 ± 503.44	14.29± 4.12	0.29±0.54	2.58 ± 3.57	11.9 ± 13.9
T2DM	0.65 ± 0.72 (N.S.)	35.16 ± 34.72 (N.S.)	15.32±10.27 (N.S.)	420.81 ± 144.09 (N.S.)	14.88± 2.46 (N.S.)	0.26±0.19 (N.S.)	3.03 ± 5.03 (N.S.)	0.003 ± 0.004 (N.S.)
T2DM OAD	0.74±0.74 (N.S.)	30.35 ± 31.49 (N.S.)	16.65 ± 7.39 (N.S.)	388.73 ± 160.48 (N.S.)	15.95 ± 2.8 (N.S.)	0.24 ± 0.26 (N.S.)	2.22 ± 2.23 (N.S.)	3.69 ± 4.98 (N.S.)
T2DM Insulin	0.56 ± 0.77 (N.S.)	39.98 ± 40.78 (N.S.)	13.99 ± 13.35 (N.S.)	452.8 ± 135.6 (N.S.)	13.82 ± 1.73 (N.S.)	0.28 ± 0.11 (N.S.)	3.84 ± 7.1 (N.S.)	2.71 ± 3.76 (N.S.)

Angulus lingual cortex								
Control	2 ± 1.36	11.07 ± 24.55	13.48±5.03	361.88 ± 111.96	16.27±1.5	0.04±0.05	0.54 ± 0.78	4.56 ± 3.9E
T2DM	1.16 ± 1.13 (N.S.)	23.16± 39.8 (N.S.)	14.45±5.26 (N.S.)	559.69 ± 346.79 (N.S.)	14.17± 3 (N.S.)	0.35±0.47 (N.S.)	2.3 ± 3.3 (N.S.)	3.13 ± 3.76(N.S.)
T2DM OAD	1.16 ± 1.16 (N.S.)	30.21 ± 30.29 (N.S.)	13.23 ± 3.61 (N.S.)	565.79 ± 317.11 (N.S.)	14.18 ± 3.55 (N.S.)	0.17 ± 0.12 (N.S.)	1.39 ± 1.48 (N.S.)	1.93 ± 1.97 (N.S.)
T2DM Insulin	1.15 ± 1.24 (N.S.)	88.47 ± 64 (N.S.)	15.66 ± 6.74 (N.S.)	553.58 ± 412.24 (N.S.)	14.17 ± 2.77 (N.S.)	0.53 ± 0.63 (N.S.)	3.2 ± 4.5 (N.S.)	4.33 ± 4.94 (N.S.)

N.S.: not significant compared to the Control group or between the T2DM groups

p value: significant when <0.05; On.N/B.Ar: osteon number per bone area; On.W.Th: osteonal wall diameter; Mean On.Ot.Ln.N: mean osteonal osteocyte lacunar number; Mean On.Mn.Lc.N: mean osteonal mineralized lacunar number; Total Mn.On.Lc.N/On.B.Ar: total mineralized osteonal lacunar number per osteonal bone area; T.Mn.Lc.N/B.Ar: total mineralized lacunar number per bone area

4.1.4 Higher carbonate-to-phosphate ratio at the buccal cortex of the molar region in T2DM as evidenced by Raman spectroscopy

Raman spectroscopy showed marginal differences in some of the observed parameters in some of the regions. The carbonate-to-phosphate ratio (v_1CO_3/v_1PO_4) was 3.2% higher in the buccal cortex of the molar region in the T2DM group (p=0.009) and 6% higher in the OAD subgroup compared with the Control group (p=0.01) (**Figure 16**). Also, crystallinity (1/FWHM (v_1PO_4)) showed a tendency towards higher values in the trabecular molar region of the T2DM group (p=0.054). Mineral-to-matrix ratio showed no differences between the groups or the subgroups in any of the observed regions. **Table 12** shows the values of Raman parameters for different bone regions.

4.1.5 Histomorphometry: Bone formation and osteocyte characteristics showing signs of increased resorption in the T2DM OAD subgroup

Histomorphometry of the trabecular bone, which included cellular and structural parameters, showed a few significant differences between the groups. Number of osteoclasts per bone perimeter (N.Oc/B.Pm) in the trabecular bone of the molar region was two times higher in the T2DM OAD subgroup compared with the Control group (p=0.042) and seven times higher compared with the T2DM Insulin subgroup (p=0.045). Moreover, osteoid volume per bone volume showed a tendency towards higher values in T2DM molar region (p=0.056) (**Figure 17**). Cortical bone thickness measurements showed no significant differences between any of the T2DM groups and the Control group. **Table 13** shows several histomorphometry parameters, while **Table 14** in the Appendix shows the values of cortical bone thickness.
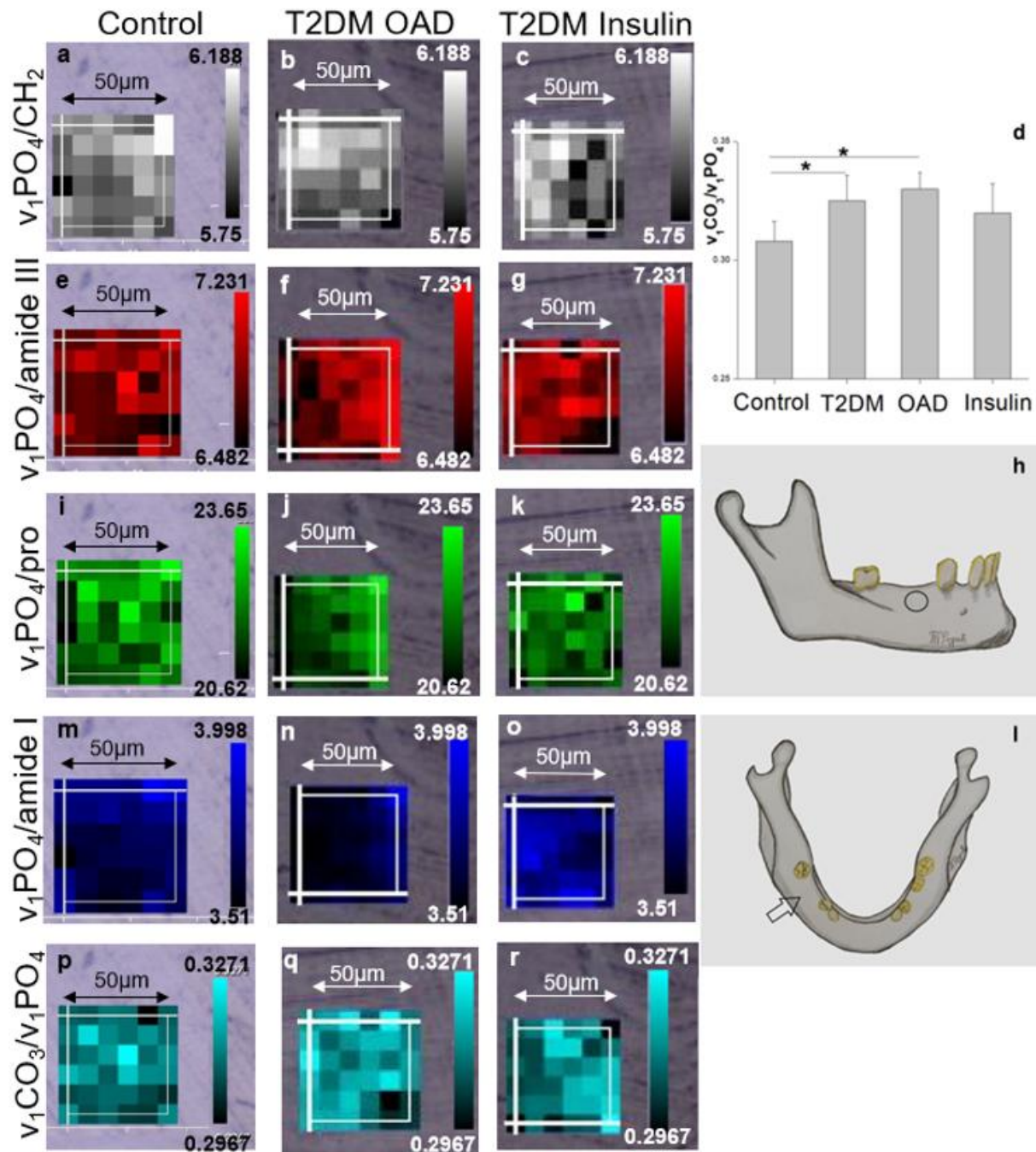
Figure 16: Bone composition of buccal cortex of the molar region. Panels show the microscopic image overlayed with pixel maps showing the spatial distribution of each parameter. (**a-c**) Phosphate-to-CH2 ratio (v1PO4/CH2 parameter). (**a**) control group, (**b**) T2DM OAD group, (**c**)T2DM Insulin group. (**d**) Bar graph represents numerical values of carbonate-to-phosphate ratio (v1CO3/v1PO4 parameter) in all groups (Origin Pro software), with statistical significance between the T2DM or T2DM OAD subgroup and the Control. (**e-g**) phosphate-to-amide III ratio (v1PO4/amide III parameter) in the buccal cortex of a molar region sample in (**e**) the Control group, (**f**) T2DM OAD group, and (**g**) T2DM Insulin group. (**h**) Drawing of a human mandible. Circle marks the trabecular bone of the molar region. (**i-k**) phosphate-to-proline ratio (v1PO4/pro parameter) in the buccal cortex of a molar region sample in (**i**) the Control group, (**j**) T2DM OAD subgroup, and (**k**) T2DM Insulin subgroup. (**l**) Drawing of a human mandible. Arrow points to the buccal cortex of the molar region. (**m-o**) phosphate-to-amide I ratio (v1PO4/amide I parameter) in the buccal cortex of a molar region sample in (**m**) the Control group, (**n**) T2DM OAD subgroup, and (**o**) T2DM Insulin subgroup. (**p-r**) carbonate-to-phosphate ratio (v1CO3/v1PO4 parameter) in the buccal cortex of a molar region sample in (**p**) the Control group, (**q**) T2DM OAD subgroup, and (**r**) T2DM Insulin subgroup. There are more surfaces in light color in the T2DM OAD subgroup (image q) compared with the Control group (image p); there are more surfaces in light color in the T2DM Insulin group (image r) compared with the Control group (image p), but not as many as in the T2DM group (image q). Raman microscope (WiRE 5.1, Renishaw).

a

b

c

200 μm

200 μm

100 μm

d

e

f

200 μm

100 μm

100 μm

g

h

i

200 μm

200 μm

100 μm

j

k

l
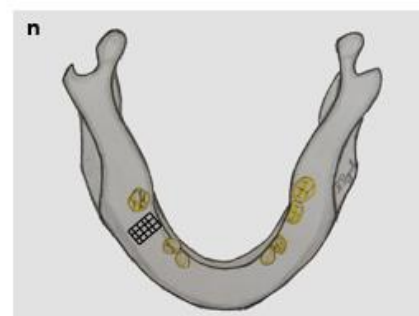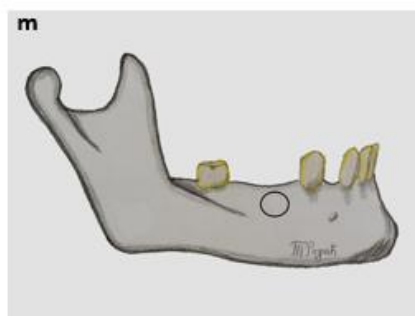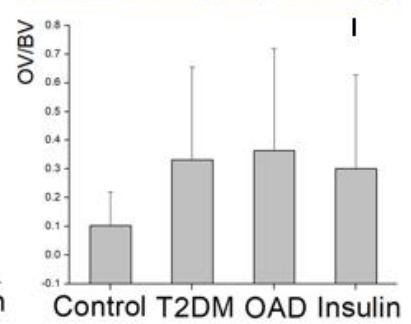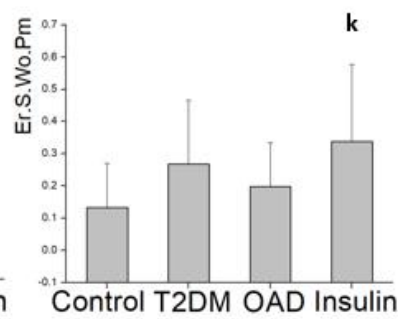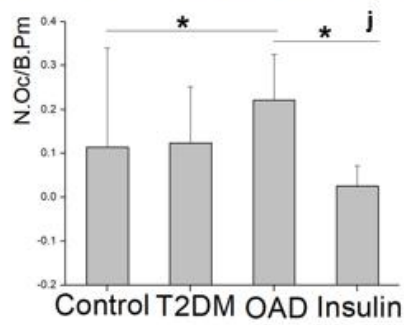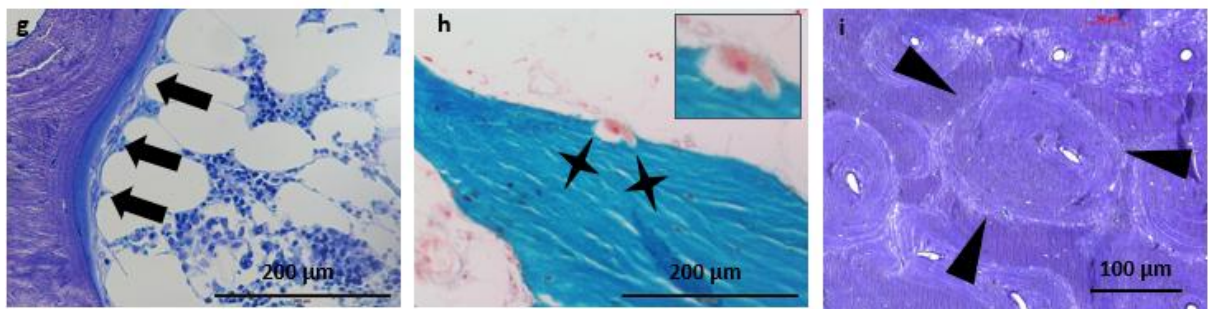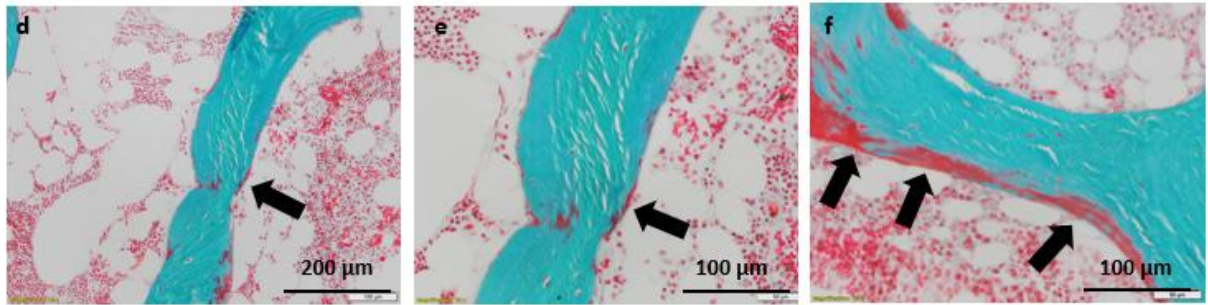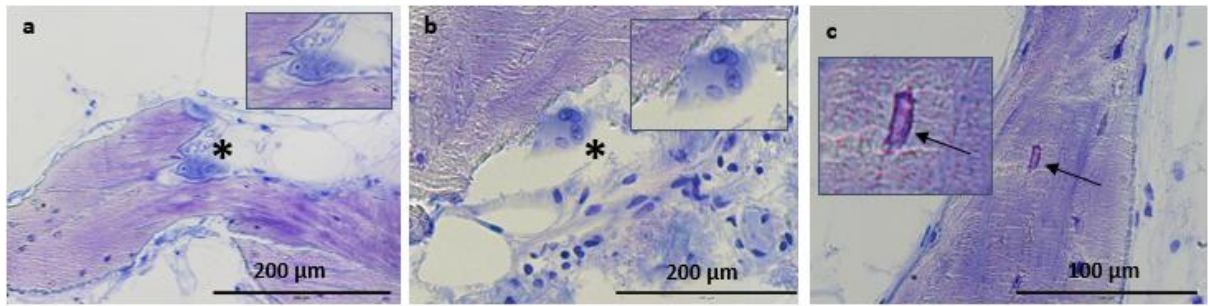
Figure 17: Bone cells and evidence of bone turnover in the molar region of different groups. (**a** and **b**) Signs of bone resorption were found in the trabecular bone of the molar region in the T2DM group. Asterisk points to an osteoclast, which is magnified in the upper right corner of the image. Toluidine staining, 40x, light microscope. (**c**) An osteocyte in its lacuna in a trabecula of the Control group molar region. The nucleus of the cell can be seen at the edge of the lacuna (arrow). Toluidine staining, 20x, light microscope. (**d**) Traces of osteoid (red areas pointed by arrow) were found on the trabecular bone surface in the molar region of the Control group. Masson Goldner staining, 20x, light microscope. (**e**) A detail of the image d. Masson Goldner staining, 40x, light microscope. (**f**) Red areas of osteoid were found in the trabecular bone of the molar region in the T2DM (arrows). Masson Goldner staining, 40x, light microscope. (**g**) Dark purple areas of osteoid were found in the trabecular bone of the molar region in the T2DM (arrows point to osteoblasts). Toluidine staining, 40x, light microscope. (**h**) A resorption cavity on the surface of the trabecular bone of the molar region in the T2DM group (stars). The cell adjacent to the cavity is not an osteoclast since only one nucleus is visible. The resorbed surface was assigned to the eroded surface without osteoclasts parameter. Masson Goldner staining, 20x, light microscope. (**I**) Triangular arrows point to an osteon in the cortical bone of the Control group molar sample. Toluidine staining, 20x, light microscope. (**j**) Bar graph represents numerical values of number of osteoclasts per bone perimeter (N.Oc/B.Pm parameter) in all of the groups (Origin Pro software). Osteoclast number was significantly higher in the T2DM OAD subgroup compared with the Control group, and in T2DM OAD subgroup compared with T2DM Insulin subgroup ($p < 0.05$(*)). (**k**) Bar graph represents numerical values of eroded surface without osteoclasts (Er.S.wo.Oc parameter) in all of the groups (Origin Pro software). Differences were close to statistical significance ($0.05 < p < 0.1$) between all T2DM groups and Control group, with more eroded surfaces in T2DM. (**l**) Bar graph represents numerical values of osteoid volume per bone volume (OV/BV parameter) in all of the groups (Origin Pro software). Differences were close to statistical significance between all T2DM groups and Control group, with more osteoid in T2DM. (**m** and **n**) Drawings of a mandible from different perspectives, with bone core site of a sample from the molar region marked by a circle and a grid.

Table 12: Values of tissue composition and maturity parameters of cortical bone and trabecular bone in the Control and T2DM groups.

	v_1PO_4/CH_2	v1PO4/amide III	v1PO4/Pro	v_1PO_4/ amide I	v_1CO_3/v_1PO_4	1/FWHM(v_1PO_4)	v_2PO_4/amide III
Molar buccal cortex							
Control	6.53±0.35	7.53±0.43	23.51±1.16	4.18±0.35	0.31±0.01	0.06±0.001	
T2DM	6.17±0.48 (N.S.)	7.14±0.53 (N.S.)	23.17±1.43 (N.S.)	4.09±0.39 (N.S.)	0.32±0.01 (p=0.009)	0.06±0.001 (N.S.)	
T2DM OAD	6.12±0.46 (N.S.)	7.16±0.55 (N.S.)	22.99±0.97 (N.S.)	4.02±0.26 (N.S.)	0.33±0.007 (p=0.01)	0.06±0.0005 (N.S.)	
T2DM Insulin	6.22±0.55(N.S.)	7.11±0.57 (N.S.)	23.36±1.89 (N.S.)	4.16±0.52 (N.S.)	0.32±0.01 (N.S.)	0.06±0.001 (N.S.)	
Angulus buccal cortex							
Control	6.13±0.48	7.19±0.66	22.51±2.4	4.05±0.19	0.32±0.02	0.06±0.001	
T2DM	5.94±0.39 (N.S.)	6.93±0.64 (N.S.)	22.11±1.57 (N.S.)	4.26±0.4 (N.S.)	0.32±0.01 (N.S.)	0.06±0.001 (N.S.)	
T2DM OAD	5.94±0.33 (N.S.)	6.75±0.31 (N.S.)	21.63±0.49 (N.S.)	4.06±0.27 (N.S.)	0.33±0.005 (N.S.)	0.062±0.001 (N.S.)	
T2DM Insulin	5.93±0.49 (N.S.)	7.1±0.87 (N.S.)	22.59±2.17 (N.S.)	4.45±0.44 (N.S.)	0.32±0.01 (N.S.)	0.06±0.002 (N.S.)	
Molar trabecular							
Control	7.17±0.67	8.98±1.12	27.47±3.94	5.87±0.34	0.38±0.03	0.06±0.0007	2.28±0.48
T2DM	6.65±0.7 (N.S.)	8.48±0.95 (N.S.)	23.75±6.39 (N.S.)	5.91±0.88 (N.S.)	0.36±0.03 (N.S.)	0.06±0.002 (N.S.)	2.15±0.37 (N.S.)
T2DM OAD	6.49±0.6 (N.S.)	8.07±0.63 (N.S.)	21.26±8.73 (N.S.)	5.55±0.63 (N.S.)	0.36±0.02 (N.S.)	0.06±0.001 (vs. T2DM Insulin p=0.084)	2.05±0.28 (N.S.)
T2DM Insulin	6.8±0.82 (N.S.)	8.9±1.09 (N.S.)	26.25±0.46 (N.S.)	6.27±1.01 (N.S.)	0.35±0.04 (N.S.)	0.06±0.002 (vs. Control p=0.054)	2.26±0.45 (N.S.)
Angulus trabecular							
Control	7.11±0.72	8.91±1.03	24.72±3.19	5.47±0.35	0.35±0.03	0.06±0.002	2.22±0.41
T2DM	6.65±0.82(N.S.)	9.25±0.92 (N.S.)	24.43±3.5 (N.S.)	6.02±1.31 (N.S.)	0.35±0.05 (N.S.)	0.06±0.001 (N.S.)	3±2.49 (N.S.)
T2DM OAD	6.9±0.82 (N.S.)	9.03±0.79 (N.S.)	22.46±0.67 (N.S.)	5.77±1.26 (N.S.)	0.37±0.03 (N.S.)	0.06±0.001 (N.S.)	2.22±0.31 (N.S.)
T2DM Insulin	6.4±0.83 (N.S.)	9.48±1.08 (N.S.)	26.4±4.18 (N.S.)	6.27±1.45 (N.S.)	0.32±0.06 (N.S.)	0.06±0.0004 (N.S.)	3.79±3.51 (N.S.)

N.S.: not significant compared to the Control group or between the T2DM groups; p value: significant when <0.05; v1CO3/v1PO4: Carbonate-to-phosphate ratio; 1/FWHM(v1PO4) crystallinity; v1PO4/amide I: area under the phosphate I peak over the area under the amide I peak (mineral-to-matrix ratio); v1PO4/CH2: area under the phosphate I peak over the area under the CH2 peak (mineral-to-matrix ratio); v1PO4/Pro: area under the phosphate I peak over the area under the proline peak (mineral-to-matrix ratio); v1PO4/amide III: area under the phosphate I peak over the area under the amide III peak (mineral-to-matrix ratio); v2PO4/amide III: area under the phosphate II peak over the area under the amide IIII peak (mineral-to-matrix ratio)

Table 13: Values of bone cellular parameters of the trabecular bone in the Control and T2DM groups.

	N.Ob/B.Pm (1/mm)	Ob.S/BS	OwoB.Ar (mm^2)	OS/BS	O.Th (µm)	OV/BV	Oc.S/BS
Molar trabecular							
Control	1.42±1.76	1.16±1.66	0.0009±0.002	2.74±3.83	2.9±3.69	0.1±0.12	0.26±0.55
T2DM	1.74±1.35 (N.S.)	2.18±1.65 (N.S.)	0.002±0.002 (N.S.)	5.22±4.7 (N.S.)	4.54±3.02 (N.S.)	0.33±0.32 (N.S.) p=0.056	0.32±0.37 (N.S.)
T2DM OAD	1.92±1.7 (N.S.)	2.53±2.05 (N.S.)	0.001±0.002 (N.S.)	6.86±6.16 (N.S.)	4.55±2.76 (N.S.)	0.36±0.35 (N.S.)	0.56±0.38 (N.S.)
T2DM Insulin	1.56±1.04 (N.S.)	1.83±1.26 (N.S.)	0.003±0.003 (N.S.)	3.58±2.27 (N.S.)	4.54±3.59 (N.S.)	0.3±0.32 (N.S.)	0.07±0.13 (N.S.)
Angulus trabecular							
Control	2.62±2.42	3.18±3.24	0.001±0.001	6.92±7.98	4.73±4.82	0.45±0.55	0.74±0.89
T2DM	2.78±2.78 (N.S.)	2.97±4.47 (N.S.)	0.003±0.007 (N.S.)	7.36±9.17 (N.S.)	2.79±2.28 (N.S.)	0.25±0.35 (N.S.)	0.39±0.49 (N.S.)
T2DM OAD	3.78±3.44 (N.S.)	5.05±5.81 (N.S.)	0.005±0.09 (N.S.)	9.53±12.15 (N.S.)	3.58±2.91 (N.S.)	0.35±0.49 (N.S.)	0.67±0.58 (N.S.)
T2DM Insulin	1.78±1.75 (N.S.)	0.89±0.66 (N.S.)	0.0009±0.0006 (N.S.)	5.19±5.24 (N.S.)	2.0±1.29 (N.S.)	0.14±0.1 (N.S.)	0.12±0.13 (N.S.)

	N.Oc/B.Pm (1/mm)	ES/BS	ErSwo.Pm (mm)	N.Ot/B.Ar (1/mm^2)	N.eOt/B.Ar (1/mm^2)	N.Oot/B.Ar (1/mm^2)
Molar trabecular						
Control	0.11±0.23	0.6±1.12	0.13±0.13	157.34±61.85	44.77±27.11	12.38±8.31
T2DM	0.12±0.13 (N.S.)	0.73±0.93 (N.S.)	0.27±0.2 (N.S.) p=0.083	169.58±40.05 (N.S.)	59.52±37.54 (N.S.)	11.47±8.07 (N.S.)
T2DM OAD	0.22±0.1 (N.S.) OAD vs. control: **p=0.042**; OAD vs. Insulin: **p=0.045**	1.34±0.98 (N.S.)	0.2±0.13 (N.S.)	200.22±26.3 (N.S.)	55.38±40.22 (N.S.)	13.62±10.93 (N.S.)
T2DM Insulin	0.03±0.04 (N.S.)	0.13±0.22 (N.S.)	0.34±0.24 (N.S.)	138.94±27.09 (N.S.)	63.65±38.87 (N.S.)	9.32±3.97 (N.S.)
Angulus trabecular						
Control	0.26±0.33	1.27±1.61	0.21±0.17	144.89±42.08	50.13±36.94	17.17±12.73
T2DM	0.2±0.28 (N.S.)	0.66±0.85 (N.S.)	0.1±0.17 (N.S.) p=0.075	135.86±58.14 (N.S.)	53.22±37.45 (N.S.)	13.48±6.47 (N.S.)
T2DM OAD	0.36±0.32 (N.S.)	1.18±0.96 (N.S.)	0.18±0.21 (N.S.)	130.85±41.24 (N.S.)	48.05±27.45 (N.S.)	14.38±7.75 (N.S.)
T2DM Insulin	0.04±0.05 (N.S.)	0.15±0.16 (N.S.)	0.02±0.03 (N.S.)	140.88±76.42 (N.S.)	58.38±48.34 (N.S.)	12.58±5.66 (N.S.)

N.S.: not significant compared to the Control group or between the T2DM groups; p value: significant when <0.05; N.Ob/B.Pm: number of osteoblasts per bone perimeter; N.Ot/B.Ar: number of osteocyte lacunae per bone area; OS/BS: osteoid surface per bone surface; ES/BS: eroded surface per bone surface; Oc.S/BS: osteoclast surface per bone surface; O.Th; osteoid thickness: N.Oc/B.Pm: number of osteoclasts per bone perimeter; OwoB.Ar: osteoid without osteoblasts bone area; ErSwo.Pm: eroded surface without osteoclasts perimeter; N.eOt/B.Ar: number of empty osteocyte lacunae per bone area; N.Oot/B.Ar: number of newly embedded osteoblasts per bone area

Table 14: Values of cortical bone thickness in the Control and T2DM groups.

	Ct. Th [μm]
Molar buccal cortex	
Control	1881.45±472.86
T2DM	1967.22±422.15 (N.S.)
T2DM OAD	1938.06±574.33 (N.S.)
T2DM Insulin	1996.39±262.67 (N.S.)
Angulus buccal cortex	
Control	1583.79±546.56
T2DM	1571.09±543.08 (N.S.)
T2DM OAD	1537.36±667.14 (N.S.)
T2DM Insulin	1604.82±464.43 (N.S.)
Molar lingual cortex	
Control	1749.57±780.58
T2DM	1700.75±464.38 (N.S.)
T2DM OAD	1914.3±523.75 (N.S.)
T2DM Insulin	1487.21±311.26 (N.S.)
Angulus lingual cortex	
Control	1387.45±526.53
T2DM	1489.61±432.15 (N.S.)
T2DM OAD	1625.13±435.2 (N.S.)
T2DM Insulin	1354.09±429.97 (N.S.)

N.S.: not significant compared to the control group or between the T2DM groups;
p value: significant when <0.05; Ct.Th: Cortical thickness

4.2 T2DM Jaw Bone Quality. Intersite comparisons (Angulus vs. Molar) in the T2DM group and T2DM subgroups

4.2.1 Higher cortical porosity in the molar region compared with the angulus region in T2DM

The results showed higher porosity of the lingual cortex and trabecular bone of the molar region compared with the same sites of the angulus region, both in the T2DM group and in the T2DM OAD subgroup. Significantly different parameters, bone sites, results, and p values are listed in **Table 15**, whereas absolute values can be found in **Tables 7 and 8**.

Table 15: Statistically significant results of microstructural analysis of T2DM group and subgroups, angulus vs. molar

T2DM group or subgroup	Parameter	Bone site	Result	p value
T2DM OAD	Po.cl	Lingual cortex	↑ in the molar region	p=0.001
T2DM OAD	Po.op	Lingual cortex	↑ in the molar region	p=0.01
T2DM OAD	Po.tot	Lingual cortex	↑ in the molar region	p=0.007
T2DM OAD	BV/TV	Lingual cortex	↑ in the angulus region	p=0.007
T2DM	Po.cl	Lingual cortex	↑ in the molar region	p=0.011
T2DM	Po.op	Lingual cortex	↑ in the molar region	p=0.011
T2DM	Po.tot	Lingual cortex	↑ in the molar region	p=0.011
T2DM	BV/TV	Lingual cortex	↑ in the angulus region	p=0.011
T2DM OAD	DA	Trabecular bone	↑ in the angulus region	p=0.009
T2DM	Tb.Th	Trabecular bone	↑ in the angulus region	p=0.008
T2DM	DA	Trabecular bone	↑ in the angulus region	p=0.002

p value: significant when <0.05; BV/TV: Bone volume per tissue volume; DA: Degree of anisotropy; Tb.Th: Trabecular thickness; Po.op: Open porosity; Po.tot: Total porosity; Po.Dm: Pore diameter

4.2.2 More mineralization variations at the molar region in the T2DM Insulin subgroup

The results of intersite comparisons in the T2DM Insulin subgroup showed more mineralization variations in the angulus region compared with the molar region. Significantly different parameters, bone sites, results, and p values are listed in **Table 16**, whereas absolute values can be found in **Table 9**.

Table 16: Statistically significant results of mineralization analysis of T2DM group and subgroups, angulus vs. molar

T2DM group or subgroup	Parameter	Bone site	Result	p value
T2DM Insulin	CaMean	Buccal cortex	↑ in the molar region	p=0.023
T2DM Insulin	StDev	Buccal cortex	↑ in the molar region	p=0.019
T2DM Insulin	CaLow	Buccal cortex	↑ in the molar region	p=0.001
T2DM Insulin	StDev	Lingual cortex	↑ in the angulus region	p=0.038

p value: significant when <0.05; CaMean: mean calcium content; StDev: heterogeneity of bone mineral distribution: CaLow: area of poorly mineralized bone above the 95th percentile value of that group

4.2.3 More mineralized lacunae at the angulus region in the T2DM Insulin subgroup

The intersite comparisons in the T2DM Insulin subgroup showed more mineralized lacunae in the buccal cortex of the angulus region compared with the buccal cortex of the molar region. Also, mean lacunar size was higher in the buccal cortex of the molar region compared with the angulus region in the T2DM Insulin subgroup. Significantly different parameters, bone sites, results, and p values are listed in **Table 17**, whereas absolute values can be found in **Table 9**.

Table 17: Statistically significant results of osteocyte analysis of T2DM group and subgroups, angulus vs. molar

T2DM group or subgroup	Parameter	Bone site	Result	p value
T2DM Insulin	Mean lacunar size	Buccal cortex	↑ in the molar region	p=0.035
T2DM Insulin	Total Mn.Lc.N/B.Ar	Buccal cortex	↑ in the molar region	p=0.025

p value: significant when <0.05; T.Mn.Lc.N/B.Ar: total mineralized lacunar number per bone area

4.2.4 Mineral-to-matrix differences between T2DM molar and angulus regions as reflected by Raman spectroscopy

The intersite comparisons of T2DM group and subgroups revealed tissue composition differences between T2DM molar and angulus regions, both in buccal cortex and in trabecular bone. Significantly different parameters, bone sites, results, and p values are listed in **Table 18**, whereas absolute values can be found in **Table 12**.

Table 18: Statistically significant results of tissue composition analysis of T2DM group and subgroups, angulus vs. molar

T2DM group or subgroup	Parameter	Bone site	Result	p value
T2DM OAD	v_1PO_4/Pro	Buccal cortex	↑ in the molar region	p=0.035
T2DM	v_1PO_4/Pro	Buccal cortex	↑ in the molar region	p=0.044
T2DM OAD	v_1PO_4/CH_2	Trabecular bone	↑ in the angulus region	p=0.037
T2DM OAD	$v_1PO_4/amide III$	Trabecular bone	↑ in the angulus region	p=0.002
T2DM	$v_1PO_4/amide III$	Trabecular bone	↑ in the angulus region	p=0.025

p value: significant when <0.05; v1PO4/CH2: area under the phosphate I peak over the area under the CH2 peak (mineral-to-matrix ratio); v1PO4/Pro: area under the phosphate I peak over the area under the proline peak (mineral-to-matrix ratio); v1PO4/amide III: area under the phosphate I peak over the area under the amide III peak (mineral-to-matrix ratio)

4.2.5 Histomorphometry: Cellular and structural differences between the angulus and molar bone regions in T2DM subgroups

The intersite comparisons of T2DM group and subgroups revealed structural and cellular differences between T2DM molar and angulus regions, both in buccal cortex and in trabecular bone. Significantly different parameters, bone sites, results, and p values are listed in **Table 19**, whereas absolute values can be found in **Table 13**.

Table 19: Statistically significant results of structural and cellular histomorphometric analysis of T2DM group and subgroups, angulus vs. molar

T2DM group or subgroup	Parameter	Bone site	Result	p value
T2DM INSULIN	ErSwo.Pm	Trabecular bone	↑ in the molar region	p=0.032
T2DM OAD	N.Ot/B.Ar	Trabecular bone	↑ in the molar region	p=0.006

p value: significant when <0.05; ErSwo.Pm: eroded surface without osteoclasts perimeter; N.Ot/B.Ar: number of osteocyte lacunae per bone area

4.3 ALC Jaw Bone Quality. Intergroup comparisons: ALC compared with Control group

4.3.1 Higher closed cortical porosity in ALC compared with Control group

Micro-CT assessment revealed significantly higher closed cortical porosity (Po(cl), [%]) in the buccal cortex of the angulus region, buccal cortex of the molar region, and lingual cortex of the molar region in the ALC group compared with the Control group. Only the lingual cortex of the angulus region showed no statistically significant difference in closed cortical porosity between the ALC group and the Control group. Po(tot), Po(op), BV/TV, and other microstructural parameters were not different between the groups in either of the regions (**Figure 18**, **Table 20**).

Trabecular bone of both regions showed no significant differences in microstructural parameters between the ALC group and the Control group (**Table 21**).

4.3.2 Lower calcium content in ALC compared with the Control group

The trabecular bone of the angulus region of the Cirrhosis group showed lower calcium content compared with the corresponding region of the Control group, as evidenced in lower CaMean and CaHigh. No other region or bone compartment showed statistically significant differences in the qBEI parameters between the groups (**Figure 19, Table 22**).

4.3.3 Lower mean lacunar size in ALC compared with the control

No differences in the osteonal morphology were found between the ALC and Control groups (**Table 23**). The trabecular bone of the molar region had significantly lower mean lacunar size (Mean Lc. size) in the Cirrhosis group than in the Control group (**Figure 20**, **Table 24**).

4.3.4 Higher tissue maturity in ALC compared with the control

Only one Raman spectroscopic parameter, v_1CO_3/v_1PO_4, was found to be significantly higher in the buccal cortex of the Cirrhosis group (**Figure 21**, **Table 25**). No other ratios interpreting the mineral to matrix ratio or other chemical structures of the bone differed between the groups, either in buccal cortex or in trabecular bone (**Figure 21**, **Tables 25 and 26**).

4.3.5 Lower osteoclast activity in ALC compared with the control

Parameters related to the resorptive activity, including ES/BS and Oc.S/BS, showed significantly lower values in the trabecular bone of the angulus of the ALC group. In fact, the values of these parameters were 0 in the ALC group, and above zero in healthy individuals (**Figure 22, Table 27**). Cortical bone thickness values showed no statistically significant differences between the ALC and the Control groups (**Table 28**).
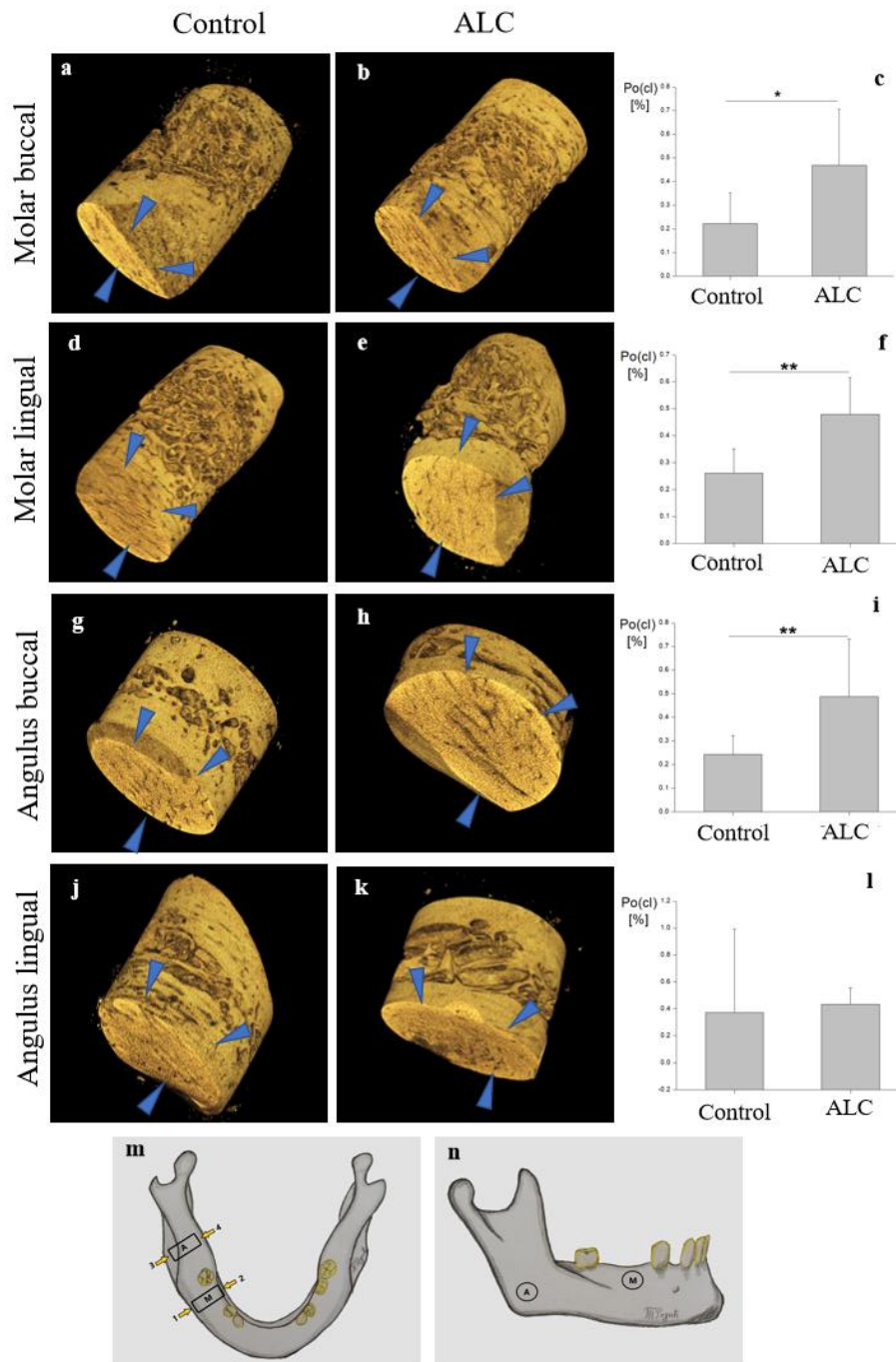
Figure 18: Higher closed cortical porosity in the ALC group compared with the Control group. (**a, b, d, e, g, h, j, k**) Sample micro-CT 3D reconstructions with arrowheads pointing to the cortex where closed cortical porosity (Po(cl)) was measured. (**c, f, i, l**) Bar charts show closed porosity values in the Control and ALC groups. (**a, b, c**) Higher closed cortical porosity was found in the buccal cortex of the molar region in the ALC group than in the Control group. (**d, e, f**) Higher closed cortical porosity was found in the lingual cortex of the molar region in the ALC group than in the Control group. (**g, h, i**) Higher closed cortical porosity was found in the buccal cortex of the angulus region in the ALC group than in the Control group. (**j, k, l**) No significant difference in closed cortical porosity was found in lingual cortex of the angulus region between the ALC and Control groups. (**m, n**) Drawings of the mandible from different perspectives, with bone core sites marked by a rectangle or a circle. Yellow arrows with numbers point to cortical regions: 1 - buccal cortex of the molar region; 2 - lingual cortex of the molar region; 3 - buccal cortex of the angulus region; 4 - lingual cortex of the angulus region.
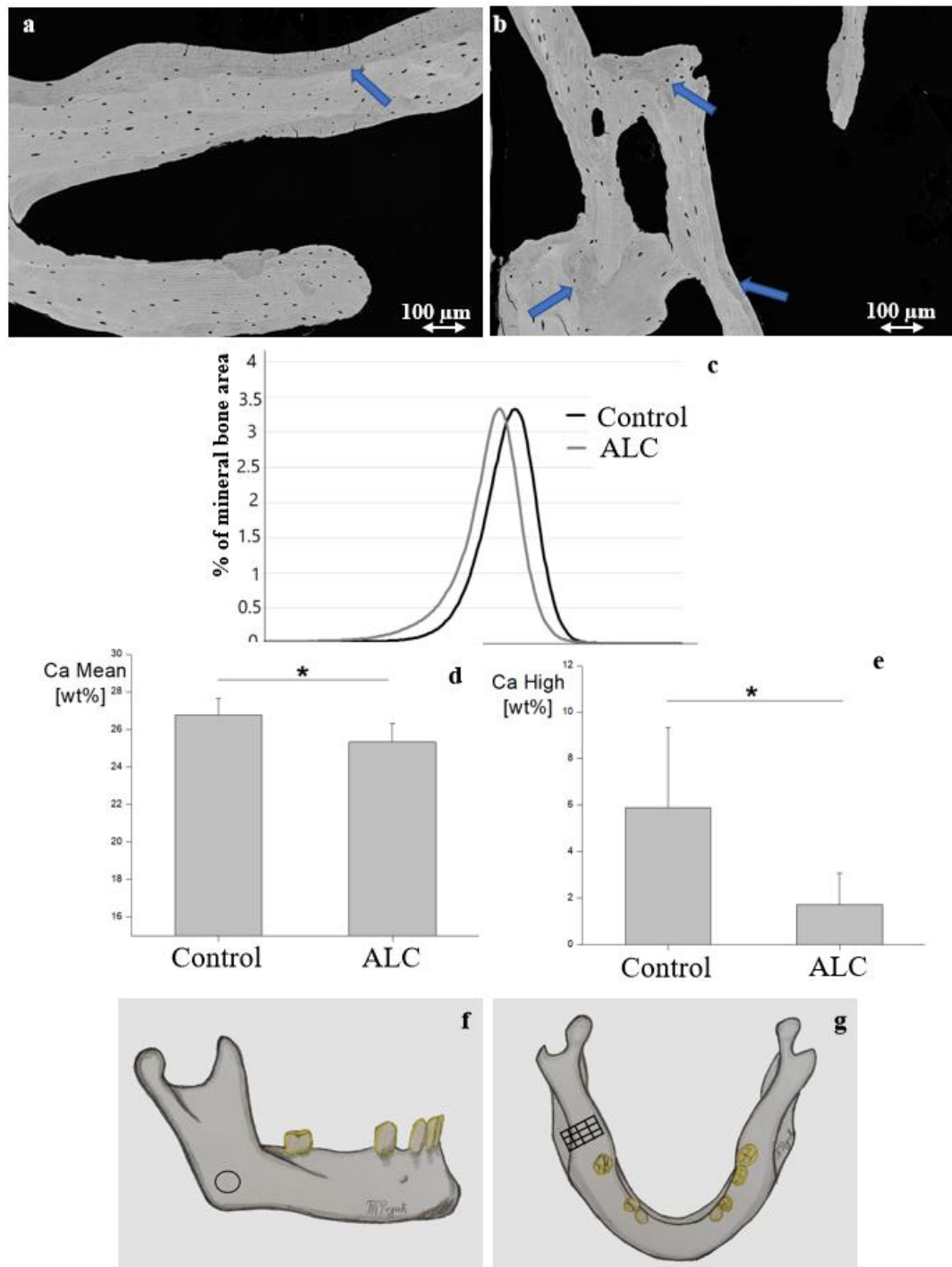
Figure 19: Lower calcium content in the trabecular bone of the angulus region of the ALC group compared with the Control group. (**a, b**) Quantitative backscattered electron microscopy images of trabecular bone in the angulus region. (**a**) Control trabecular bone has dominant light grey areas with high calcium content and few dark grey areas with low calcium content (blue arrow). (**b**) ALC trabecular bone has several low calcium content areas (blue arrows). (**c**) Calcium weight chart of the ALC group is shifted towards lower values compared with the Control group. (**d, e**) Bar charts show lower CaMean and CaHigh values in the ALC group compared with the Control group in the angulus trabecular bone region. (**f, g**) Drawings of the mandible from different perspectives, with bone core site of the samples from the angulus region marked by a circle and a grid.

43
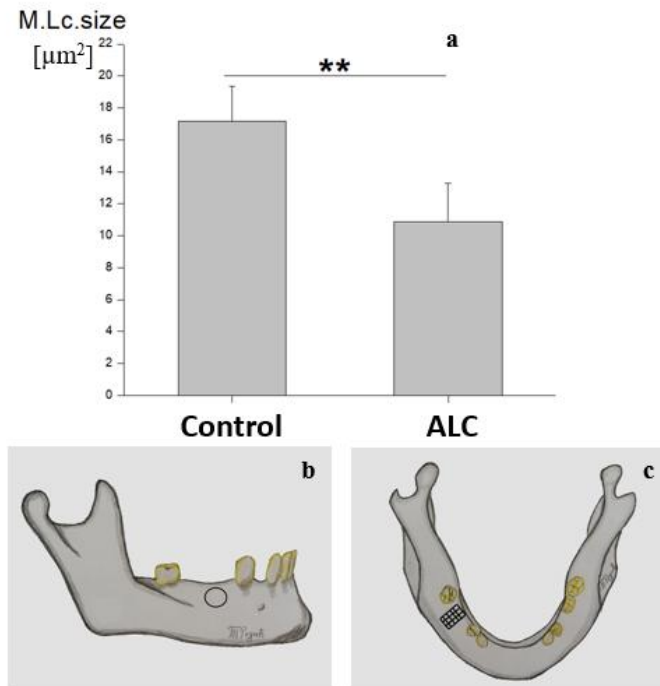
Figure 20: Lower mean lacunar size in the ALC group compared with the Control group. (**a**) Bar chart shows lower mean lacunar size in the ALC group compared with the Control group. (**b, c**) Drawings of the mandible from different perspectives, with the trabecular bone of the molar region marked by a circle and a grid.
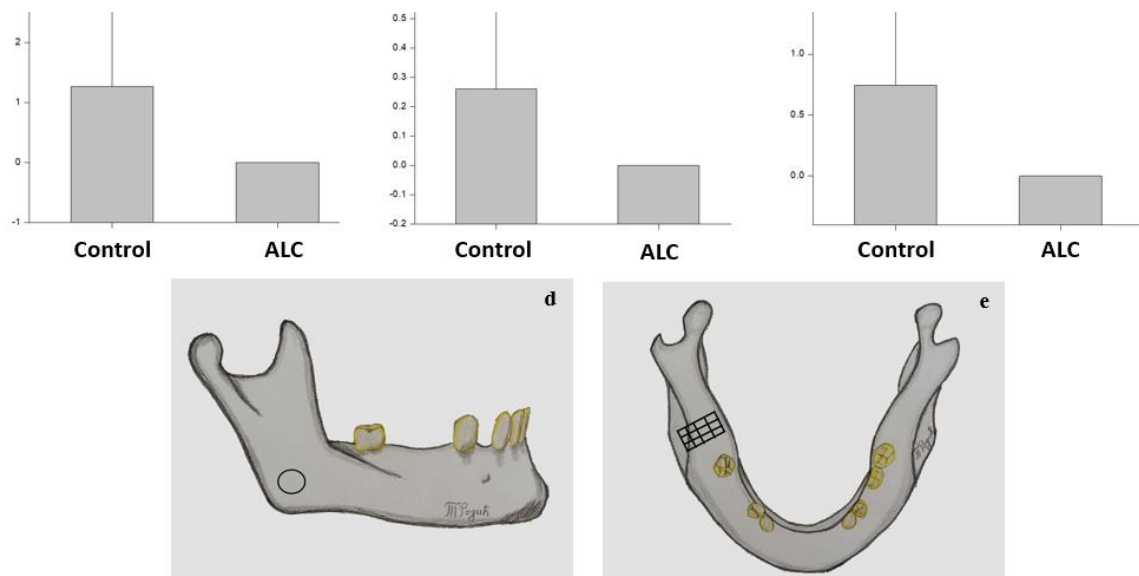
Figure 21: Lower osteoclast activity in the ALC group compared with the Control group. (**a, b, c**) Bar charts show lower resorption parameters (eroded surface per bone surface, osteoclast number per bone perimeter, osteoclast surface per bone surface) in the ALC group compared with the Control group. (**d, e**) Drawings of the mandible from different perspectives, with the trabecular bone of the angulus region marked by a circle and a grid.
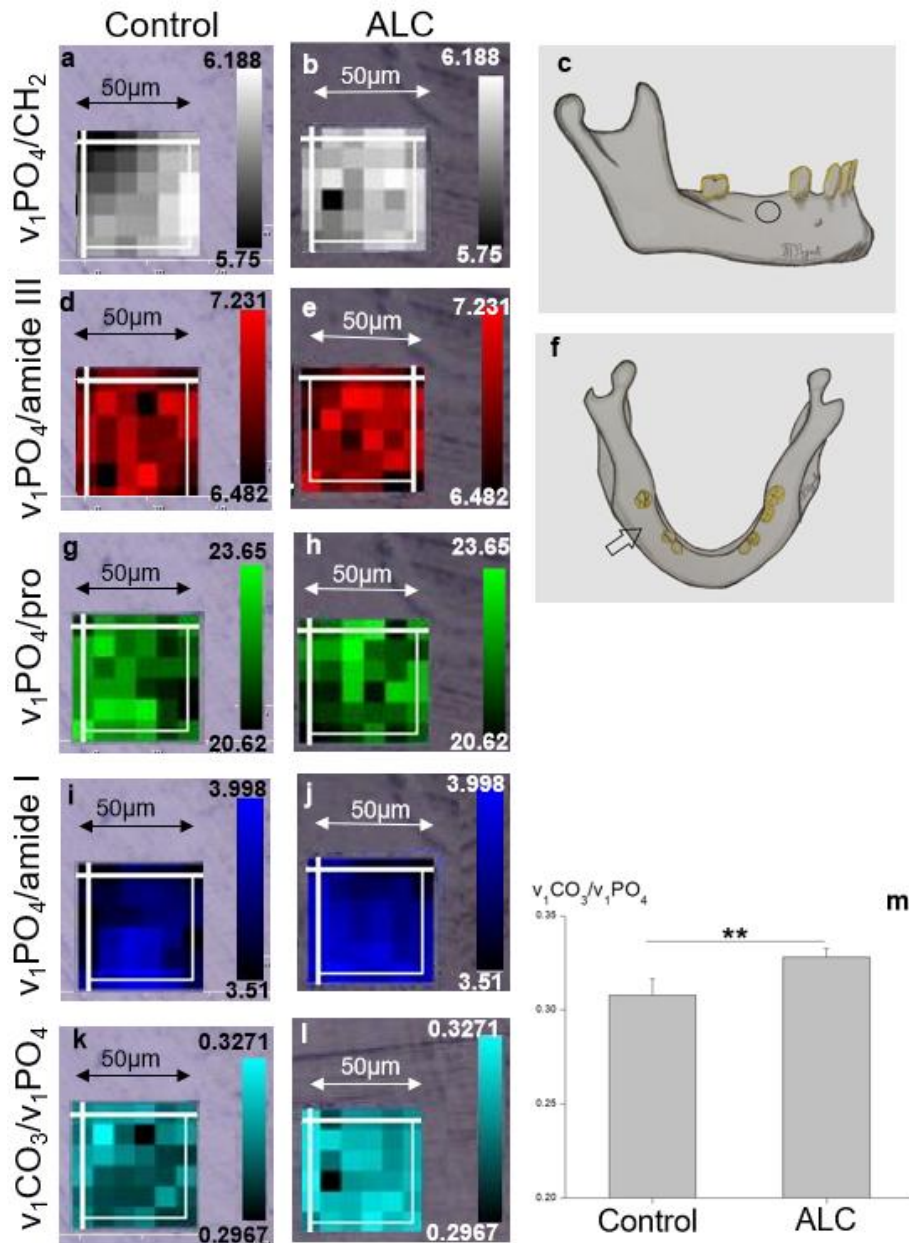
Figure 22: Bone composition of buccal cortex of the molar region in the ALC group. Panels show the microscopic image overlayed with pixel maps showing the spatial distribution of each parameter (**a, b**) Phosphate-to-CH_2 ratio (v_1PO_4/CH_2 parameter) (**a**) Control group (**b**) ALC group (**c**) Drawing of the human mandible. Circle marks the buccal cortex of the molar region (**d, e**) phosphate-to-amide III ratio (v_1PO_4/amide III parameter) in the buccal cortex of a molar region sample (**d**) Control group (**e**) ALC group (**f**) Drawing of the human mandible. Arrow points to the buccal cortex of the molar region. (**g, h**) phosphate-to-proline ratio (v_1PO_4/pro parameter) in the buccal cortex of a molar region sample (**g**) Control group (**h**) ALC group (**i, j**) Phosphate-to-amide I ratio (v_1PO_4/amide I parameter) in the buccal cortex of a molar region sample (**i**) Control group (**j**) ALC group (**k, l**) Carbonate to phosphate ratio (v_1CO_3/v_1PO_4 parameter) in the buccal cortex of a molar region sample (**k**) Control group (**l**) ALC group. There are more surfaces in light color in the ALC group (image l) compared to the Control group (image k). Raman microscope (WiRE 5.1, Renishaw). (**m**) Bar graph represents numeric values of carbonate-to-phosphate ratio (v_1CO_3/v_1PO_4 parameter) in the Control group and the ALC group (Origin Pro software), with statistical significance between the ALC group and the Control group.

Table 20: Comparison of the 3D microstructural parameters in the cortical bone between the Control group and the ALC group.

		BV/TV [%]	Po.cl [%]	Po.op [%]	Po.tot [%]	Po.Dm [mm]
Molar buccal cortex	**Control**	94.07±5.5	0.22±0.13	5.71±5.58	5.92±5.49	0.11±0.07
	ALC	95.24±1.13 (N.S.)	0.47±0.24 **p=0.02**	4.31±1.02 (N.S.)	4.76±1.13 (N.S.)	0.11±0.02 (N.S.)
Molar lingual cortex	**Control**	95.29±1.84	0.26±0.09	4.45±1.85	4.7±1.85	0.1±0.03
	ALC	87.84±17.26 (N.S.)	0.48±0.13 **p=0.003**	11.73±17.33 (N.S.)	12.14±17.27 (N.S.)	0.26±0.41 (N.S.)
Angulus buccal cortex	**Control**	96.08±2.81	0.24±0.08	3.69±2.83	3.92±2.8	0.1±0.04
	ALC	81.69±35.23 (N.S.)	0.49±0.24 **p=0.007**	3.33±1.28 (N.S.)	3.81±1.19 (N.S.)	0.09±0.03 (N.S.)
Angulus lingual cortex	**Control**	96.07±1.42	0.37±0.62	3.74±1.42	3.92±1.42	0.13±0.07
	ALC	97.16±2.26 (N.S.)	0.43±0.12 (N.S.)	2.41±2.22 (p=0.098)	2.83±2.26 (N.S.)	0.08±0.03 (p=0.098)

N.S.: not significant compared to the control group or between the T2DM groups; p value: significant when <0.05; BV/TV: Bone volume per tissue volume; Po.cl: closed porosity; Po.op: pen porosity; Po.tot: total porosity; Po.Dm: pore diameter

Table 21: Comparison of the 3D microstructural parameters in the trabecular bone between the Control group and the ALC group.

	BV/TV [%]	SMI	DA	FD	Tb.Th [mm]	Tb.N [mm]	Tb.Pf [1/mm]	Tb.Sp [mm]	Conn.Dn [1/mm^3]
Molar trabecular									
Control	30.44±10.24	-0.06±1.24	1.8±0.66	2.51±0.1	0.24±0.06	1.18±0.3	-1.54±4.28	0.75±0.3	12.85±6.02
ALC	40.07±23.08(N.S.)	-3.91±6.33 (N.S.)	1.72±0.23 (N.S.)	2.45±0.13(N.S.)	0.25±0.05 (N.S.)	1.73±1.24 (N.S.)	-7.5±11.8 (N.S.)	0.72±0.33 (N.S.)	-5.11±18.39 (N.S.)
Angulus trabecular									
Control	32.21±18.51	-0.51±2.27	3.29±0.84	2.31±0.42	0.25±0.06	1.25±0.52	-1.73±4.25	0.76±0.27	2.29±13.27
ALC	22.87±8.83 (N.S.)	0.78±0.94 (N.S.)	3.2±0.66 (N.S.)	2.3±0.07 (N.S.)	0.26±0,05 (N.S.)	0.84±0.18 (N.S.)	0.92±2.7 (N.S.)	0.87±0.18 (N.S.)	4.44±3.24 (N.S.)

N.S.: not significant compared to the control group or between the T2DM groups**;** p value: significant when <0.05; BV/TV: bone volume per tissue volume; SMI: structure model index; DA: degree of anisotropy; FD: fractal dimension; Tb.Th: trabecular thickness; Tb.N: trabecular number; Tb.Pf: trabecular pattern factor; Tb.Sp: trabecular separation; Conn.Dn: connectivity density

Table 22: Values of the qBEI parameters in the Control and the ALC group.

	CaMean [wt %]	CaPeak [wt %]	StDev [wt %]	CaLow [wt %]	CaHigh [wt %]
Molar buccal cortex					
Control	26.55±0.62	27.2±0.63	2.49±0.26	5.92±2.33	6.28±3.88
ALC	26.12±0.88 (N.S.)	27.04±0.86 (N.S.)	2.94±0.53 (N.S.)	9.62±4.59 (N.S.)	6.26±5.7 (N.S.)
Molar lingual cortex					
Control	25.92±0.39	26.59±0.24	2.78±0.35	5.34±2.42	4.96±1.54
ALC	25.47±1.02 (N.S.)	26.34±0.89 (N.S.)	3.02±0.63 (N.S.)	8.71±5.35 (N.S.)	3.55±2.02 (N.S.)
Angulus buccal cortex					
Control	26.59±0.5	27.17±0.35	2.58±0.6	4.82±3.35	5.01±2.7
ALC	25.73±0.68 (N.S.)	26.5±0.58 (N.S.)	2.7±0.76 (N.S.)	8±5.2 (N.S.)	2.07±1.92 (N.S.)
Angulus lingual cortex					
Control	26.37±0.49	26.94±0.46	2.35±0.14	5.04±2.09	5.63±3.28
ALC	26.32±0.23 (N.S.)	26.85±0.36 (N.S.)	2.3±0.24 (N.S.)	4.58±1.25 (N.S.)	3.73±1.83 (N.S.)
Molar trabecular bone					
Control	25.58±0.75	26.48±0.48	2.98±0.53	7.02±4.71	5.31±3.02
ALC	25.26±1.06 (N.S.)	26.4±0.75 (N.S.)	3.5±0.62 (N.S.)	11.21±6.98 (N.S.)	6.42±2.87 (N.S.)
Angulus trabecular bone					
Control	26.76±0.9	27.26±0.98	2.52±0.18	5.82±4.36	5.88±3.45
ALC	25.32±0.98 (**p=0.042**)	26.18±0.43 (N.S.)	2.85±0.52 (N.S.)	14.81±11.01 (N.S.)	1.72±1.34 (**p=0.036**)

N.S.: not significant compared to the control group or between the T2DM groups; p value: significant when <0.05; CaMean: mean calcium content; CaPeak; peak calcium content; CaWidth: heterogeneity of bone mineral distribution: CaHigh: area of highly mineralized bone below the 5th percentile value of that group; CaLow: area of poorly mineralized bone above the 95th percentile value of that group

Table 23: Comparison of osteonal morphology parameters and osteocyte lacunar parameters of cortical bone between the Control group and the ALC group.

	On.N/B.Ar (1/mm^2)	On.W.Th (μm)	Mean On.Ot.Ln.N	Lc.N/B.Ar (1/mm^2)	Mean Lc. size (μM^2)	MEan On.Mn.Lc.N	T.Mn.On.Lc.N/On. B.Ar (1/mm^2)	T.Mn.Lc.N/B. Ar (1/mm^2)
Molar buccal cortex								
Control	3.85 ± 2.48	14.59 ± 32.46	11±5	533.13 ± 66.76	15.31± 1.58	0.09 ± 0.12	1.72 ± 3.01	5.79 ± 5.69
ALC	3.14±7.61 (N.S.)	81.2±29.54 (N.S.)	8.5±3.35 (N.S.)	897.61±515.31 (N.S.)	12.75±4.43 (N.S.)	0.05±0.11 (N.S.)	0.77±1.72 (N.S.)	4.15±2.98 (N.S.)
Molar lingual cortex								
Control	1.31 ±1.79	41.18 ± 39.18	15±6	627.12 ± 164.68	15.04± 3.15	0.11±0.08	0.59 ± 1.32	1.51 ± 2.13
ALC	3.28±1.45 (N.S.)	74.77±25.74 (N.S.)	12.1±4.62 (N.S.)	997.03±519.5 (N.S.)	12.74±3.63 (N.S.)	0.01±0.03 (N.S.)	0.46±1.03 (N.S.)	3.37±2.51 (N.S.)
Angulus buccal cortex								
Control	1.78 ± 1.44	16.06 ± 35.76	9.28±3.01	662.93 ± 503.44	14.29± 4.12	0.29±0.54	2.58 ± 3.57	11.9 ± 13.9
ALC	3.68±1.94 (N.S.)	77.47±25.61 (N.S.)	15.83±8.61 (N.S.)	888.89±934.07 (N.S.)	13.72±2.67 (N.S.)	0.02±0.05 (N.S.)	0.44±1 (N.S.)	2.06±1.35 (N.S.)
Angulus lingual cortex								
Control	2 ± 1.36	11.07 ± 24.55	13.48±5.03	361.88 ± 111.96	16.27±1.5	0.04±0.05	0.54 ± 0.78	4.56 ± 3.9
ALC	2±1.1 (N.S.)	71.09±27.62 (N.S.)	13.2±5.35 (N.S.)	419.7±136.92 (N.S.)	15.5±1.75 (N.S.)	0.02±0.05 (N.S.)	0.85±1.9 (N.S.)	2.33±2.14 (N.S.)

N.S.: not significant compared to the Control group or between the T2DM groups; p value: significant when <0.05; On.N/B.Ar: osteon number per bone area; On.W.Th: osteonal wall diameter; Mean On.Ot.Ln.N: mean osteonal osteocyte lacunar number; Lc.N/B.Ar: lacunar number per bone area; Mean Lc. size: mean lacunar size; Mean On.Mn.Lc.N: mean osteonal mineralized lacunar number; Total Mn.On.Lc.N/On.B.Ar: total mineralized osteonal lacunar number per osteonal bone area; T.Mn.Lc.N/B.Ar: total mineralized lacunar number per bone area

Table 24: Comparison of osteocyte lacunar parameters of trabecular bone between the Control group and ALC group.

	Lc.N/B.Ar (1/mm^2)	Mean Lc. size (µm^2)	T.Mn.Lc.N/B.Ar (1/mm^2)
Molar trabecular			
Control	452.21± 61.54	17.19± 2.15	3.93 ± 5.47
ALC	1356.8±866.23 (N.S.)	10.87±2.39 (p=0.002)	9.48±6.14 (N.S.)
Angulus trabecular			
Control	362.04± 117.91	16.97± 3.33	15.8 ± 11
ALC	591.43±304.41 (N.S.)	13.71±3.49 (N.S.)	5.24±3.7 (N.S.)

N.S.: not significant compared to the Control group or between the T2DM groups; p value: significant when <0.05; T.Mn.Lc.N/B.Ar: total mineralized lacunar number per bone area; Lc.N/B.Ar: lacunar number per bone area; Mean Lc. size: mean lacunar size

Table 25: Values of tissue composition and maturity parameters of cortical bone in the Control group and ALC group.

	v_1PO_4/CH_2	$v_1PO_4/amideIII$	v_1PO_4/Pro	$v_1PO_4/amideI$	v_1CO_3/v_1PO_4	1/FWHM (v_1PO_4)
Molar buccal cortex						
Control	6.53±0.35	7.53±0.43	23.51±1.16	4.18±0.35	0.31±0.01	0.06±0.001
ALC	6.29±0.71 (N.S.)	7.15±0.84 (N.S.)	22.98±1.34 (N.S.)	4.22±0.74 (N.S.)	0.33±0.004 (**p=0.008**)	0.06±0.0008 (N.S.)
Angulus buccal cortex						
Control	6.13±0.48	7.19±0.66	22.51±2.4	4.05±0.19	0.32±0.02	0.06±0.001
ALC	5.7±0.34 (N.S.)	6.72±0.37 (N.S.)	22.63±1.17 (N.S.)	3.94±0.23 (N.S.)	0.33±0.01 (N.S.)	0.06±0.0009 (N.S.)

Table 26: Values of tissue composition and maturity parameters of trabecular bone in the Control group and ALC group.

	v_1PO_4/CH_2	$v_1PO_4/amideIII$	v_1PO_4/Pro	$v_1PO_4/amideI$	v_1CO_3/v_1PO_4	$v_2PO_4/amideIII$	1/FWHM (v_1PO_4)
Molar trabecular							
Control	7.17±0.67	8.98±1.12	27.47±3.94	5.87±0.34	0.38±0.03	2.28±0.48	0.06±0.0007
ALC	6.76±0.8 (N.S.)	8.53±1.41 (N.S.)	26.81±1.85 (N.S.)	5.91±0.86 (N.S.)	0.37±0.02 (N.S.)	2.15±0.13 (N.S.)	0.06±0.002 (N.S.)
Angulus trabecular							
Control	7.11±0.72	8.91±1.03	24.72±3.19	5.47±0.35	0.35±0.03	2.22±0.41	0.06±0.002
ALC	6.19±0.55 (N.S.)	8.24±1.16 (N.S.)	26.18±2.98 (N.S.)	5.68±0.84 (N.S.)	0.33±0.04 (N.S.)	3.21±2.86 (N.S.)	0.06±0.0006 (N.S.)

N.S.: not significant compared to the control group or between the T2DM groups; p value: significant when <0.05; v_1CO_3/v_1PO_4: Carbonate-to-phosphate ratio; 1/FWHM(v_1PO_4) crystallinity; $v_1PO_4/amideI$: area under the phosphate I peak over the area under the amide I peak (mineral-to-matrix ratio); v_1PO_4/CH_2: area under the phosphate I peak over the area under the CH_2 peak (mineral-to-matrix ratio); v_1PO_4/Pro: area under the phosphate I peak over the area under the proline peak (mineral-to-matrix ratio); $v_1PO_4/amideIII$: area under the phosphate I peak over the area under the amide III peak (mineral-to-matrix ratio); $v_2PO_4/amideIII$: area under the phosphate II peak over the area under the amide IIII peak (mineral-to-matrix ratio)

Table 27: Values of bone cellular parameters of the trabecular bone in the Control group and the ALC group.

	OV/BV	OS/BS	ES/BS	Oc.S/BS	O.Th (µm)	OwOb.Ar (mm^2)
Molar trabecular bone						
Control	0.1±0.12	2.74±3.83	0.6±1.12	0.26±0.55	2.9±3.69	0.0009±0.002
ALC	0.44±0.53 (N.S.)	7.76±7.72 (N.S.)	0.48±0.69 (N.S.)	0.31±0.47 (N.S.)	4.41±4.6 (N.S.)	0.0002±0.0005 (N.S.)
Angulus trabecular bone						
Control	0.45±0.55	6.92±7.98	1.27±1.61	0.74±0.89	4.73±4.82	0.00097±0.001
ALC	0.33±0.46 (N.S.)	5.12±7.36 (N.S.)	0±0 (**p=0.034**)	0±0 (**p=0.022**)	3.74±4.86 (N.S.)	0.00132±0.003 (p=0.056)

	N.Ob/B.Pm (1/mm)	N.Oc/B.Pm (1/mm)	ErSwO.Pm (mm)	N.eOt/B.Ar (1/mm^2)	N.Ot/B.Ar (1/mm^2)	N.Oot/B.Ar (1/mm^2)
Molar trabecular bone						
Control	1.42±1.76	0.11±0.23	0.13±0.13	44.77±27.11	157.34±61.85	12.38±8.31
ALC	2.24±2.25 (N.S.)	0.12±0.18 (N.S.)	0.14±0.12 (N.S.)	47.05±13 (N.S.)	192.76±45.38 (N.S.)	8.71±6.76 (N.S.)
Angulus trabecular bone						
Control	2.62±2.42	0.26±0.33	0.21±0.17	50.13±36.94	144.89±42.08	17.17±12.73
ALC	1.68±2.38 (N.S.)	0±0 (**p=0.032**)	0.16±0.11 (N.S.)	52.73±14.69 (N.S.)	104.92±35.51 (p=0.056)	6.37±9.1 (p=0.092)

N.S.: not significant compared to the Control group or between the T2DM groups; p value: significant when <0.05; N.Ob/B.Pm: number of osteoblasts per bone perimeter; N.Ot/B.Ar: number of osteocyte lacunae per bone area; OS/BS: osteoid surface per bone surface; ES/BS: eroded surface per bone surface; Oc.S/BS: osteoclast surface per bone surface; O.Th; osteoid thickness: N.Oc/B.Pm: number of osteoclasts per bone perimeter; OwoB.Ar: osteoid without osteoblasts bone area; ErSwo.Pm: eroded surface without osteoclasts perimeter; N.eOt/B.Ar: number of empty osteocyte lacunae per bone area; N.Oot/B.Ar: number of newly embedded osteoblasts per bone area

Table 28: Values of cortical bone thickness in the Control and ALC groups.

	Ct. Th [µm]
Molar buccal cortex	
Control	1881.45±472.86
ALC	1955.62±414.03 (N.S.)
Angulus buccal cortex	
Control	1583.79±546.56
ALC	1236.31±562.99 (N.S.)
Molar lingual cortex	
Control	1749.57±780.58
ALC	1909.15±678.91 (N.S.)
Angulus lingual cortex	
Control	1387.45±526.53
ALC	1253.34±378.99 (N.S.)

N.S.: not significant compared to the Control group or between the T2DM groups; p value: significant when <0.05; Ct.Th: cortical thickness

4.4 ALC Jaw Bone Quality. Intersite comparisons (Angulus region vs. Molar region) in the ALC group

4.4.1 Microstructural differences in trabecular geometry in the ALC group

Intersite comparison of the angulus and molar regions in the ALC group revealed significant differences in DA and FD. Significantly different parameters, bone sites, results, and p values are listed in **Table 29**, whereas absolute values are shown in **Table 21**.

Table 29: Statistically significant results of microstructural analysis of ALC angulus vs. molar region

Group	Parameter	Bone site	Result	p value
ALC	DA	Trabecular bone	↑ in the angulus region	p=0.001
ALC	FD	Trabecular bone	↑ in the molar region	p=0.033

p value: significant when <0.05; DA: degree of anisotropy; FD: Fractal dimension

4.4.2 No intersite mineralization variations in ALC

Statistical analysis of qBEI mineralization parameters showed no significant intersite differences in the ALC group.

4.4.3 Osteocyte lacunar intersite differences in the ALC group

Intragroup comparisons of the angulus and molar regions in the ALC group revealed significant differences in two of the parameters regarding osteocyte lacunae.

Significantly different parameters, bone sites, results, and p values are listed in **Table 30**, whereas absolute values can be found in **Table 24**.

Table 30: Statistically significant results of osteonal analysis of ALC angulus vs. molar region

Group	Parameter	Bone site	Result	p value
ALC	Mean On.Ot.Ln.N	Buccal cortex	↑ in the angulus region	p=0.025
ALC	T.Mn.Lc.N/B.Ar	Buccal cortex	↑ in the molar region	p=0.037

p value: significant when <0.05; Mean On.Ot.Ln.N: mean osteonal osteocyte lacunar number; T.Mn.Lc.N/B.Ar: total mineralized lacunar number per bone area

4.4.4 Mineral-to-matrix intersite differences in the ALC group

Comparisons of the angulus and molar regions in the ALC group revealed a statistically significant difference in one of the parameters of tissue composition (v_1PO_4/CH_2). This parameter, its bone site, result, and p value are listed in **Table 31**, whereas absolute values can be found in **Tables 25 and 26**.

Table 31: Statistically significant results of tissue composition analysis of ALC angulus vs. molar region

Group	Parameter	Bone site	Result	p value
ALC	v_1PO_4/CH_2	Trabecular bone	↑ in molar region	p=0.015

p value: significant when <0.05; v_1PO_4/CH_2: area under the phosphate I peak over the area under the CH_2 peak (mineral-to-matrix ratio)

4.4.5 Cellular parameters and cortical thickness intersite differences in the ALC group

Histomorphometry revealed an intersite difference in osteocyte number between the angulus and the molar regions in the ALC group. Furthermore, cortical thickness of the buccal cortex differed between the angulus and molar bone cores in the ALC group. Significantly different parameters, bone sites, results, and p values are listed in **Table 32**, whereas absolute values can be found in **Tables 27 and 28**.

Table 32: Statistically significant results of histomorphometry analysis of Control angulus vs. molar region

Group	Parameter	Bone site	Result	p value
ALC	N.Ot/B.Ar	Trabecular bone	↑ in the molar region	p<0.001
ALC	Ct.Th	Buccal cortex	↑ in the molar region	p=0.002

p value: significant when <0.05; N.Ot/B.Ar: number of osteocyte lacunae per bone area; Ct.Th: cortical thickness

4.5 Intersite comparisons (Angulus region vs. Molar region) in the Control group

4.5.1 Microstructural differences in geometry in the Control group

Statistical analysis revealed microstructural differences in geometry between the angulus and the molar region in the Control group. Significantly different parameters, bone sites, results, and p values are listed in **Table 33**, whereas absolute values can be found in **Table 8**.

Table 33: Statistically significant results of microstructural analysis of the angulus vs. molar region of the Control group

Group	Parameter	Bone site	Result	p value
Control	DA	Trabecular bone	↑ in the angulus region	p=0.001
Control	Conn.Dn	Trabecular bone	↑ in the molar region	p=0.007

p value: significant when <0.05; DA: degree of anisotropy; Conn.Dn: connectivity density

4.5.2 No intersite mineralization variations in the Control group

Statistical analysis of qBEI mineralization parameters showed no significant intersite differences in the Control group.

4.5.3 Osteonal number intersite variations in the Control group

Statistical analysis revealed significant differences in osteonal number between the angulus and the molar regions of the Control group. Parameter, bone site, result, and p value are listed in **Table 34**, whereas absolute values can be found in **Table 10**.

Table 34: Statistically significant results of osteonal morphology analysis of the angulus vs. molar regions in the Control group

Group	Parameter	Bone site	Result	p value
Control	On.N/B.Ar	Trabecular bone	↑ in the molar region	p=0.033

p value: significant when <0.05; On.N/B.Ar: osteon number per bone area

4.5.4 Mineral-to-matrix intersite differences in the Control group

Comparisons of the angulus and molar regions of Control group revealed statistically significant difference in one parameter related to tissue composition. This parameter, its bone site, result, and p value are listed in **Table 35**, whereas absolute values can be found in **Table 12**.

Table 35: Statistically significant results of microstructural analysis of the angulus vs. molar regions in the Control group

Group	Parameter	Bone site	Result	p value
Control	v_1PO_4/amideI	Trabecular bone	↑ in the molar region	p=0.048

p value: significant when <0.05; v_1PO_4/amideI: area under the phosphate I peak over the area under the amide I peak (mineral-to-matrix ratio)

### 4.5.5 No cellular, structural and cortical thickness inter-site differences in the Control group

Statistical analysis of cellular, structural and cortical thickness parameters showed no significant inter-site differences in the Control group.

5. Discussion

In this post mortem study, we compared the parameters of jaw bone microstructure, composition and bone cells in individuals with T2DM and healthy controls, and investigated the influence of antidiabetic drugs vs. insulin in a site-specific manner in these groups of individuals. We observed substantial inter-group variability in T2DM affecting bone quality as summarized below per each site investigated:

- the *trabecular* bone of the *molar* region showed a lower fractal dimension, higher calcium content heterogeneity and higher osteoclast number per bone perimeter in T2DM vs. controls;
- the *lingual* cortex of the *molar* region showed no difference in T2DM;
- the *buccal* cortex of the *molar* region had a lower mineralized osteocyte lacunar bone number and higher carbonate-to-phosphate ratio in T2DM;
- the *trabecular* bone of the *angulus* region had thicker trabeculae, fewer mineralized osteocyte lacunae and smaller lacunae;
- the *lingual* cortex of the *angulus* region had lower porosity in T2DM;
- the *buccal* cortex of the *angulus* region showed more packets of highly mineralized bone in T2DM (**Figure 23**).

Firstly, micro-CT evaluation of the trabecular bone of the molar region showed a lower fractal dimension parameter in the micro-CT evaluation in T2DM group, which signifies lower structural complexity in this bony region in T2DM irrespective of anti-diabetic treatment. A recent study compared mandibular bone fractal dimension on digital panoramic radiographs of T2DM to controls, but found no significant difference [Kurşun-Çakmak, 2018]. Fractal dimension analysis was conducted on a digital panoramic X-ray using a box-counting method in the Image J software. Absolute values reported for the T2DM molar region were lower than in our post mortem research (1.28±0.1 vs. 2.39±0.13). Notably, in this research a two-dimensional radiograph underwent significant computation prior to its analysis in Image J software, in contrast to our micro-CT-based fractal dimension calculation, which was performed automatically on 3D bone biopsy scans. Other differences to our research were: clinical research (in contrast to our cadaveric post mortem research), patients' age (48.6±9.5 yrs), and no missing teeth. Since in our research a tooth had been previously extracted in the molar region, trabecular bone of the edentulous molar region was likely remodeled in a different way under the influence of T2DM, which is discussed in detail in the next section. Bearing in mind that such alteration in microstructure was not affected by the type of therapy (OAD vs. insulin), it can be assumed that a decrease in fractal dimension in the mentioned research was caused by T2DM itself.
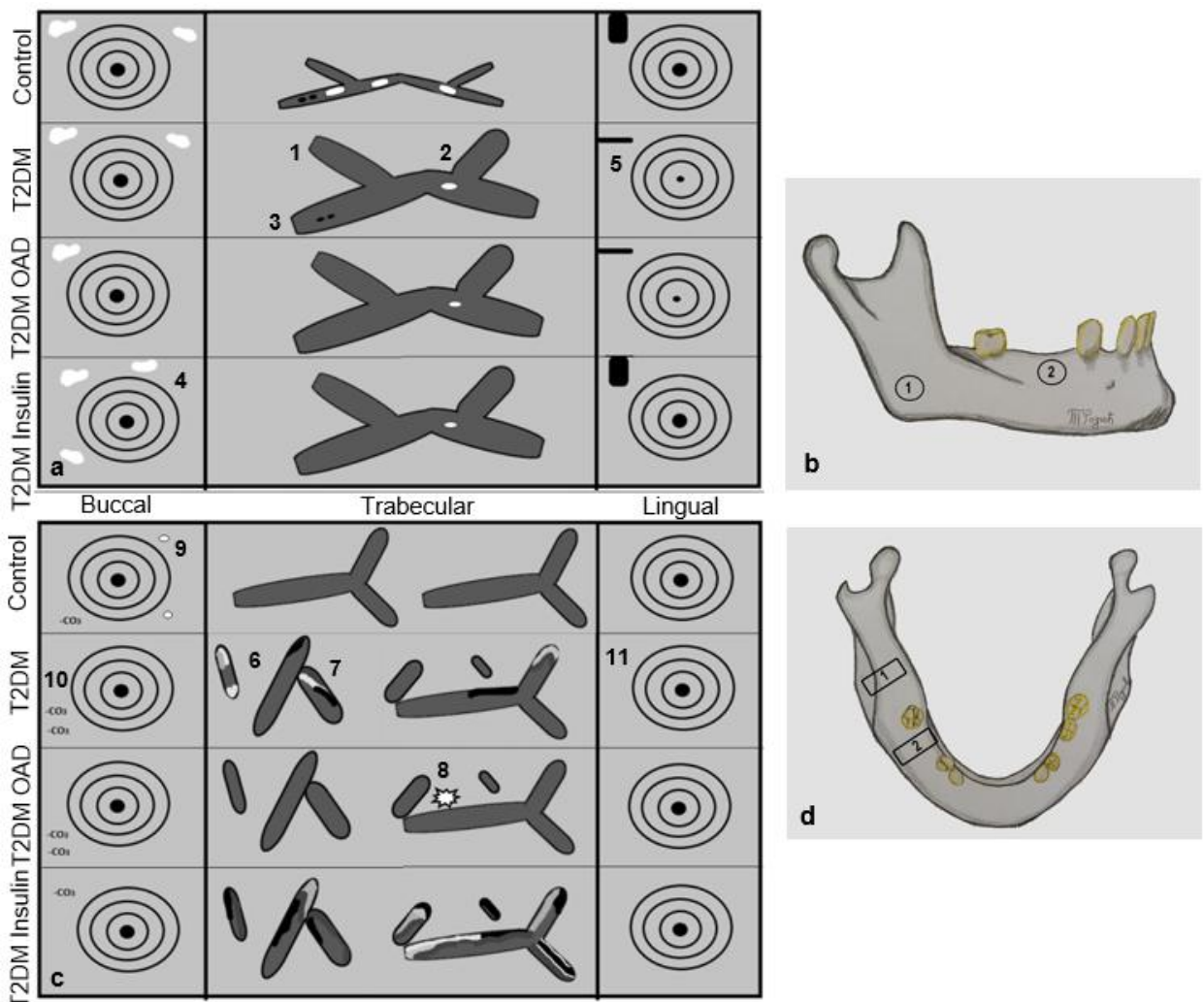
Figure 23: Schematic representation of bone microstructural, compositional, and cellular alterations in all T2DM and Control groups (**a** and **c**) Schematic representations of angulus and molar samples. Rows represent groups (Control, T2DM, T2DM OAD and T2DM Insulin) and columns represent bony sites within a sample (buccal cortex, trabecular bone and lingual cortex). (**a**) Angulus sample. 1: Trabeculae were thicker in all T2DM groups compared to the control. 2: The same bony site showed fewer mineralized lacunae in all T2DM groups compared to the control. 3: Osteocyte lacunae were smaller in T2DM compared to the control. 4: Significantly higher number of hypermineralized bone packets was found in buccal cortex of the angulus region in T2DM Insulin subgroup compared to the T2DM OAD. 5: Open porosity was lower in T2DM and T2DM OAD in lingual cortex of the angulus compared to the control. (**c**) Molar sample. 6: Trabecular bone had inferior geometry pattern in all T2DM groups compared to the control.7: Heterogeneity of calcium content was higher in T2DM and T2DM Insulin groups compared to the control. 8: T2DM OAD subgroup revealed higher osteoclast number per bone perimeter in trabecular bone of the molar region compared to controls and T2DM Insulin. 9: Buccal cortex of the molar region had fewer mineralized lacunae in T2DM compared to the Control group.10: There were fewer crystal impurities in T2DM Insulin subgroup compared to the Control in buccal cortex of the molar region. 11: Lingual cortex remained unchanged by all evaluated parameters in all T2DM groups. (**b** and **d**) Drawings of mandible from different perspectives. 1: bone core site of a sample from the angulus region, 2: bone core site of a sample from the molar region

T2DM had been diagnosed at least 3 years prior to tooth extraction in individuals in our research. Therefore, bone remodeling of tooth socket could have been affected by diabetic conditions. Literature data regarding bone remodeling during DM are somewhat contradictory. For example, one study found no statistical differences between delayed healing after tooth extraction and age, gender, diabetic state, blood glucose level or smoking, between T2DM patients treated by oral antidiabetics and healthy patients [Huang 2013]. Also, it was found that insulin-dependent T2DM patients, if well controlled, tend to heal well following dental extractions but with a small but not statistically different rate of post-extraction complications including infection [Power 2019]. Next, there are evidences of osteoblast insufficiency and enhanced bone resorption [Pietschmann 2019] during T2DM. There are evidences of low bone formation, although evidences of increased bone resorption in T2DM are not consistent [Palermo 2017, Murray 2019]. In vitro and animal studies report an unaltered rate of bone resorption [Achemlal 2005], whereas some studies have suggested increased osteoclastic activity in diabetes mellitus under certain conditions, such as periodontal disease [Pacios 2013] and osteoporosis [Yamagishi 2012]. Other studies have even reported inhibited osteoclast function and differentiation in a diabetic environment [Kasahara 2010, Wittrant 2008, He 2004]. Due to the conflicting evidence and generally negligent effect that has been observed in osteoclasts, it seems likely that the impaired bone formation in diabetes mellitus is primarily due to inhibited osteoblastic and progenitor cell activity rather than an alteration of bone resorption. However, further research is needed to clarify the effect of diabetes mellitus on osteoclastic function and differentiation. In our research osteoclast activity seemed enhanced in T2DM in the molar region, especially in the OAD group, which might be assigned to the OAD treatment [Guja 2019] and local conditions of biting forces [Ferrato 2017].

Further analysis of the trabecular bone of the edentulous molar region based on the subgroups, revealed higher heterogeneity of the calcium content in the Insulin subgroup compared to the OAD subgroup and Control. Higher mineralization heterogeneity in insulin-treated cases in this region might indicate the presence of younger remodeled bone packets in addition to older bone packets. Considering that insulin has anabolic effects on bone [Thraillkil 2005], trabecular bone had likely been previously remodeled intensely, displaying bone layers of different tissue age simultaneously at the time of the observation. Nevertheless, Raman spectroscopy showed a tendency towards higher crystallinity in the trabecular bone of the edentulous molar region in the Insulin subgroup than in controls, indicating a more mature mineral [Shah 2019]. Mineral crystallinity parameter reflects crystallite size and perfection, and was shown to increase with post-extraction healing time in healthy persons [Shah 2019]. Recently, Shah et al. (2019) analyzed human mandible bone biopsies by Raman spectroscopy and quantitative backscattered electron microscopy and compared matrix composition and mineralization between healthy persons in different stages of alveolar socket remodeling (less than 4yrs post-extraction and 4-5 yrs post-extraction). This research divided groups by duration of healing time, whereas we divided groups by therapy (OAD or insulin). They found that mineral crystallinity and bone mineral density were positively correlated, which can be put in relation to our findings of crystallinity and higher heterogeneity of calcium content in the trabecular molar region. In our study Raman-based mineral-to-matrix ratios showed no significant differences between the T2DM groups and control. This can be because T2DM likely causes only short-term disturbances in healing during post-extraction time, with no evidence of poor healing in the long-term [Marin 2020]. Also, unchanged mineral-to-matrix ratio in our

research was in agreement with qBEI-derived mean Calcium content, which was also unchanged in T2DM.

T2DM OAD subgroup revealed higher osteoclast number per bone perimeter in trabecular bone of the molar region compared to controls and T2DM Insulin. Moreover, the same region showed a tendency towards higher osteoid volume per bone volume in the same group. These findings suggest more intense alveolar trabecular bone turnover in molar region in T2DM. Although high standard deviations and strict statistical tests applied to the T2DM subgroups may partially explain the lack of statistical significance in majority of osteoclast- and osteoblasts-related parameters (Table 8), we can still notice trends towards higher bone turnover in T2DM trabecular bone in molar region compared to control. Also, osteoclast differentiation might be favored by OAD therapy. Since to our knowledge there are no contemporary papers dealing with possible mechanisms of alveolar bone turnover in partially edentulous T2DM individuals, we refer to clinical studies including T2DM patients with periodontitis and soft tissue inflammation, with regards to differences in study design. Findings in the contemporary literature regarding alveolar bone turnover in T2DM patients with periodontitis are somewhat contradictory. Several studies including periodontitis reported higher osteoclast formation and activity and lower bone formation through increase in RANKL/OPG ratio (receptor activated nuclear k-B ligand/osteoprotegerin ratio) and the inflammation mediators such as interleukin-17 (IL-17) [Wu 2015, Liu 2006, Pacios 2012, Xiao 2017]. Other studies in diabetic humans on non-maxillofacial sites speak for lower bone formation in T2DM [Yamamoto 2012, Jiajue 2014]. However, since our study includes human male alveolar bone, but does not involve periodontitis, wound healing process or local inflammation, we expect that mechanisms of bone turnover inside edentulous molar region and angulus region might slightly differ from mechanisms described in periodontitis, wound healing process or local inflammation [Marin 2020]. For example, osteoclasts might not be activated by the RANKL/OPG ratio imbalance, since this pathway also causes osteoblast apoptosis [Wu 2015], but possibly via monocyte-colony-stimulating factor (MCSF), but this assumption needs further investigation. Moreover, our findings do not contradict the fact that Insulin treatment has a proven anabolic effect on bone tissue, while OADs have varying effects on bone remodeling [He 2004, Thraillkil 2005].

To place all findings of molar region trabecular bone into relation, the fact that a tooth had been extracted at this site should be kept in mind. This bony site had been remodeled several years prior to sample collection, when T2DM was most likely already present. It seems that T2DM treated by either OAD or Insulin favors bone remodeling in this region, forming geometric irregularities among trabeculae. Insulin causes mineralization heterogeneity and more mature crystals, whereas OAD therapy favors osteoclast differentiation in the molar region.

The lingual cortex of the molar region showed no T2DM related changes in microstructure or mineralization or any other evaluated parameters. Since this cortex is rarely damaged during tooth extraction, there was no need for a significant degree of bone remodeling in this region. Consequently, bone quality at this site was not evidently different in T2DM compared to healthy individuals by methods applied in this study.

The buccal cortex of the molar region, which is often damaged during tooth extraction, showed fewer mineralized lacunae in the T2DM group regardless of the therapy. From cellular perspective, this suggests younger bone tissue characteristics in the T2DM group compared to the same region of the controls [71,72]. It may be speculated that T2DM OAD favored new bone formation in buccal cortex, like in the

trabecular bone of the moral region. However, since no cellular histomorphometry parameters were evaluated for the cortical bone, our conclusion is based only on lower mineralized lacunar number in T2DM.

The same region presented with more crystal impurities inside bone, which was represented by higher carbonate-to-phosphate ratio (v_1CO_3/v_1PO_4) Raman parameter in the T2DM whole group, as well as in the OAD subgroup compared to the Control. Higher carbonate-to-phosphate ratio was interpreted as carbonate substitution in the hydroxyapatite crystal [Paschalis 2017, Creecy 2017]. Higher carbonate content is a predictor of bone susceptibility to fracture [Paschalis 2017, Mansur 2019]. This bony site might be more prone to fracture due to its higher carbonate content in T2DM but this requires further research. To put the findings regarding the buccal cortex of the molar region in relation, we can speculate that bone in this region is younger and slightly altered in chemical content in T2DM compared to controls.

The trabecular bone of the angulus region showed higher trabecular thickness in T2DM and T2DM OAD groups. This finding is in agreement with an experiment on a diabetic pig model where mandibular bone microstructure of the jaw rim below the molar region was evaluated [von Wilmowsky 2016]. In this animal study, implants were placed in mandibular rim of domestic pigs with chemically induced diabetes. After three months histomorphometry was performed and new bone height (NBH), bone-to-implant-contact (BIC), area of newly formed bone (NFB), bone-density (BD), and bone mineralization (BM) were measured. Authors stated that samples from the diabetic group had "irregularly shaped and thicker trabeculae", but did not quantify these findings. OADs can enhance bone formation [Kanazava 2018], which might have contributed to trabecular thickening in this subgroup. However, our histomorphometry results showed no significant differences in the trabecular angulus region. This might be because bone formation which led to trabecular thickening occurred at the time of tooth extraction, when occlusion height and muscle traction changed. If that had been the case, no obvious osteoid would be present at the time of sample collection, only mineralized bone tissue.

The same region showed a lower mineralized osteocyte lacunar number in all T2DM groups compared to controls. Since the rarity of mineralized lacunae is a general hallmark of younger bone, as suggested by other studies [Milovanovic 2015, Busse 2010, Weinkammer 2019], a low number of mineralized lacunae in this area may suggest that bone was entirely remodeled. However, a lower number of mineralized osteocyte lacunae in T2DM compared to controls might suggest even younger tissue age due to T2DM-related more intense remodeling. Potential mechanisms have been discussed in the section regarding trabecular bone of the molar region.

Next, buccal cortex of the angulus region showed a higher number of highly mineralized bone packets in the Insulin subgroup compared to the OAD group. Since insulin acts as an anabolic agent for bone tissue, it can be assumed that these hypermineralized bone packets were formed as a mineralization irregularity caused by T2DM and insulin therapy. Insulin binds to its intracellular receptors in osteoblasts through insulin receptor substrate (IRS) molecules, termed IRS-1 to IRS-4 [Thraillkil 2005]. It could be speculated that impaired insulin signaling in bone-forming cells results in a secondary and local insulin-growth factor (IGF) deficiency [Ogata 2000]. Perhaps it is the varying level of IGF that caused heterogeneity in bone mineralization, but this requires further investigation. The mineralization irregularity caused by insulin therapy in our research was comparable in two sites of the angulus region (trabecular bone and buccal cortex).

Finally, lingual cortex of the angulus region had less porous bone tissue in the T2DM whole group and in the OAD subgroup compared to the Control. More precisely, there was a bone filling effect of the open pores, which was evident in the micro-CT parameters depicting the open and total porosity as well as pore diameter, and in toluidine stainings as well. This finding is in agreement with our findings on other bone sites where bone formation was favored by OAD therapy, such as trabecular angulus and trabecular molar.

Since there was no tooth extraction in the region of angulus, or any other evident bone tissue damage which might have triggered targeted bone remodeling, microstructural changes of the angulus region in the T2DM can be caused by a combination of systemic factors (hyperglycemia, OAD or insulin therapy) and local factors (muscle traction, occlusion height) which acted upon bone tissue simultaneously. Hyperglycemia, OAD therapy and muscle traction could have triggered trabecular thickening in the angulus region, and cortical pore filling could be an adaptive mechanism to altered systemic and local conditions. Additionally, local factors which might have contributed to bone microstructure alterations in the molar region were: biting forces acting directly on the edentulous alveolar ridge, presence of a denture etc.

Additionally, the cortical thickness parameters were unchanged in the T2DM group in all regions. Since the cortical bone provides most of the primary stability for a dental implant, this parameter alone might encourage oral surgeons for a dental implant placement in T2DM patients. However, the surgeon should bear in mind other changed features which alter bone quality and affect long-term implant stability, such as hypermineralized bone areas, pore filling effect, crystal impurities etc.

Inter-site differences between angulus and molar regions in T2DM are in agreement with our proposed pathophysiological mechanism of bone tissue alterations in this disease. Bone volume ratio (BV/TV) was higher in lingual cortex of the angulus region in T2DM group and T2DM OAD subgroup compared to the same bony site of molar region. This finding speaks in favor of bone-filling effect in T2DM OAD angulus. Mineral-to-matrix ratio (v_1PO_4/pro) was higher in buccal cortex of the molar region in T2DM and T2DM OAD compared to the same bony site of angulus region. This finding can be put into relation with hydroxyapatite substitutions which have likely taken place at the tooth extraction site, as explained above. Also, calcium content showed higher variations in buccal cortex of the molar region of T2DM Insulin compared to the same cortex of the angulus. Similarly to intergroup findings, mineralization disturbance could have been caused by insulin, the anabolic agent, as explained above.

There are a couple of limitations to this study to acknowledge. Firstly, there was a limited number of individuals in the T2DM OAD and Insulin subgroups (n=5 in each subgroup). Secondly, values of glycosylated hemoglobin of T2DM individuals (HbA1c) were not known and could not have been accessed as a covariate in statistical analysis. However, since this is a pioneer research of bone quality in T2DM on human jaw bone, it offers valuable information both to researchers and clinicians in spite of these limitations.

Similar to T2DM jaw bone quality study, we compared the parameters of jaw bone microstructure, composition and bone cells in individuals with ALC and healthy controls in a site-specific manner. We observed substantial variability in bone quality between ALC and healthy controls as summarized below per each site investigated:
- the *trabecular* bone of the *molar* region showed smaller lacunae in ALC vs. controls;

61

- the *lingual* cortex of the *molar* region showed higher closed porosity in ALC compared to controls;
- the *buccal* cortex of the *molar* region had higher closed porosity and higher carbonate-to-phosphate ratio in ALC;
- the *trabecular* bone of the *angulus* region had lower calcium content, fewer highly mineralized bone packets, fewer octeoclasts and a tendency towards lower osteoblast number in ALC compared to Control;
- the *lingual* cortex of the *angulus* region showed a tendency towards higher open porosity and pore diameter in ALC;
- the *buccal* cortex of the *angulus* region showed higher closed porosity in ALC compared to controls (**Figure 24**).

Trabecular bone of the molar region showed significantly smaller osteocyte lacunae in ALC. This finding can be interpreted as a consequence of systemic inflammatory state present in ALC [Handzlik-Orlik 2016, Lopez-Larramona 2013]. As pointed out by González-Reimers (2014), ALC features direct toxic effect of ethanol on cellular viability, and possibly defective protein synthesis, which might cause formation of smaller osteocytes, and consequentially smaller osteocyte lacunae. qBEI method determined only the lacunar size and not the osteocyte size directly, so our assumption regarding smaller osteocytes in ALC remains to be quantified by other methods, such as transmission electron microscopy.

Lingual cortex of the molar region revealed higher closed porosity in ALC. Since higher porosity decreases bone strength, we can say that our finding is in agreement with previously published work on ALC at other skeletal sites, such as femur and lumbar spine [Wakolbinger 2019, Jadzic 2020, Culafic 2015]. Wakolbinger et al. (2019) found 32% higher cortical porosity of the femoral cortex using high-resolution peripheral quantitative computed tomography in clinical setting. Jadzic et al. (2020) reported microarchitectural deterioration of trabecular bone in lumbar spine of ALC cadaveric samples, manifested in reduced parameters such as BV/TN, Tb.Th and Tb.N. Culafic 2015 found thinner proximal femoral cortex in patients with ALC by hip structure analysis of dual X-ray absorptiometry (DXA) scans. Although bony site and local factors differ compared to our study, possible mechanism might be the same, that is, bone turnover might be disrupted by systemic inflammatory conditions, which result in ALC showing higher bone resorption in some skeletal sites. Stimulation of IL-6 production by ethanol, which activates RANKL and osteoclasts, is a possible mechanism for higher closed porosity found in our research [Wakolbinger 2019, Magdaleno 2017, Farbega 2005].
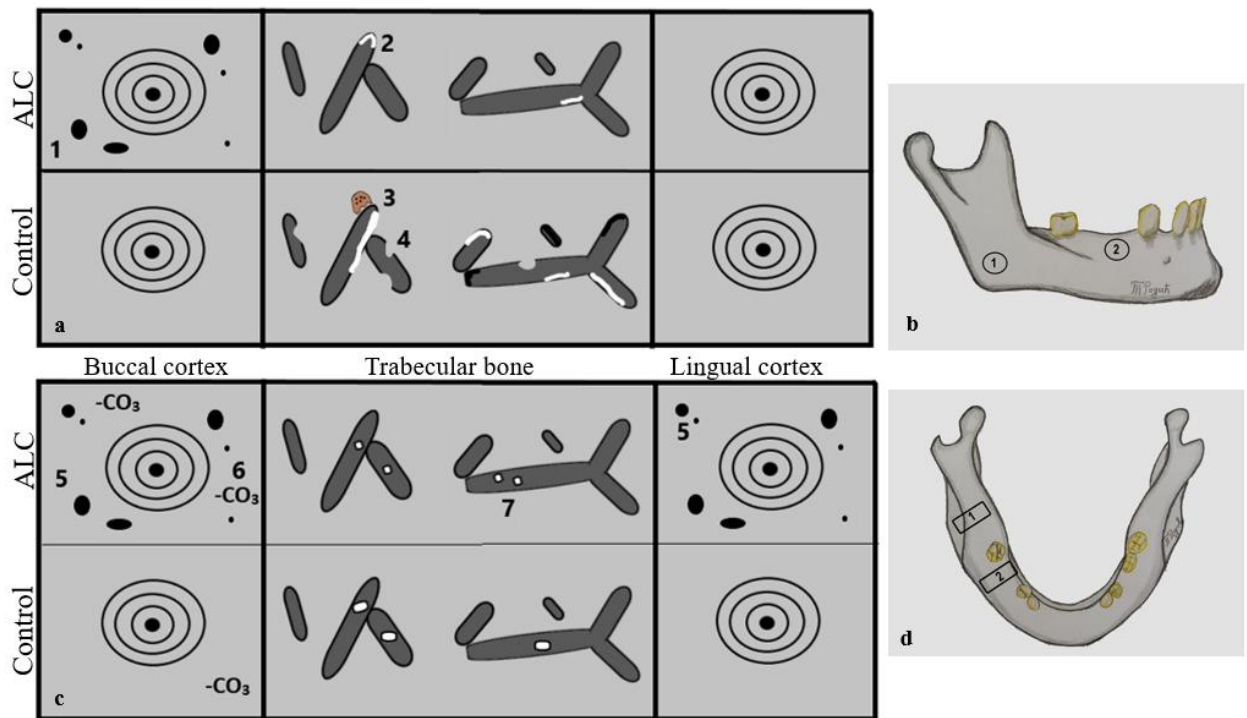
Figure 24: Schematic representation of bone microstructural, compositional, and cellular alterations in ALC and Control groups (**a** and **c**) Schematic representations of angulus and molar samples. Rows represent groups (ALC and Control) and columns represent bony sites within a sample (buccal cortex, trabecular bone and lingual cortex). (**a**) Angulus sample. 1: Higher closed porosity in buccal cortex in ALC group. 2: Lower calcium content in trabecular bone in ALC group. 3: Lower osteoclast number in trabecular bone in ALC group. 4: Lower eroded surface area in trabecular bone in ALC group. (**c**) Molar sample. 5: Higher closed porosity in buccal and lingual cortex in ALC group. 6: Higher carbonate content in buccal cortex in ALC group. 7: Higher lacunar number and lower lacunar area in trabecular bone in ALC group. (**b** and **d**) Drawings of mandible from different perspectives. 1: bone core site of a sample from the angulus region, 2: bone core site of a sample from the molar region

Buccal cortex of the molar region of the ALC group showed higher carbonate-to-phosphate ratio (v1CO3/v1PO4) and closed cortical porosity. As indicated in the T2DM section, higher carbonate values are present in bone tissue when the carbonate substitution inside hydroxyapatite crystals dominates over other possible substitutions such as fluoride, sodium etc. [Arcos 2020]. Carbonate substitutions of hydroxyapatite are interpreted as crystal impurities, which might increase crystal solubility [Arcos 2020, Boskey 2013]. Carbonate substitutions increase with age, impair mechanical features of bone tissue and result in higher risk of femoral neck fractures [Boskey 2013, Carretta 2013, Ojanen 2015]. Moreover, buccal cortex is often damaged during lower first molar extraction [Chrcanovic 2012]. Since ALC causes disturbances in bone formation, oxidative damage of bone cells and defective protein synthesis [González-Reimers, 2014], both higher closed cortical porosity and higher carbonate-to-phosphate ratio in this bony site are understandable findings.

The trabecular bone of the angulus region showed significantly lower values of mean calcium (Ca Mean) and hypermineralized bone (Ca High) in ALC compared to the Control. This bony site is less mineralized and has fewer packets of hypermineralized bone in ALC. Such bone possibly has altered mechanical characteristics, similar to osteoporotic bone which also had lower calcium values, as shown by Milovanovic 2015. Similarly, Culafic 2015 found lower areal BMD in proximal femora of patients' bone samples using DXA, linking the result to lower bone strength. Additionally, laboratory test revealed decreased osteocalcin and C telopeptide of collagen type 1 values, which signified reduced bone formation and increased bone resorption [Culafic 2015]. Giuliani et al. found reduced osteoblast proliferation and fewer colony-forming units for fibroblasts in ALC, which can explain lower BMD in these patients [Giuliani 1999]. Our finding of a tendency towards reduced osteoblast number in the trabecular bone of the angulus region is in agreement with Guiliani's work. It can therefore be assumed that ALC reduced an intake of minerals into the bone matrix of this jaw bone compartment. There is also a question of regional differences, since no other observed bony region in our research revealed similar feature of lower mean calcium and hypermineralized bone packets. Regional differences might be interpreted by the influence of local biomechanical factors. As for clinical significance of our finding, an oral or a maxillofacial surgeon should bear in mind that the trabecular bone of angulus region is softer in patients with ALC compared to healthy individuals. This would mean that a different amount of force is necessary for a bone transplant extraction from the ramus or that a titanium screw can be inserted with lower force from this region.

We found significantly lower resorption parameters and lower number of the newly embedded osteocytes and a tendency towards lower osteoblast number in the trabecular bone of the angulus region in the ALC group. The osteoclastic activity was zero in this region in ALC, unlike the corresponding region of the control group and all other regions of the ALC group. There is an ongoing debate on effects of ALC on bone turnover [Jeong & Kim, 2019; Monegal et al. 2007a]. It is generally accepted that ethanol decreases bone formation, but there is some controversy regarding its effects on bone resorption. According to some studies, ethanol causes both decreased bone formation and increased bone resorption [Gonzales-Reimers, 2015]. Our findings seem to be in agreement with current understanding of bone tissue dynamics in ALC.

Lingual cortex of the angulus region had unchanged closed porosity in ALC, but had a tendency towards higher open porosity and higher pore diameter. Higher open porosity could be a sign of a greater bone tissue fragility. Differences between lingual cortex of the angulus region and other cortices could result from a different microenvironment in terms of the forces acting on the bone, the age of the bone, lower remodeling rate, lower viability of the tissue etc.

We showed that angulus and molar regions were differently affected by ALC, as described above. Direct inter-site comparisons revealed that microstructural parameter fractal dimension was higher in molar region compared to angulus in ALC, which speaks for inferior geometric structure of the angulus bony site [Kurşun-Çakmak, 2018]. Likely explanation is that trabecular bone in the molar region was remodeled after tooth extraction, under the influence of local and biomechanical factors as well. Next, there was higher cortical thickness of buccal cortex of the molar region relative to the angulus region, likely due to the reparatory process after tooth extraction in the molar region [Thomes, 2021]. Lastly, higher mineral-to-matrix ratio in trabecular bone of the molar region of ALC compared to the angulus region may suggest lower strength of the

angulus region in individuals with ALC [Boskey 2013, Milovanovic 2015, Rolvien 2018].

There are a couple limitations of the ALC study to acknowledge. First, sample number in the ALC group was limited to n=6. Second, the duration of alcohol consumption and duration of ALC diagnosis were unknown. If there had been a larger sample number that could have been divided into subgroups based on the duration of ALC, possibly the obtained results would have revealed more information on jaw bone quality in ALC. However, since this is pioneer research on jaw bone quality in ALC, it offers valuable information both to researchers and clinicians in spite of these limitations.

6. Conclusion

First, the results of our post-mortem study indicated that T2DM caused microarchitectural alterations of the jaw bone, manifested by simpler microarchitectural geometry of the trabecular molar region and higher trabecular thickness at the trabecular angulus. Both insulin and OAD therapy favored bone remodeling, where OADs caused more intense resorption in the trabecular molar region several years after tooth extraction, and Insulin therapy predominantly caused alterations in matrix mineralization. OAD therapy had a filling effect of cortical pores in the lingual cortex of the angulus region. Insulin therapy created packets of highly mineralized bone and layers of bone tissue of different calcium content in both of the observed regions of the mandible. Bone tissue in cases receiving OAD therapy had altered carbonate content compared with the healthy bone. Lower number of mineralized lacunae in T2DM compared with controls might suggest even younger tissue age due to DM-related faster remodeling. Cortical thickness of the jaw remained unchanged in T2DM. Taken together, all alterations to bone quality must have developed under a combination of local and systemic factors specific for each bony site of the jaw. Further research is required to explain the mechanisms of such bone tissue alterations in diabetic patients. Based on the current data, there is generally no contraindication for the implant placement in T2DM patients as far as bone microstructure and composition are concerned. Nevertheless, alterations to bone quality might affect implant's long-term stability, which requires further studies.

Second, we found that ALC causes microstructural alterations of the jaw bone, manifested by higher closed cortical porosity in cortical bone, as well as lower lacunar size in the trabecular bone of the molar region. Trabecular bone of the angulus region had lower calcium content and lower resorptive activity in the ALC individuals than in the corresponding regions of the healthy individuals. Bone chemical composition was altered in buccal cortex of the molar region, with higher carbonate content in ALC compared with healthy individuals. Such bone tissue characteristics must have developed under a combination of systemic and local factors specific for each bony site of the jaw. Our findings lead to a conclusion that jaw bone quality is altered in ALC in terms of microstructure, mineralization, tissue composition and cellular activity. It is possible that jaw bone in ALC has altered mechanical characteristics, but this needs further research. Oral and maxillofacial surgeons should approach patients with ALC with caution during surgical procedures involving bone, due to alterations in jaw bone quality.

This thesis found that T2DM and ALC alter bone quality of the mandible, and that alterations caused by T2DM and ALC differentially affect various bony sites and compartments of the mandible. Moreover, site-specific differences in bone quality between the angulus region of the mandible and the edentulous alveolar bone in the region of first lower molar are of interest to oral and maxillofacial surgeons. This thesis indirectly provided more possibilities for dental implant insertion and the titanium screw placement in patients with T2DM. In ALC patients, surgeons should bear in mind altered jaw bone tissue characteristics when performing interventions involving bone tissue. Taken together, the results provided by this thesis likely provide the structural basis for consideration during making treatment plan in oral and maxillofacial surgery of these patients.

All in all, this research has shed more light on the microarchitectural and microstructural characteristics of the jaw bone of individuals with T2DM and ALC. These findings are of interest to oral and maxillofacial surgeons since they offer more possibilities during the dental implant insertion and titanium screw placement in these patients. Oral implantology protocols might be altered after this research and alcohol consumption might no longer be considered a relative contraindication for oral interventions on bone, at least when it comes to the bone tissue status of these patients.

7. References

Achemlal L, Tellal S, Rkiouak F, et al. Bone metabolism in male patients with type 2 diabetes. Clin Rheumatol. 2005;24(5):493-496. doi:10.1007/s10067-004-1070-9

Andrade VFC, Besen D, Chula DC, Borba VZC, Dempster D, Moreira CA. Bone Marrow Adiposity in Premenopausal Women With Type 2 Diabetes With Observations on Peri-Trabecular Adipocytes. J Clin Endocrinol Metab. 2021 Aug 18;106(9):e3592-e3602. doi: 10.1210/clinem/dgab322. PMID: 33974069.

Aguilar-Salvatierra A, Calvo-Guirado JL, González-Jaranay M, Moreu G, Delgado-Ruiz RA, Gómez-Moreno G (2016) Peri-implant evaluation of immediately loaded implants placed in esthetic zone in patients with diabetes mellitus type 2: a two-year study. Clin Oral Implants Res. 27(2):156-61. doi: 10.1111/clr.12552

Akyol UK, Güngörmüş M (2010) Effect of biostimulation on healing of bone defects in diabetic rats. Photomed Laser Surg. 28(3):411-6. doi: 10.1089/pho.2008.2478

Alrabiah M, Al-Aali KA, Al-Sowygh ZH, Binmahfooz AM, Mokeem SA, Abduljabbar T (2018) Association of advanced glycation end products with peri-implant inflammation in prediabetes and type 2 diabetes mellitus patients.Clin Implant Dent Relat Res. 20(4):535-540. doi: 10.1111/cid.12607

Alsaadi G, Quirynen M, Komárek A, van Steenberghe D (2008) Impact of local and systemic factors on the incidence of late oral implant loss.Clin Oral Implants Res. 19(7):670-6. doi: 10.1111/j.1600-0501.2008.01534.x

Arcos D, Vallet-Regí M. Substituted hydroxyapatite coatings of bone implants. J Mater Chem B. 2020 Mar 4;8(9):1781-1800. doi: 10.1039/c9tb02710f. PMID: 32065184; PMCID: PMC7116284.

Bernhard A, Milovanovic P, Zimmermann EA, Hahn M, Djonic D, Krause M, Breer S, Püschel K, Djuric M, Amling M, Busse B (2013) Micro-morphological properties of osteons reveal changes in cortical bone stability during aging, osteoporosis, and bisphosphonate treatment in women. Osteoporos Int. 24(10):2671-80. doi: 10.1007/s00198-013-2374-x

Boskey AL. Bone composition: relationship to bone fragility and antiosteoporotic drug effects. Bonekey Rep. 2013 Dec 4;2:447. doi: 10.1038/bonekey.2013.181. Erratum in: Bonekey Rep. 2015;4:710. PMID: 24501681; PMCID: PMC3909232.

Bulut E, Baş B, Altunkaynak BZ, Bekçioğlu B, Erdem Koç G, Gönülol E, Önger ME, Kaplan S (2014) Efficacy of Ankaferd Blood Stopper on bone healing in diabetic rats: a stereological and histopathological study, Biotechnic & Histochemistry, 89:7, 535-543. doi:10.3109/10520295.2014.906657

Burghardt AJ, Issever AS, Schwartz AV, Davis KA, Masharani U, Majumdar S, Link TM. High-resolution peripheral quantitative computed tomographic imaging of cortical and trabecular bone microarchitecture in patients with type 2 diabetes mellitus. J Clin Endocrinol Metab. 2010 Nov;95(11):5045-55. doi: 10.1210/jc.2010-0226. Epub 2010 Aug 18. PMID: 20719835; PMCID: PMC2968722.

Busse B, Djonic D, Milovanovic P, Hahn M, Püschel K, Ritchie RO, Djuric M, Amling M (2010) Decrease in the osteocyte lacunar density accompanied by hypermineralized lacunar occlusion reveals failure and delay of remodeling in aged human bone. Aging Cell. 9(6):1065-75. doi: 10.1111/j.1474-9726.2010.00633.x

Carretta R, Stüssi E, Müller R, Lorenzetti S. Within subject heterogeneity in tissue-level post-yield mechanical and material properties in human trabecular bone. J Mech Behav Biomed Mater. 2013 Aug;24:64-73. doi: 10.1016/j.jmbbm.2013.04.014. Epub 2013 Apr 23. PMID: 23683760.

Castellanos-Cosano L, Rodriguez-Perez A, Spinato S, Wainwright M, Machuca-Portillo G, Serrera-Figallo MA, Torres-Lagares D (2019) Descriptive retrospective study analyzing relevant factors related to dental implant failure. Med Oral Patol Oral Cir Bucal. 24(6):e726-e738. doi: 10.4317/medoral.23082

Cirovic A, Vujacic M, Petrovic B, Cirovic A, Zivkovic V, Nikolic S, Djonic D, Bascarevic Z, Djuric M, Milovanovic P. Vascular Complications in Individuals with Type 2 Diabetes Mellitus Additionally Increase the Risk of Femoral Neck Fractures Due to Deteriorated Trabecular Microarchitecture. Calcif Tissue Int. 2022 Jan;110(1):65-73. doi: 10.1007/s00223-021-00894-5. Epub 2021 Jul 24. PMID: 34302494; PMCID: PMC8302969.

Chrcanovic BR, Albrektsson T, Wennerberg A (2014) Diabetes and oral implant failure: a systematic review. J Dent Res. 93(9):859-67. doi: 10.1177/0022034514538820

Chrcanovic BR. Fixation of mandibular angle fractures: clinical studies (2014) Oral Maxillofac Surg. 18(2):123-52. doi: 10.1007/s10006-012-0374-1

Chrcanovic BR. Factors influencing the incidence of maxillofacial fractures. Oral Maxillofac Surg. 2012 Mar;16(1):3-17. doi: 10.1007/s10006-011-0280-y. Epub 2011 Jun 9. PMID: 21656125.

Creecy A, Uppuganti S, Merkel AR, O'Neal D, Makowski AJ, Granke M, Voziyan P, Nyman JS (2016) Changes in the Fracture Resistance of Bone with the Progression of Type 2 Diabetes in the ZDSD Rat. Calcif Tissue Int. 99(3):289-301. doi: 10.1007/s00223-016-0149-z

Creecy A, Uppuganti S, Unal M, Clay Bunn R, Voziyan P, Nyman JS (2018) Low bone toughness in the TallyHO model of juvenile type 2 diabetes does not worsen with age. Bone. 110:204-214. doi: 10.1016/j.bone.2018.02.005

Culafić Dj, Djonic D, Culafic-Vojinovic V, Ignjatovic S, Soldatovic I, Vasic J, Beck TJ, Djuric M. Evidence of degraded BMD and geometry at the proximal femora in male patients with alcoholic liver cirrhosis. Osteoporos Int. 2015 Jan;26(1):253-9.

Cunha JS, Ferreira VM, Maquigussa E, Naves MA, Boim MA. Effects of high glucose and high insulin concentrations on osteoblast function in vitro. Cell Tissue Res. 2014 Oct;358(1):249-56. doi: 10.1007/s00441-014-1913-x. Epub 2014 May 25. PMID: 24859221.

Dempster DW, Compston JE, Drezner MK, Glorieux FH, Kanis JA, Malluche H, Meunier PJ, Ott SM, Recker RR, Parfitt AM (2013) Standardized nomenclature, symbols, and units for bone histomorphometry: a 2012 update of the report of the ASBMR Histomorphometry Nomenclature Committee. J Bone Miner Res. 28(1):2-17. doi: 10.1002/jbmr.1805

El Maghraoui A, Sadni S, Rezqi A, Bezza A, Achemlal L, Mounach A. Does Rheumatoid Cachexia Predispose Patients with Rheumatoid Arthritis to Osteoporosis and Vertebral Fractures? J Rheumatol. 2015 Sep;42(9):1556-62. doi: 10.3899/jrheum.141629. Epub 2015 Aug 1. PMID: 26233497.

Eskow CC, Oates TW (2017) Dental Implant Survival and Complication Rate over 2 Years for Individuals with Poorly Controlled Type 2 Diabetes Mellitus. Clin Implant Dent Relat Res. 19(3):423-431. doi: 10.1111/cid.12465.

Fan Y, Wei F, Lang Y, Liu Y. Diabetes mellitus and risk of hip fractures: a meta-analysis. Osteoporos Int. 2016 ;27(1):219-28.

Fábrega E, Orive A, García-Suarez C, García-Unzueta M, Antonio Amado J, Pons-Romero F. Osteoprotegerin and RANKL in alcoholic liver cirrhosis. Liver Int. 2005 Apr;25(2):305-10.

Ferrato G, Falisi G, Ierardo G, Polimeni A, Di Paolo C (2017) Digital evaluation of occlusal forces: comparison between healthy subjects and TMD patients. Ann Stomatol (Roma). 8(2):79-88. doi: 10.11138/ads/2017.8.2.089

Fiedler IAK, Schmidt FN, Wölfel EM, Plumeyer C, Milovanovic P, Gioia R, Tonelli F, Bale HA, Jähn K, Besio R, Forlino A, Busse B (2018) Severely Impaired Bone Material Quality in Chihuahua Zebrafish Resembles Classical Dominant Human Osteogenesis Imperfecta. J Bone Miner Res. 33(8):1489-1499. doi: 10.1002/jbmr.3445

Gennari L, Merlotti D, Valenti R, Ceccarelli E, Ruvio M, Pietrini MG, Capodarca C, Franci MB, Campagna MS, Calabrò A, Cataldo D, Stolakis K, Dotta F, Nuti R. Circulating sclerostin levels and bone turnover in type 1 and type 2 diabetes. J Clin Endocrinol Metab. 2012 May;97(5):1737-44. doi: 10.1210/jc.2011-2958. Epub 2012 Mar 7. PMID: 22399511.

González-Reimers E, Santolaria-Fernández F, Martín-González MC, Fernández-Rodríguez CM, Quintero-Platt G. Alcoholism: a systemic proinflammatory condition. World J Gastroenterol. 2014 Oct 28;20(40):14660-71. doi: 10.3748/wjg.v20.i40.14660. PMID: 25356029; PMCID: PMC4209532.

González-Reimers E, Quintero-Platt G, Rodríguez-Rodríguez E, Martínez-Riera A, Alvisa-Negrín J, Santolaria-Fernández F. Bone changes in alcoholic liver disease. World J Hepatol. 2015 May 28;7(9):1258-64. doi: 10.4254/wjh.v7.i9.1258. PMID: 26019741; PMCID: PMC4438500.

Giuliani N, Girasole G, Vescovi PP, Passeri G, Pedrazzoni M. Ethanol and acetaldehyde inhibit the formation of early osteoblast progenitors in murine and human bone marrow cultures. Alcohol Clin Exp Res 1999; 23: 381-385 [PMID: 10069572 DOI: 10.1111/j.1530-0277.1999.tb04126.x]

Grønkjær LL, Holmstrup P, Schou S, Schwartz K, Kongstad J, Jepsen P, Vilstrup H. Presence and consequence of tooth periapical radiolucency in patients with cirrhosis. Hepat Med. 2016 Sep 13;8:97-103.

Goss AN, Sambrook PJ (2013) Diabetes, wound healing and complications: authors' reply. Aust Dent J. 58(4):536-7. doi: 10.1111/adj.12117_2

Guggenheimer J, Eghtesad B, Close JM, Shay C, Fung JJ. Dental health status of liver transplant candidates. Liver Transpl. 2007 Feb;13(2):280-6

Guja C, Guja L, Miulescu RD (2019) Effect of type 2 diabetes medications on fracture risk. Ann Transl Med. 7(20):580. doi: 10.21037/atm.2019.09.51

Hammond MA, Gallant MA, Burr DB, Wallace JM (2014) Nanoscale changes in collagen are reflected in physical and mechanical properties of bone at the microscale in diabetic rats. Bone. 60:26-32. doi: 10.1016/j.bone.2013.11.015

He C, Shan Y, Song W. Targeting gut microbiota as a possible therapy for diabetes. Nutr Res. 2015 May;35(5):361-7. doi: 10.1016/j.nutres.2015.03.002. Epub 2015 Mar 14. PMID: 25818484.

He B, Li SQ, Wang W, Han P (2004) [Maternal serum lipid at 36-42 weeks' gestation and their relationship to newborn weight in pregnant women with gestational diabetes

mellitus and type 1 and type 2 diabetes mellitus]. Zhonghua Fu Chan Ke Za Zhi 39(10):675–677 (Chinese)

Huang S, Dang H, Huynh W, Sambrook PJ, Goss AN. The healing of dental extraction sockets in patients with Type 2 diabetes on oral hypoglycaemics: a prospective cohort. Aust Dent J. 2013;58(1):89-93. doi:10.1111/adj.12029

Jadzic J, Cvetkovic D, Milovanovic P, Tomanovic N, Zivkovic V, Nikolic S, Djuric M, Djonic D. The micro-structural analysis of lumbar vertebrae in alcoholic liver cirrhosis. Osteoporos Int. 2020 Jun 24.

Javid AZ, Hormoznejad R, Yousefimanesh HA, Haghighi-Zadeh MH, Zakerkish M (2019) Impact of resveratrol supplementation on inflammatory, antioxidant, and periodontal markers in type 2 diabetic patients with chronic periodontitis. Diabetes Metab Syndr. 13(4):2769-2774. doi: 10.1016/j.dsx.2019.07.042

Jeong HM, Kim DJ. Bone Diseases in Patients with Chronic Liver Disease. Int J Mol Sci. 2019 Aug 31;20(17):4270. doi: 10.3390/ijms20174270. PMID: 31480433; PMCID: PMC6747370.

Jiajue R1, Jiang Y, Wang O, Li M, Xing X, Cui L, Yin J, Xu L, Xia W (2014) Suppressed bone turnover was associated with increased osteoporotic fracture risks in non-obese postmenopausal Chinese women with type 2 diabetes mellitus. Osteoporos Int. 25(8):1999-2005. doi: 10.1007/s00198-014-2714-5

Jokanovic, dr Vukoman. (2014). Инструменталне методе кључ разумевања нанотехнологије и наномедицине. 10.13140/2.1.2949.5684.

Kanazawa I, Sugimoto T (2018) Diabetes Mellitus-induced Bone Fragility. Intern Med. 57(19):2773-2785. doi: 10.2169/internalmedicine.0905-18

Karim L, Moulton J, Van Vliet M, Velie K, Robbins A, Malekipour F, Abdeen A, Ayres D, Bouxsein ML. Bone microarchitecture, biomechanical properties, and advanced glycation end-products in the proximal femur of adults with type 2 diabetes. Bone. 2018 Sep;114:32-39. doi: 10.1016/j.bone.2018.05.030. Epub 2018 May 30. PMID: 29857063; PMCID: PMC6141002.

Kasahara T, Imai S, Kojima H, Katagi M, Kimura H, Chan L, Matsusue Y. Malfunction of bone marrow-derived osteoclasts and the delay of bone fracture healing in diabetic mice. Bone. 2010 Sep;47(3):617-25. doi: 10.1016/j.bone.2010.06.014. Epub 2010 Jun 19. PMID: 20601287; PMCID: PMC2926189.

Kudiyirickal MG, Pappachan JM (2015) Diabetes mellitus and oral health. Endocrine. 49(1):27-34. doi: 10.1007/s12020-014-0496-3

Kurşun-Çakmak EŞ, Bayrak S (2018) Comparison of fractal dimension analysis and panoramic-based radiomorphometric indices in the assessment of mandibular bone changes in patients with type 1 and type 2 diabetes mellitus. Oral Surg Oral Med Oral Pathol Oral Radiol. 126(2):184-191. doi: 10.1016/j.oooo.2018.04.010

Liu R, Bal HS, Desta T, Krothapalli N, Alyassi M, Luan Q, Graves DT (2006) Diabetes enhances periodontal bone loss through enhanced resorption and diminished bone formation. J. Dent. Res 85 510–514. doi: 10.1177/154405910608500606.

Magdaleno F, Blajszczak CC, Nieto N. Key Events Participating in the Pathogenesis of Alcoholic Liver Disease. Biomolecules. 2017 Jan 27;7(1):9.

Mandair GS, Morris MD (2015) Contributions of Raman spectroscopy to the understanding of bone strength. Bonekey Rep. 4:620. doi: 10.1038/bonekey.2014.115

Mansur SA, Mieczkowska A, Flatt PR, Chappard D, Irwin N, Mabilleau G (2019) The GLP-1 Receptor Agonist Exenatide Ameliorates Bone Composition and Tissue Material Properties in High Fat Fed Diabetic Mice.Front Endocrinol (Lausanne). 10:51. doi: 10.3389/fendo.2019.00051

Marchand F, Raskin A, Dionnes-Hornes A, Barry T, Dubois N, Valéro R, Vialettes B (2012) Dental implants and diabetes: conditions for success. Diabetes Metab. 38(1):14-9. doi: 10.1016/j.diabet.2011.10.002.

Mauri-Obradors E, Merlos A, Estrugo-Devesa A, Jané-Salas E, López-López J, Viñas M (2018) Benefits of non-surgical periodontal treatment in patients with type 2 diabetes mellitus and chronic periodontitis: A randomized controlled trial. J Clin Periodontol. 45(3):345-353. doi: 10.1111/jcpe.12858

Milovanovic P, Zimmermann EA, Riedel C, vom Scheidt A, Herzog L, Krause M, Djonic D, Djuric M, Püschel K, Amling M, Ritchie RO, Busse B (2015) Multi-level characterization of human femoral cortices and their underlying osteocyte network reveal trends in quality of young, aged, osteoporotic and antiresorptive-treated bone. Biomaterials. 45:46-55. doi: 10.1016/j.biomaterials.2014.12.024

Milovanovic P, Vom Scheidt A, Mletzko K, Sarau G, Püschel K, Djuric M, Amling M, Christiansen S, Busse B (2018) Bone tissue aging affects mineralization of cement lines. Bone. 110:187-193. doi: 10.1016/j.bone.2018.02.004

Monegal A, Navasa M, Peris P, Alvarez L, Pons F, Rodés J, Guañabens N. Serum osteoprotegerin and its ligand in cirrhotic patients referred for orthotopic liver transplantation: relationship with metabolic bone disease. Liver Int. 2007 May;27(4):492-7. doi: 10.1111/j.1478-3231.2007.01448.x. PMID: 17403189.

Murray CE, Coleman CM. Impact of Diabetes Mellitus on Bone Health. Int J Mol Sci. 2019 Sep 30;20(19):4873. doi: 10.3390/ijms20194873. PMID: 31575077; PMCID: PMC6801685.

Naujokat H, Kunzendorf B, Wiltfang J (2016) Dental implants and diabetes mellitus-a systematic review. Int J Implant Dent. 2(1):5. doi: 10.1186/s40729-016-0038-2.

NCD Risk Factor Collaboration (NCD-RisC) (2016) Worldwide trends in diabetes since 1980: a pooled analysis of 751 population-based studies with 4.4 million participants. Lancet 387(10027):1513–1530. https://doi.org/10.1016/S0140-6736(16)00618-8

Napoli N, Chandran M, Pierroz DD, Abrahamsen B, Schwartz AV, Ferrari SL (2017) IOF Bone and Diabetes Working Group. Mechanisms of diabetes mellitus-induced bone fragility. Nat Rev Endocrinol. 13(4):208-219. doi: 10.1038/nrendo.2016.153

Nemtoi A, Ladunca O, Dragan E, Budacu C, Mihai C, Haba D (2013) Quantitative and qualitative bone assessment of the posterior mandible in patients with diabetes mellitus: a cone beam computed tomography study. Rev Med Chir Soc Med Nat Iasi. 117(4):1002-8

Oates TW Jr, Galloway P, Alexander P, Vargas Green A, Huynh-Ba G, Feine J, McMahan CA. (2014) The effects of elevated hemoglobin A(1c) in patients with type 2 diabetes mellitus on dental implants: Survival and stability at one year. J Am Dent Assoc. 145(12):1218-26. doi: 10.14219/jada.2014.93

Oates TW, Huynh-Ba G, Vargas A, Alexander P, Feine J (2013) A critical review of diabetes, glycemic control, and dental implant therapy. Clin Oral Implants Res. 24(2):117-27. doi: 10.1111/j.1600-0501.2011.02374.x

Oettinger-Barak O, Machtei EE, Barak S, Baruch Y, Ardekian L, Peled M. Periodontal changes in liver cirrhosis and post-transplantation patients. II: radiographic findings: J Periodontol. 2002 Mar;73(3):313-6.

Ogata N, Chikazu D, Kubota N, Terauchi Y, Tobe K, Azuma Y, Ohta T, Kadowaki T, Nakamura K, Kawaguchi H (2000) Insulin receptor substrate-1 in osteoblast is indispensable for maintaining bone turnover. J Clin Invest. 105(7):935-43. doi: 10.1172/JCI9017.

Ojanen X, Isaksson H, Töyräs J, Turunen MJ, Malo MK, Halvari A, Jurvelin JS. Relationships between tissue composition and viscoelastic properties in human trabecular bone. J Biomech. 2015 Jan 21;48(2):269-75. doi: 10.1016/j.jbiomech.2014.11.034. Epub 2014 Dec 3. PMID: 25498367.

Osima M, Kral R, Borgen TT, Høgestøl IK, Joakimsen RM, Eriksen EF, Bjørnerem Å. Women with type 2 diabetes mellitus have lower cortical porosity of the proximal

femoral shaft using low-resolution CT than nondiabetic women, and increasing glucose is associated with reduced cortical porosity. Bone. 2017 Apr;97:252-260. doi: 10.1016/j.bone.2017.01.037. Epub 2017 Feb 1. PMID: 28161589.

Pacicca DM, Brown T, Watkins D, Kover K, Yan Y, Prideaux M, Bonewald L. Elevated glucose acts directly on osteocytes to increase sclerostin expression in diabetes. Sci Rep. 2019 Nov 22;9(1):17353. doi: 10.1038/s41598-019-52224-3. PMID: 31757981; PMCID: PMC6874765.

Pacios S, Andriankaja O, Kang J, Alnammary M, Bae J, de Brito Bezerra B, Schreiner H, Fine DH, Graves DT. Bacterial infection increases periodontal bone loss in diabetic rats through enhanced apoptosis. Am J Pathol. 2013 Dec;183(6):1928-1935. doi: 10.1016/j.ajpath.2013.08.017. Epub 2013 Oct 8. PMID: 24113454; PMCID: PMC5745547.

Pacios S, Kang J, Galicia J, Gluck K, Patel H, Ovaydi-Mandel A, Petrov S, Alawi F, Graves DT (2012) Diabetes aggravates periodontitis by limiting repair through enhanced inflammation. FASEB J 26 1423–1430. doi: 10.1096/fj.11-196279.

Palermo A, D'Onofrio L, Buzzetti R, Manfrini S, Napoli N. (2017) Pathophysiology of Bone Fragility in Patients with Diabetes. Calcif Tissue Int. 100(2):122-132. doi: 10.1007/s00223-016-0226-3

Parihar AS, Madhuri S, Devanna R, Sharma G, Singh R, Shetty K (2020) Assessment of failure rate of dental implants in medically compromised patients. J Family Med Prim Care 9:883-5. doi: 10.4103/jfmpc.jfmpc_989_19.

Pascart T, Falgayrac G, Migaud H, Quinchon J, Norberciak L, Budzik JF, Paccou J, Cotten A, Penel G, Cortet B (2017) Region specific Raman spectroscopy analysis of the femoral head reveals that trabecular bone is unlikely to contribute to non-traumatic osteonecrosis. Sci Rep. 7(1):97. doi: 10.1038/s41598-017-00162-3

Paschalis EP, Gamsjaeger S, Tatakis DN, Hassler N, Robins SP, Klaushofer K (2015) Fourier transform Infrared spectroscopic characterization of mineralizing type I collagen enzymatic trivalent cross-links. Calcif Tissue Int. 96(1):18-29. doi: 10.1007/s00223-014-9933-9

Paschalis EP, Gamsjaeger S, Klaushofer K (2017) Vibrational spectroscopic techniques to assess bone quality. Osteoporos Int. 28(8):2275-2291. doi: 10.1007/s00198-017-4019-y

Peled M, Ardekian L, Tagger-Green N, Gutmacher Z, Machtei EE (2003) Dental implants in patients with type 2 diabetes mellitus: a clinical study. Implant Dent. 12(2):116-22. doi: 10.1097/01.id.0000058307.79029.b1.

Picke AK, Campbell G, Napoli N, Hofbauer LC, Rauner M (2019) Update on the impact of type 2 diabetes mellitus on bone metabolism and material properties. Endocr Connect. 8(3):R55-R70. doi: 10.1530/EC-18-0456

Pietschmann P, Patsch JM, Schernthaner G. Diabetes and bone. Horm Metab Res. 2010 Oct;42(11):763-8. doi: 10.1055/s-0030-1262825. Epub 2010 Aug 13. PMID: 20711953

Power DJ, Sambrook PJ, Goss AN. The healing of dental extraction sockets in insulin-dependent diabetic patients: a prospective controlled observational study. Aust Dent J. 2019;64(1):111-116. doi:10.1111/adj.12669

Rao W, Benzi R (2007) Single mandibular first molar implants with flapless guided surgery and immediate function: preliminary clinical and radiographic results of a prospective study. J Prosthet Dent. 97(6 Suppl):S3-S14. doi: 10.1016/S0022-3913(07)60003-1

Rigawa A, Oka S, Tanaka S, Nakano M, Aoyama T, Watari I, Aikata H, Arihiro K, Chayama K. Small bowel metastasis of hepatocellular carcinoma detected by capsule endoscopy. Case Rep Gastroenterol. 2013 Nov 28;7(3):492-7.

Rolvien T, Vom Scheidt A, Stockhausen KE, Milovanovic P, Djonic D, Hubert J, Hawellek T, Wacker A, Jebens V, Püschel K, Zimmermann EA, Djuric M, Amling M, Busse B (2018) Inter-site variability of the osteocyte lacunar network in the cortical bone underpins fracture susceptibility of the superolateral femoral neck. Bone. 112:187-193. doi: 10.1016/j.bone.2018.04.018

Roschger P, Paschalis EP, Fratzl P, Klaushofer K (2008) Bone mineralization density distribution in health and disease. Bone. 42(3):456-66. doi: 10.1016/j.bone.2007.10.021.

Saito M, Kida Y, Kato S, Marumo K (2014) Diabetes, collagen, and bone quality. Curr Osteoporos Rep. 12(2):181-8. doi: 10.1007/s11914-014-0202-7

Schneider, C.A., Rasband, W.S., Eliceiri, K.W (2012) "NIH Image to ImageJ: 25 years of image analysis". Nature Methods 9, 671-675. doi: 10.1038/nmeth.2089.

Schuppan D, Afdhal NH. Liver cirrhosis. Lancet. 2008 Mar 8;371(9615):838-51.

Sella-Tunis T, Pokhojaev A, Sarig R, O'Higgins P, May H (2018) Human mandibular shape is associated with masticatory muscle force. Sci Rep. 8(1):6042. doi: 10.1038/s41598-018-24293-3

Silva Santos PS, Fernandes KS, Gallottini MH. Assessment and management of oral health in liver transplant candidates. J Appl Oral Sci. 2012 Mar-Apr;20(2):241-5.

Singh R, Parihar AS, Vaibhav V, Kumar K, Singh R, Jerry JJ (2020) A 10 years retrospective study of assessment of prevalence and risk factors of dental implants failures. J Family Med Prim Care 9:1617-9.

Shanbhogue VV, Mitchell DM, Rosen CJ, Bouxsein ML. Type 2 diabetes and the skeleton: new insights into sweet bones. Lancet Diabetes Endocrinol. 2016 Feb;4(2):159-73. doi: 10.1016/S2213-8587(15)00283-1. Epub 2015 Sep 11. PMID: 26365605.

Shah FA, Sayardoust S, Thomsen P, Palmquist A (2019) Extracellular matrix composition during bone regeneration in the human dental alveolar socket. Bone. 127:244-249. doi: 10.1016/j.bone.2019.06.003

Smeets R1, Henningsen A, Jung O, Heiland M, Hammächer C, Stein JM (2014) Definition, etiology, prevention and treatment of peri-implantitis--a review. Head Face Med. 10:34. doi: 10.1186/1746-160X-10-34

Thrailkill KM, Lumpkin CK Jr, Bunn RC, Kemp SF, Fowlkes JL (2005) Is insulin an anabolic agent in bone? Dissecting the diabetic bone for clues. Am J Physiol Endocrinol Metab. 289(5):E735-45. doi: 10.1152/ajpendo.00159.2005.

Tomczyk S, Whitten T, Holzbauer SM, Lynfield R(2018) Combating antibiotic resistance: a survey on the antibiotic-prescribing habits of dentists. Gen Dent. 66(5):61-68

Wakolbinger R, Muschitz C, Scheriau G, Bodlaj G, Kocijan R, Feichtinger X, Schanda JE, Haschka J, Resch H, Pietschmann P. Bone microarchitecture and bone turnover in hepatic cirrhosis. Osteoporos Int. 2019 Jun;30(6):1195-1204. doi: 10.1007/s00198-019-04870-6. Epub 2019 Feb 20. PMID: 30788527; PMCID: PMC6546655.

Ward III NH, Wainwright DJ (2015) Outcomes Research: Mandibular Fractures in the Diabetic Population. Journal of Cranio-Maxillofacial Surgery. doi: 10.1016/j.jcms.2015.09.001

Weinkamer R, Kollmannsberger P, Fratzl P (2019) Towards a Connectomic Description of the Osteocyte Lacunocanalicular Network in Bone.Curr Osteoporos Rep. 17(4):186-194. doi: 10.1007/s11914-019-00515-z

WHO: Global Report on Diabetes 2017; NCD-RisC https://apps. who.int/iris/bitstream/handle/10665/204871/9789241565257_eng.pdf;jsessionid=A3890 983DA4DA8727ABC73AD6167E736?sequence=1.Accessed Nov 2019

Wittrant Y, Gorin Y, Woodruff K, Horn D, Abboud HE, Mohan S, Abboud-Werner SL. High d(+)glucose concentration inhibits RANKL-induced osteoclastogenesis. Bone.

2008 Jun;42(6):1122-30. doi: 10.1016/j.bone.2008.02.006. Epub 2008 Feb 29. PMID: 18378205; PMCID: PMC2696157.

von Wilmowsky C, Schlegel KA, Baran C, Nkenke E, Neukam FW, Moest T (2016) Peri-implant defect regeneration in the diabetic pig: A preclinical study. J Craniomaxillofac Surg. 44(7):827-34. doi: 10.1016/j.jcms.2016.04.002

Wölfel EM, Jähn-Rickert K, Schmidt FN, Wulff B, Mushumba H, Sroga GE, Püschel K, Milovanovic P, Amling M, Campbell GM, Vashishth D, Busse B. Individuals with type 2 diabetes mellitus show dimorphic and heterogeneous patterns of loss in femoral bone quality. Bone. 2020 Nov;140:115556. doi: 10.1016/j.bone.2020.115556. Epub 2020 Jul 28. PMID: 32730921.

Wu YY, Xiao E, Graves DT. Diabetes mellitus related bone metabolism and periodontal disease (2015) Int J Oral Sci. 7(2):63-72. doi: 10.1038/ijos.2015.2

Xiao E, Mattos M, Vieira GHA, Chen S, Correa JD, Wu Y, Albiero ML, Bittinger K, Graves DT (2017) Diabetes enhances IL-17 expression and alters the oral microbiome to increase its pathogenicity. Cell Host Microbe 22:120–128. doi: 10.1016/j.chom.2017.06.014.

Yamagishi S, Maeda S, Matsui T, Ueda S, Fukami K, Okuda S. Role of advanced glycation end products (AGEs) and oxidative stress in vascular complications in diabetes. Biochim Biophys Acta. 2012 May;1820(5):663-71. doi: 10.1016/j.bbagen.2011.03.014. Epub 2011 Apr 2. PMID: 21440603.

Yamagishi S. Potential clinical utility of advanced glycation end product cross-link breakers in age- and diabetes-associated disorders. Rejuvenation Res. 2012;15(6):564-572. doi:10.1089/rej.2012.1335

Yamamoto M1, Yamaguchi T, Nawata K, Yamauchi M, Sugimoto T (2012) Decreased PTH levels accompanied by low bone formation are associated with vertebral fractures in postmenopausal women with type 2 diabetes. J Clin Endocrinol Metab. 97(4):1277-84. doi: 10.1210/jc.2011-2537

Biography of the candidate

Dr Teodora Rodic was born on the 28th of September in 1989 in Bijeljina, Republic of Srpska, Bosnia and Herzegovina. She finished high school in her hometown as a Vuk's degree graduate. She enrolled at the Faculty of Dentistry, University of Belgrade, in 2008. She was awarded as the best student of the first and second year of studies. She was a scholar of the "Dr Milan Jelic" Fund from Banja Luka for the year 2012/13, as well as a scholar of the Ministry of Science of Republic of Srpska in 2015. She graduated in 2014 with an average grade of 9.56.

Dr Teodora Rodic enrolled at the PhD studies in Skeletal Biology in 2014 at the Faculty of Medicine, University of Belgrade. She was a scholar of the Ministry of Science on the subproject *"Age-related bone micro-architectural and mechanical bone properties: implications for increased bone fragility"* within the project 45005 (*Functional, Functionalized and Advanced Nano-materials;* Ministry of Science of Republic of Serbia, Nr. 45005) from 2016 until 2018, and since 2018 has been employed as an Assistant Researcher on the same project. She won a DAAD scholarship for a six-months research stay at the University Medical Center Hamburg- Eppendorf in Hamburg, Germany, in 2018. Dr Rodic has recently been engaged on two research projects of the Science Fund of Serbia. First, since July 2020, "*DiaBonet: Effects of diabetes mellitus on osteocytic, neural and vascular networks in bone: implications for increased fracture susceptibility at the proximal femur*", led by Assistant Professor Dr Petar Milovanovic. Second, since January 2022, "*IDEAS: Changes in bone structure and composition leading to increased fracture risk in aged population with chronic comorbidities*", lead by Professor Dr Marija Djuric.

Dr Teodora Rodic enrolled in the specialization in Orthodontics at the Faculty of Medical Sciences of University of Kragujevac in December 2018.

Изјава о ауторству

Име и презиме аутора: Др Теодора М. Родић

Број индекса: BS-01/14

Изјављујем

да је докторска дисертација под насловом

АНАЛИЗА КВАЛИТЕТА ВИЛИЧНИХ КОСТИЈУ КОД ТИПА 2 ДИЈАБЕТЕСА И АЛКОХОЛНЕ ЦИРОЗЕ ЈЕТРЕ: АНАТОМСКА И МИКРОСТРУКТУРНА АНАЛИЗА

- резултат сопственог истраживачког рада;
- да дисертација у целини ни у деловима није била предложена за стицање друге дипломе према студијским програмима других високошколских установа;
- да су резултати коректно наведени и
- да нисам кршила ауторска права и користила интелектуалну својину других лица.

Потпис аутора

У Београду, 6.7. 2022.год.

Теодора Родић

Изјава о истоветности штампане и електронске верзије докторског рада

Име и презиме аутора: Др Теодора М. Родић

Број индекса: BS-01/14

Студијски програм: Биологија скелета

Наслов рада: Анализа квалитета виличних костију код типа 2 дијабетеса и алкохолне цирозе јетре: анатомска и микроструктурна анализа

Ментор: Доц. др Петар Миловановић, Институт за анатомију, Медицински факулет, Универзитет у Београду

Изјављујем да је штампана верзија мог докторског рада истоветна електронској верзији коју сам предала ради похрањивања у **Дигиталном репозиторијуму Универзитета у Београду.**

Дозвољавам да се објаве моји лични подаци везани за добијање академског назива доктора наука, као што су име и презиме, година и место рођења и датум одбране рада.

Ови лични подаци могу се објавити на мрежним страницама дигиталне библиотеке, у електронском каталогу и у публикацијама Универзитета у Београду.

Потпис аутора

У Београду, 6.7. 2022.год.

Изјава о коришћењу

Овлашћујем Универзитетску библиотеку „Светозар Марковић" да у Дигитални репозиторијум Универзитета у Београду унесе моју докторску дисертацију под насловом:

АНАЛИЗА КВАЛИТЕТА ВИЛИЧНИХ КОСТИЈУ КОД ТИПА 2 ДИЈАБЕТЕСА И АЛКОХОЛНЕ ЦИРОЗЕ ЈЕТРЕ: АНАТОМСКА И МИКРОСТРУКТУРНА АНАЛИЗА

која је моје ауторско дело.

Дисертацију са свим прилозима предала сам у електронском формату погодном за трајно архивирање.

Моју докторску дисертацију похрањену у Дигиталном репозиторијуму Универзитета у Београду и доступну у отвореном приступу могу да користе сви који поштују одредбе садржане у одабраном типу лиценце Креативне заједнице (Creative Commons) за коју сам се одлучио/ла.

1. Ауторство (CC BY)

2. Ауторство – некомерцијално (CC BY-NC)

3. Ауторство – некомерцијално – без прерада (CC BY-NC-ND)

4. Ауторство – некомерцијално – делити под истим условима (CC BY-NC-SA)

5. Ауторство – без прерада (CC BY-ND)

6. Ауторство – делити под истим условима (CC BY-SA)

(Молимо да заокружите само једну од шест понуђених лиценци.
Кратак опис лиценци је саставни део ове изјаве).

Потпис аутора

У Београду, 6.7. 2022.год.
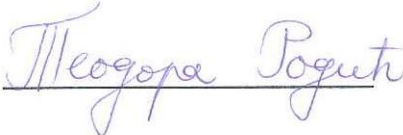
1. **Ауторство.** Дозвољавате умножавање, дистрибуцију и јавно саопштавање дела, и прераде, ако се наведе име аутора на начин одређен од стране аутора или даваоца лиценце, чак и у комерцијалне сврхе. Ово је најслободнија од свих лиценци.

2. **Ауторство – некомерцијално.** Дозвољаı   множавање, дистрибуцију и јавно саопштавање дела, и прераде, ако се на⎯⎯⎯ име аутора на начин одређен од стране аутора или даваоца лиценце. Ова лиценца не дозвољава комерцијалну употребу дела.

3. **Ауторство – некомерцијално – без прерада.** Дозвољавате умножавање, дистрибуцију и јавно саопштавање дела, без промена, преобликовања или употребе дела у свом делу, ако се наведе име аутора на начин одређен од стране аутора или даваоца лиценце. Ова лиценца не дозвољава комерцијалну употребу дела. У односу на све остале лиценце, овом лиценцом се ограничава највећи обим права коришћења дела.

4. **Ауторство – некомерцијално – делити под истим условима.** Дозвољавате умножавање, дистрибуцију и јавно саопштавање дела, и прераде, ако се наведе име аутора на начин одређен од стране аутора или даваоца лиценце и ако се прерада дистрибуира под истом или сличном лиценцом. Ова лиценца не дозвољавакомерцијалну употребу дела и прерада.

5. **Ауторство – без прерада.** Дозвољавате умножавање, дистрибуцију и јавно саопштавање дела, без промена, преобликовања или употребе дела у свом делу, ако се наведе име аутора на начин одређен од стране аутора или даваоца лиценце. Ова лиценца дозвољава комерцијалну употребу дела.

6. **Ауторство – делити под истим условима.** Дозвољавате умножавање, дистрибуцијуи јавно саопштавање дела, и прераде, ако се наведе име аутора на начин одређен од стране аутора или даваоца лиценце и ако се прерада дистрибуира под истом или сличном лиценцом. Ова лиценца дозвољава комерцијалну употребу дела и прерада. Слична је софтверским лиценцама, односно лиценцама отвореног кода.